Pharmacological characterisation of the [alpha]4 neuronal nicotinic acetylcholine receptor

Stephens, Mark William

Award date:
1993

Awarding institution:
University of Bath

PHARMACOLOGICAL CHARACTERISATION OF THE α4ß2 NEURONAL NICOTINIC ACETYLCHOLINE RECEPTOR

Submitted by MARK WILLIAM STEPHENS for the degree of Ph.D. of the University of Bath

1993.

SIGNED

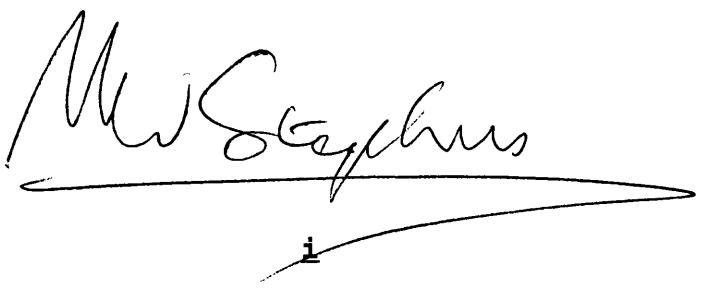

ProQuest LLC
789 East Eisenhower Parkway
P.O. Box 1346
Ann Arbor, MI 48106-1346

To Ray, Egon and Peter

"Everything in this book may be wrong"

From **Illusions** by Richard Bach

SUMMARY

This study was undertaken to investigate the mechanisms by which a variety of effectors - agonists and antagonists - interact with the predominant neuronal nicotinic acetylcholine receptor (nAChR), the $\alpha 4\beta 2$ subtype. The transfected M10 cell line expresses this subtype upon induction, and was used extensively here.

The four agonists - acetylcholine, (-)nicotine, cytisine and (+)anatoxin - appeared to be mechanistically similar in their action at the agonist binding sites of the M10 cell line. All had a very narrow concentration range over which they could activate the receptor and elicit $^{86}Rubidium^{+}$ influx, usually in the micromolar range. Dose-response curves were invariably bell-shaped, suggesting a rapid desensitisation at higher agonist concentrations. Extended exposure to agonists promoted a large (two to three orders of magnitude) increase in the binding affinity. (+)Anatoxin was exceptional, having a high affinity in functional studies (EC_{50} = 48nM), and steeper dose-response curves. However, affinity for the desensitised state was approximately equal to that of the other agonists.

The antagonists were assayed for their ability to attenuate agonist-induced $^{86}Rubidium^{+}$ flux into M10 cells, and for their effects on [^{3}H]nicotine binding to Triton X-100 extracts of rat brain membranes. Dihydro-ß-erythroidine behaved as a competitive antagonist, reducing the apparent affinity of the nAChR for the agonist. The data was

consistent with MK-801 acting as an open-channel blocker, though this form of antagonism has an unusually small allosteric component and thus only limited effects on high affinty agonist binding. Mecamylamine and chlorisondamine had profound, and distinctive effects on agonist binding. Mecamylamine may stabilise a structurally discrete conformation of the receptor, distinct from that resulting from agonist-induced desensitisation. Possible modes of antagonism are fully discussed within a general framework.

ACKNOWLEDGEMENTS

Many thanks to....

....my supervisors: Dr. Susan Wonnacott (University of Bath) and Dr. Paul Whiting (Merck, Sharp & Dohme). I would especially like to thank them for their professional guidance, and more importantly, their tolerance of my many idiosyncrasies. May they both live long and prosper.

....all the inhabitants, past and present, of the Nicotine Research Lab at the University of Bath. They provided a constant source of amusement, even when not aware of doing so! Special mentions go to Graham (who had the good sense to produce results complimentary to those presented here) and Phil (for the 3-D structures, and for being a Clanger).

....the other members of the School of Biological Sciences with whom I have chatted/drank/sympathised over the years.

....all the people (especially the Hockey team) at MSD Research Laboratories who made Essex bearable.

....the SERC and MSD for their financial support.

....my family, who, whilst probably not really understanding my research, gave uncompromising support as I played with my test-tubes.

PUBLICATIONS

Communications

Stephens, M.W., Wonnacott, S. & Whiting, P. (1991) The interaction of non-competitive antagonists with the nicotinic acetylcholine receptor. Eur. J. Neurosci. (Suppl 4) 2145

Stephens, M.W., Wonnacott, S. & Whiting, P. (1991) Non-competitive antagonists alter the affinity of nicotinic acetylcholine receptors for agonist. Soc. Neurosci. Abs. 17 384.12

Wilkie, G.I., Hutson, P.H., Stephens, M.W., Whiting, P. & Wonnacott, S. (1993) Hippocampal nicotinic autoreceptors modulate acetylcholine release. Biochem. Soc. Trans. 21/2 429-431

Wilkie, G.I., Stephens, M.W., Hutson, P.H., Whiting, P. & Wonnacott, S. (1993) Pharmacological characterisation of presynaptic nicotinic autoreceptors in the rat hippocampus. Soc. Neurosci. Abs. 19 123.1

Refereed papers

Thomas, P., Stephens, M.W., Wilkie, G.I., Amar, M., Lunt, G.G., Whiting, P., Gallagher, T., Periera, E., Alkondon, M., Albuquerque, E.X. & Wonnacott, S. (1992) (+)-Anatoxin-a is a potent agonist at neuronal nicotinic acetylcholine

receptors. J. Neurochem. 60 2308-2311

Wilkie, G.I., Stephens, M.W., Whiting, P., Hutson, P.H., Bertrand, S., Bertrand, D. & Wonnacott, S. (1993) Pharmacological comparison of a nicotinic autoreceptor in rat hippocampus with the reconstituted α4ß2 nicotinic receptor subtype. Br. J. Pharmacol. (Submitted)

Book review

Stephens, M.W. & Wonnacott, S. (1991) **Fidia Research Foundation Neuroscience Award Lectures, Vol. 4, 1988-1989.** Neurochem. Int. 19 619

ABBREVIATIONS

ACh	-	acetylcholine
AChR	-	acetylcholine receptor
α-BgTX	-	α-bungarotoxin
AnTX	-	anatoxin-a
Bmax	-	maximum density of ligand binding sites
BSA	-	bovine serum albumin
BSS	-	balanced salt solution
CPZ	-	chlorpromazine
DMEM	-	Dulbecco's modified eagle medium
EC_{50}	-	agonist concentration which gives half-maximal response
EDTA	-	diaminoethanetetra-acetic acid disodium salt
EGTA	-	ethyleneglycol-bis-(ß-aminoethylether)-N,N,N',N'-tetraacetic acid
GART	-	goat anti-rat IgG
HEPES	-	(N-[2-hydroxyethyl]piperazine-N'-[2-ethane sulphonic acid
HTX	-	histrionicotoxin
H_{12}-HTX	-	perhydrohistrionicotoxin
IC_{50}	-	ligand concentration which reduces radio-ligand binding or functional response to half-maximal
IgG	-	immunoglobulin G
k_{-1}	-	dissociation rate
Kd	-	dissociation binding constant
Ki	-	inhibiton constant

k_{obs}	-	observed association rate
mAb	-	monoclonal antibody
MK-801	-	dizoclipine
nAChR	-	nicotinic acetylcholine receptor
NCI	-	non-competitive inhibitor
NMDA	-	N-methyl-D-aspartate
NMDAR	-	N-methyl-D-aspartate receptor
PBS	-	phosphate buffered saline
PMSF	-	phenylmethylsulphonyl flouride
PCP	-	phencyclidine
SDS	-	sodium dodecoyl sulphate
TPMP	-	triphenylmethyl phosphonium
TRIS	-	Tris[hydroxymethyl]amino-methane

CONTENTS

LIST OF TABLES

LIST OF FIGURES

LIST OF SEQUENCES

1 GENERAL INTRODUCTION

Most intercellular signalling molecules do not permeate the plasma membrane, but interact with surface receptors. Neurotransmitters generally fit into this group, acetylcholine (ACh) for instance, acting at two different classes of receptor (the nicotinic and muscarinic), each containing a number of subtypes. The members of the nicotinic acetylcholine receptor (nAChR) family may, in structural and pharmacological terms, be broadly divided into two groups: "muscle-" (including those from Torpedo and Electrophorus electric organs) and "neuronal-type" receptors. The identification and biochemical characterisation of nAChR in neurons has lagged considerably behind that in electric organ and muscle; a primary aim of this project is to help redress this imbalance.

Generically, nAChR may be considered to consist of three distinct domains: the region involved in signal recognition, a cation selective ion channel, and a region accessible to intracellular regulatory processes, such as phosphorylation. Although each region is spatially discrete, events at one may influence the others; the very act of signal transduction is based on ACh binding leading to an opening of the channel. The receptor conforms to the classical definition of an allosteric protein (Monod et al., 1963). The project aims to examine possible allosteric interactions in neuronal receptors, allowing comparison with the more extensively studied muscle types, where

applicable, and speculation as to the effect such mechanisms have on receptor function.

1.1 nAChR STRUCTURE

1.1.1 The receptor macromolecule

Early structural evidence from Torpedo, based on x-ray diffraction (Ross et al., 1977), immunoelectron microscopy (Klymkowsky et al., 1979) and neutron scattering (Wise et al., 1981), suggested a protein 110-120Å in length, enclosing a central pore at least 6.5Å in diameter (Dwyer et al., 1980). The bulk of the protein was shown to be in the extracellular domain (extending 50-60Å from the membrane, compared with 10-20Å on the cytoplasmic side; see Fig 1.1A), with regions of regular secondary structure, probably α-helix (though see section 1.1.3), perpendicular to the membrane. These dimensions relate to the quaternary structure of an oligomeric molecule; each receptor, in Torpedo, actually consists of 5 subunits around a pseudo five-fold axis (Brisson & Unwin, 1985). The subunits are not identical, but homologous proteins: α (of which there are two in each receptor), ß, τ and δ (Raftery et al., 1980). They are believed to be arranged such that the ß separates the two α subunits, with the τ and δ next to each other (Kubalak et al., 1987, see Fig. 1.1Bi). This has recently been disputed however, because such an arrangement gives rise to a non-symmetrical positioning of the agonist binding sites (Pedersen & Cohen, 1990; see Fig. 1.1Bii). Reports indicate that a pentameric arrangement, including

two agonist binding sites, is maintained in neuronal nAChR (Anand et al., 1991 and Cooper et al., 1991). This is not immediately obvious, as it appears that only two types of subunits, α and ß, are usually present in neuronal nAChR, though multiple subtypes of each have been described (see section 1.1.2).

1.1.2 **Subunit heterogeneity**

The subunit composition of neuronal nAChR contrasts markedly with that of the muscle-type receptor, most notably in the number of different subunits that appear to exist. Thus far, a further ten subunits have been cloned from neuronal cDNA libraries (see Table 1.1). Seven of these have been identified, by sequence homology and/or functional expression, as agonist-binding subunits, analogous to the α of muscle nAChR. These neuronal α subunits, α2 to α8 (that of muscle having been designated, retrospectively, α1), contain residues homologous to those labelled by affinity probes in Torpedo nAChR (most notably cysteines 192 and 193; see section 1.2.1). These residues are not present in the remaining three subunits, which have been alternatively designated as ß2 to ß4 or nonα1 to nonα3, depending upon the species from which they were originally cloned (rat or chicken respectively).

The ligand-gated cation channels formed in the Xenopus oocyte expression system appear, usually, to consist of only one type of agonist-binding subunit, and one type of structural subunit. As the interaction of

Table 1.1 Published neuronal nAChR subunits cloned from rat and chicken sources.

Subunit	Rat	Chicken
α2	Wada et al. (1988)	Nef et al. (1988)
α3	Boulter et al. (1986)	
α4	Goldman et al. (1987)	
α5	Boulter et al. (1990)	Couturier et al. (1990b)
α6	-	
α7	-	Couturier et al. (1990a), Schoepfer et al. (1990)
α8	-	Schoepfer et al. (1990)
ß2 (nonα1)	Deneris et al. (1988)	Nef et al. (1988)
ß3 (nonα2)	Deneris et al. (1989)	-
ß4 (nonα3)	Duvoison et al. (1989)	Couturier et al. (1990b)

agonists and antagonists with nAChR is dependent upon both the α and non-α subunits present within the oligomer (see section 1.2.1), the existence of multiple subunits raised the possiblity of multiple pharmacological profiles amongst neuronal nAChR. This was demonstrated to some extent by Couturier et al. (1990a), who showed that sensitivity to ACh varied with subunit composition; the subtype displaying the highest affinity, α4ß2, is the main interest of this project (see section 3.1). Not all the subunits discovered appear to form part of a functional nicotinic receptor in the Xenopus system however, limiting the theoretical diversity. For example, neither α5 nor ß3 form functional receptors when combined with any subunit (Boulter et al.,1990; Couturier et al., 1990b; Deneris et al., 1989); there is other evidence which suggests that α5 can combine with two other subunits in a single heterooligomer however (Conroy et al., 1992). Similarly, there are no published data refering to α6 as being able to form functional channels. Conversely, the α7 subunit is able to form homo-oligomeric ion channels; coinjection with ß subunits had no effect on the agonist sensitivity of the resultant receptor (Couturier et al., 1990a). However, Schoepfer et al. (1990) have suggested that α8 may combine with α7 to form yet another receptor subtype.

1.1.3 Subunit topography

Hydropathy profiles of subunit sequence data (Fig. 1.1C), initially from Torpedo, revealed two main

hydrophilic and four hydrophobic domains (M1, M2, M3 and M4), the latter of sufficient length to span the plasma membrane as α-helices. These data provided the basis of the earliest structural model (Noda et al., 1982, 1983; Claudio et al., 1983 and Devillers-Thiery et al., 1983). Consensus glycosylation site sequences where located in the first of the hydrophilic domains, whilst the intracellular domain was situated between the two putative transmembrane helices M3 and M4 (Fig. 1.1D). This model was challenged (for example by Guy, 1984 and Finer-Moore & Stroud, 1984). The lack of a suitably hydrophilic transmembrane segment to line the channel lumen, and the existence of an extracellular carboxy-terminal (unlike most other membrane protein structures determined at that time) were regarded as particularly significant in this context. However, the location of a channel-blocker binding site to M2 (see section 1.3.1.2), and confirmation of the carboxy-terminal orientation (McCrea et al., 1987) added weight to the initial model, as well as serving to emphasise the unconventionality of the the ligand-gated ion channels. However, the recent generation of a 9Å resolution structure of the Torpedo nAChR by Unwin (1993), has once again raised doubt as to the accuracy of this model of subunit structure. Only a single α-helix, postulated to be the M2 segment, was seen in the membrane spanning domain of each subunit; no other secondary structures could be resolved in this region. Based on these data, Unwin hypothesised that the M1, M3 and M4 segments form ß-strands.

1.2 THE "THREE DOMAIN" MODEL

1.2.1 Signal recognition: the agonist binding site

The nAChR has two agonist binding sites (Reynolds & Karlin, 1978), both of which must be occupied to open the ion channel (Dionne et al., 1978). Binding curves, from Torpedo, suggested these sites to be non-identical and capable of interacting with positive cooperativity (Oswald & Changeux, 1982). Combination of α with other subunits appears to be the basis of these phenomena (Blount & Merlie, 1989). Agonist binding sites are now believed to be at the interfaces of α and non-α subunits, both in muscle- (Pedresen & Cohen, 1990) and neuronal-type (Luetje & Patrick, 1991) nAChR. Affinity labelling with competitive antagonists has been used to identify those residues involved in agonist binding. Such studies have picked out residues in three different regions of the N-terminal domain of the α subunit: tyrosines 93 and 190, tryptophan 149 and cysteines 192 and 193 (Torpedo numbering; see Sequence 1.1). These are conserved in all α, and absent in all non-α, subunits (in most cases: neuronal ß subunits contain aromatic residues homologous to tyrosine 93 and tryptophan 149). Similarly, Chiara & Cohen (1992) have recently reported the labelling of homologous tryptophan residues on the τ and δ subunits. A 13 residue loop, anchored by a disulphide bridge between cysteines 128 and 142, has been suggested to play a role in agonist binding (Cockcroft et al., 1990). This structure certainly appears to be a key one; deletion of one of the cysteine residues

leads to a drastic reduction in nAChR expression and activity (Mishina et al., 1985; Gehle & Sumikawa, 1991). However, the presence of the "cys-loop" in non-α subunits, and in other members of the ligand gated ion channel super family (Betz et al., 1990), tends to support a more generalised structural role for this motif.

1.2.2 **The ion channel**

In nAChR, the central "pore", framed by surrounding subunits, can be divided into three regions: two wide openings, approximately 25Å in diameter, on either side of the plasma membrane, divided by a much narrower channel, less than 10Å wide. The boundries between these different areas are very sharp and occur at the level of the phospholipid head groups (Fig. 1.1D). Although the outer regions may have a role in channel function (see section 1.2.2.3), it is the organisation of the transmembrane domain, central to nAChR action as a cation selective channel, which is addressed here.

1.2.2.1 M2 as the pore-lining segment

Identification of the channel lining segment proved one of the decisive factors in the adoption of the current model of subunit topology (See section 1.1.2). Support for M2 in this role came from several lines of investigation. Using DNA expression and single channel recording, it was shown that the conductance of a chimeric channel was dependent on the M2 segment and adjacent hinge regions

(Imoto et al., 1986; see also section 1.2.2.2). Binding data, using photoaffinity radiolabels based on channel blockers such as chlorpromazine (CPZ) and triphenylmethyl -phosphonium (TPMP) further implicated M2 as the pore lining region, as well as providing information on those residues involved in the high affinity site for such compounds (see section 1.3.1.2).

1.2.2.2 Barriers to ion permeation

Unwin (1989), noting the preponderance of negatively charged residues in the extracellular domain of nAChR, elaborated a possible role for this region in ion selectivity. The cylindrical shape of the channel in this region (see Fig. 1.1C) was envisaged as serving a dual function: wide enough so as not to inhibit ion diffusion, but sufficiently narrrow that the charged residues exert significant electrostatic effects (that is, attracting cations and repelling anions). The main effectors of ion selectivity, however, are likely to be located close to, or within, the narrow portion of the pore.

By analysis of single channel currents, Imoto et al. (1988) identified three clusters of negatively charged and glutamine residues as major determinants of the rate of ion transport through Torpedo nAChR. These clusters, adjacent to the M2 region - hence confirming earlier observations, see section 1.2.2.1 - were suggested to form three "rings" of charged residues. Using the nomenclature given in the review by Changeux (1990), these are: the

INNER- (homologous to α-aspartate 238), OUTER- (α-glutamate 262) and INTERMEDIATE (α-glutamate 241) charged rings (see Sequence 1.2 for positions relative to M2). Mutations in the intermediate ring exerted the strongest influence on single channel conductance, as well as on ion selectivity (Konno et al., 1991), which may imply that the residues of this ring come into closest contact with permeating cations. The other rings have been suggested to have a role in regulating ion access to the channel. It is worth emphasising at this point that these observations fully support the still strictly hypothetical α-helical configuration assigned to the transmembrane regions, at least for M2; the other putative membrane spanning segments may be different (see Unwin, 1993).

Dani (1989) showed that one cation binding site exists within the pore, through which every ion must pass. This narrow region was calculated, by streaming potentials, to be approximately 3-6Å long (a distance equivalent to one or two α-helical turns). A ring of polar residues within the central region of the pore could, by donating a hydrogen bond to the carbonyl oxygen on the next helical turn, form such a site (Perutz, 1989). It is tempting to equate the cation binding site with that for channel blockers labelled by CPZ and TPMP (See section 1.3.1.2), which is located two helical turns from the intermediate charged ring (See Fig. 1.2). Both sites may, after all, be envisaged as constrictions within the channel. However, changes in conductance elicited by mutations at this site

were negligible (Leonard et al., 1988 and Charnet et al., 1990). Recently, Imoto et al. (1991) have shown a ring of hydrophilic residues, homologous to α-threonine 244 (position 2; Sequence 1.2), to have profound effects on single channel currents when mutated. It was suggested that this HYDROPHILIC ring, and the intermediate charged ring, form the constriction which is the basis of the cation binding site. In favour of this hypothesis are: the size of this putative site, calculated to be approximately 5.4Å, and the high degree of conservation evident at these positions, the hydrophilic ring residues are invariably serine or threonine in the muscle and neuronal subunits of birds and mammals. Channel blockers, whilst also interacting with hydrophilic residues, may simply be incapable of penetrating beyond their high affinity site; Furois-Corbin & Pullman (1989) calculated the M2 helices to tilt approximately 7°, creating, in effect, a narrowing channel. Interestingly, White & Cohen (1992) reported that the location of channel blocker binding is dictated by the degree of access allowed to the antagonist. They showed that whilst a channel blocker (3-(trifluoromethyl)-3-(m-[^{125}I]iodophenyl)diazarine) labelled Torpedo nAChR in both the absence and presence of an agonist, only in the latter case was antagonist bound at the high-affinity channel blocker site.

The possible application of this four-ring "structure" to the neuronal α4ß2 subtype using sequence alignments, is illustrated in Fig. 1.3.

1.2.3 **Intracellular modulation - phosphorylation**

Protein phosphorylation is a major regulatory mechanism, likely to have a role in the control of almost all cellular pathways. The effectors of this system are the protein kinases and phosphatases. The former catalyse the covalent transfer of the τ-phosphate of adenosine trisphosphate (ATP) to specific - serine, threonine or tyrosine - residues of the target protein; the latter, its removal. The addition of such a charged group would be envisaged to cause changes in protein structure, thereby regulating function.

1.2.3.1 Subunit specificities

It has long been established that isolated post synaptic membranes from Torpedo have protein kinase activity (Gordon et al., 1977a), and that this was able to act on nAChR (Gordon et al., 1977b). Later studies were able to associate this activity with three endogenous kinases: cAMP dependent kinase, phosphorylating τ and δ subunits (Huganir & Greengard, 1983), protein kinase C, acting on α1 and δ subunits (Huganir et al., 1983), and a tyrosine specific kinase, targetting ß, τ and δ subunits (Huganir et al., 1984).

Avian and mammalian muscle-type receptors were shown to be similarly phosphorylated by means of radiolabelling, with phosphorus-32, both primary cultures and clonal cell lines. Under basal conditions, chick myotubes were found to have labelled τ and δ subunits (Ross

et al., 1987), whilst those from rat (Miles et al., 1987) and and BC3H1 myocytes (Smith et al., 1987) had phosphorylated ß1 and δ subunits. Additionally, forskolin (an activator of adenylate cyclase) and cAMP analogues induced labelling of the α1 subunit in BC3H1 cells. Recently, again using similar techniques, neuronal nAChR have been shown to be phosphoproteins. Using chick cilliary ganglia, Vijayaraghavan et al. (1990) reported α3 to be phosphorylated in response to cAMP analogues. Whiting (unpublished results) has demonstrated α4 to be basally phosphorylated in the M10 cell line, whilst forskolin treatment promotes the phosphorylation of ß2 subunits.

1.2.3.2 Functional effects of phosphorylation

It was postulated that, if nAChR could be phosphorylated (see section 1.2.3.1), then this must modulate channel function (Saitoh & Changeux, 1981). However, as purified receptor preparations were active in the absence of ATP (Tank et al., 1983), phosphorylation could not be a prerequisite of normal activity. Huganir et al. (1986) showed that, although no difference was apparent in initial conductance rates, or indeed sensitvity to agonist, the rate of desensitization of purified and reconstituted Torpedo nAChR was greater for phosphorylated receptors. Investigations using muscle-type receptors in less artificial systems confirmed this, as well as the involvement of the endogenous kinases. Application of forskolin to rat soleus muscle end plates (Middleton et

al., 1986) caused a rapid increase in the rate of desensitisation; analogues which could not activate adenylate cyclase had no effect (Albuquerque et al., 1986). Activation of protein kinase C in chick myotubes had previously been shown to reduce the sensitvity of nAChR to agonist (Eusebi et al., 1985).

The situation for neuronal nAChR appears less clear. Acute treatment of PC12 cells with forskolin had no effect on receptor properties (McGee & Liepe, 1984). Although a reduction in response was observed in rat sympathetic ganglia (Akagi & Kudo, 1985), this may have been due to a direct inhibition by forskolin (McHugh & McGee, 1985). Conversely, in chick ciliary ganglia, cAMP analogues increased the overall ACh response, whilst only having a small effect on desensitisation rate (Margiotta et al., 1987). This was achieved by an increase in the number of functional channels, though apparently not by a stimulation of de novo synthesis.

As well as these direct effects, it has been suggested that phosphorylation may have a role in nAChR biosynthesis and agregation at the synapse. In chick muscle cultures, for example, the phosphorylation status of the δ subunit changes as it is incorporated into the complete oligomer (Ross et al.,1987). Such alterations are likely in other subunits.

1.3 MODELS OF nAChR FUNCTION

1.3.1 The "four-state" model

As with many other features of nAChR, the kinetic model of its interaction with agonists is derived from extensive analysis of data from the muscle-type receptor. As this has been reviewed in great detail elsewhere (Ochoa et al., 1989 and Changeux, 1990 for example), only the key features of the model, and the some of the experimental observations behind them, are dealt with here.

Prolonged exposure to agonist was found to lead to a time-dependent reversible decrease of the response called "desensitisation" (Katz & Thesleff, 1957). This phenomenon was found to be kinetically complex, consisting of two distinct processes: a fast one, which led to a thousand-fold decrease in ion transport, and a slow one, in which ion movement through the channel was undetectable (Walker et al., 1982).

Early attempts to correlate the opening of the ion channel with agonist binding met with a puzzling paradox. The dissociation constant (Kd) of ACh was found to be in the region of 10nM (Weber & Changeux, 1974), some 4 to 5 orders of magnitude below that for the permeability response. Studies using either [^{3}H]ACh (Boyd & Cohen, 1980), or a flourescent agonist, Dansyl-C_6-Choline (Hiedmann & Changeux, 1979), showed that under resting conditions around one fifth of the receptor population exists in a state of high affinity for agonists, the rest in one of low affinty. Two major conformational transitions were resolved

during extended exposure to agonists, the slower of which was characterised by high affinty agonist binding and formed the majority at equilibrium.

Comparisons, performed in parallel, of the kinetics of agonist binding and receptor desensitisation revealed that the slow transition state of the former coincided exactly with the slow desensitisation phase of the latter (Neubig et at., 1982). The faster transition, which gave rise to an intermediate binding state with an apparent affinity of approximately 1μM (Heidemann & Changeux, 1979), fitted with the fast desensitisation.

The simplest minimal model compatible with these observations is an adapted version of the concerted model for allosteric transitions (Monod et al., 1965) and that proposed by Katz & Thesleff (1957) to account for desensitisation (see Fig 1.4A). It has four discrete, interconvertible states, namely: resting (R), active (A), intermediate (I) and desensitised (D). The channel is open in the A state, whilst the I and D states are the products of rapid and slow desensitisation, respectively. The same agonist binding sites are presumed to be involved in all four states, though their affinity increases from R to D, via A and I.

1.3.2 The model and neuronal nAChR

Depending upon their subunit composition, neuronal nAChR vary in their basic physiological properties such as agonist sensitivity (see section 1.1.2). Does this extend

to other aspects of receptor function, such as desensitisation? Both α (Gross et al., 1991) and ß (Cachelin & Jaggi, 1991) subunits appear to have a role in defining the desensitisation profile of a given subtype. The molecular mechanisms underlying desensitisation of the neuronal subtypes are assumed, on the basis of structural homologies, to be similar to those in the muscle nAChR (see section 1.3.1). The α4ß2 subtype, in these terms is very similar to the muscle receptor; its affinity for ACh when in the R state is micromolar (Bertrand et al., 1990; see section 3.1.3.1), whilst, a biphasic desensitisation is believed to give rise to a D state which binds agonist with high (nanomolar) affinity (Whiting & Lindstrom, 1986; see section 3.1.1). Other subtypes appear less like the muscle-type nAChR in this respect.

In the rat phoechromocytoma PC12 cell line, the affinity of the receptor for ACh increases only moderately during an extended period of exposure to the agonist (Kemp & Morley, 1986). PC12 cells are unlikely to express only one receptor subtype however. The α3 subunit is certainly present, this cell line having been the source of the original clone (Boulter et al., 1986). Analysis of total PC12 RNA by Rogers et al. (1992) has shown α5, ß2, ß3 and ß4 to also be present. A similar range of subunits has been reported to present in sympathetic ganglia (Listeraud et al., 1991), though this is unsurprising when the adrenal origin of the PC12 cell is considered (Greene & Tischler, 1976). Sympathetic ganglia also have high levels of α7

subunit gene expression, whilst PC12 cells have been shown to bind α-BgTX (Patrick & Stallcup, 1977). The relative levels of expression suggest that the dominant receptor subtype contains α3 and ß4 subunits; α5 may also be coexpressed, as appears to be the case in ciliary ganglia (Vernallis et al., 1993). Interestingly, a combination of α3 and ß4 subunits in Xenopus oocytes has been shown recently to desensitise only slightly, with the rapid initial phase reducing peak response by only 10 to 20% at high agonist concentrations (Cachelin & Jaggi, 1991). It seems likely that the small increase in agonist affinity and this limited desensitisation are linked, and that the underlying mechanisms at the α3ß4 subtype are similar to those in muscle nAChR. A comparative lack of desensitisation may be inferred from functional dose-response data for agonists at PC12 cells. Lukas (1989) showed agonist-induced ion flux to fall only slightly at concentrations above those which elicited maximal response in most instances. An exception was ACh, which produced a profound attenuation of ion movement. This effect was observed at very high (5 to 10mM) concentrations, probably sufficient for ACh to sterically block the ion channel.

The α7 homo-oligomer also appears to have a desensitisation profile differing from the muscle-type nAChR. Desensitisation was found to be both very fast and very thorough (Couturier et al., 1990a). Of greater interest are the recent studies in which the structural basis of desensitisation has been probed, using this

receptor as a model. Mutation of a leucine residue in the M2 region (position 9; see Sequence 1.2) not only disrupted the high affinity channel blocker binding site (see section 1.4.1.2), but additionally decreased the rate of desensitisation of the response (Revah et al., 1991). One of the mutants (in which the leucine residue was changed to a threonine) was found to exhibit a second conductance state. This was only seen under conditions in which the wild-type receptor would be desensitised, namely: in the presense of competitive antagonists, or after extended exposure to agonists (Bertrand et al., 1992). These observations have given rise to a modification of the four-state model. The nAChR is now considered to have multiple, structurally discrete desensitised states instead of just one as formerly believed (see Fig. 1.4B). In at least one of these conformations, the ion channel is occluded by a ring of highly conserved, homologous leucine (position 9, see sequence 1.2) residues.

1.4 NON-COMPETITIVE INHIBITORS

1.4.1 Sites and modes of action

"Non-competitve inhibitors" (NCI) are taken here to be compounds which attenuate ACh-induced ion flux through the nAChR channel, but do not, primarily, compete with agonists at their recognition site. Often such interactions promote and stabilize a desensitised form of the receptor. Heterogeneity of NCI action led Heidmann et al. (1983) to propose three "sites" at which such molecules may bind to

nAChR, namely:

(i) a single "high affinity" site, located within the ion channel ("perhydrohistrionicotoxin (H_{12}-HTX) sensitive").
(ii) multiple "low affinity" sites, possibly at the protein/lipid interface.
(iii) the agonist binding site, classically that at which competitive antagonists act.

A combination of NCI structure, concentration and relative affinity for each site, it was suggested, determined observed effects. To these criteria, the subunit composition of nAChR should probably be added (see section 1.4.3). Of these "sites", interaction at the ion channel is probably the best characterised (see sections 1.4.1.1 and 1.4.1.2) and may be the most common mode of action, though, is by no means universal.

1.4.1.1 Characteristics of the "channel block" mechanism

The mechanism of NCI channel block was first characterised for single channels in the seminal work of Neher & Steinbach (1978), using a local anesthetic, QX-222. Classically, channel block is both "agonist-" and "use-dependent", that is: the NCI reaches its site by an aqueous path accessible only when the channel is open, usually in the presence of agonist; the number of channels available to subsequent stimulation decreasing in the presence of the blocking agent. Recent evidence however, suggests uncharged

NCI may reach the channel via the lipid bilayer (Blanton et al., 1988), though the exact mechanism involved is unclear. Once in the channel the molecule binds, at least partially, into a hydrophobic pocket, in which molecular motion is restricted (Herz et al., 1987). This interaction appears to elicit only a small change in the overall conformation of the protein (McCarthy & Stroud, 1989).

1.4.1.2 The high affinity channel blocker site

Some of the residues which constitute this site were highlighted during investigations aimed at identifying the channel forming regions of nAChR subunits (see section 1.2.2.1). CPZ (Giraudat et al., 1986a, 1986b and 1989) and TPMP (Hucho et al., 1986) both labelled homologous serine residues of α, ß and τ subunits (position 6; Sequence 1.2), whilst retaining a 1:1 stoichiometry with the whole complex. CPZ also labelled a further serine of the ß subunit (position 9) and, in addition, was recently shown to label the τ subunit (positions 2, 6 and 9, Revah et al., 1990). Point mutation studies in mouse muscle receptor further emphasised the importance of serine 6; conversion to a non-polar residue severely reduced QX-222 affinity (Charnet et al., 1990). (This is a local anaesthetic showing some structural similarity to CPZ and TPMP; see section 1.4.2). The same study suggested that residue 10 may have a role; mutation from polar to non-polar character enhanced QX-222 affinity. Comparison of these sequences with other muscle and neuronal subunit data from higher

species (see Sequence 1.2) suggests that homologous residues are present, and thus may interact in these receptors in a similar fashion. Thus, all NCIs which act by a mechanism of channel blockade, based on their mutual competition, appear to operate at a common site, or at least overlapping multiple sites; these labelled residues (especially the serines at positions 6 and 9) are strong candidates for such a site.

1.4.2 Structural features of NCI

The "structural requirements" of nAChR NCI have not as yet been clearly defined. However, analogous data are available for a class of glutamate receptors, the n-methyl-d-aspartate (NMDA) subtype. Examination of the literature suggests that there is some degree of similarity in the molecular architecture in the ion channel of NMDAR and nAChR. For example, some drugs, notably phencyclidine (PCP) and MK-801, appear to antagonize both classes of receptor in a pharmacologically similar fashion (ie by channel block). In addition, Moriyoshi et al. (1991) have reported the cloning of what appears to be an NMDAR subunit, the putative M2 region of which has serine/threonine residues homologous to those in nAChR (see section 1.2.2.2), and is flanked by negatively charged amino acids (which may form the equivalent of the "charged rings" postulated to exist in nAChR; see section 1.2.2.2).

Using analogues of MK-801, Leeson et al. (1990) demonstrated that H-bonding through an amino group was

energetically the most important interaction of NCI with NMDAR. Previously, the presence of a phenyl ring had also shown to be vital (Kozikowski & Pang, 1989). Use of rigid PCP analogues indicated that ideally the ring should be orientated at 90° to the amino group. Examination of common nAChR NCIs structures (See Fig. 1.5) shows most to include both features. Those which do not, have mechanisms which appear to deviate from pure open channel block. For example, hexamethonium, which lacks a phenyl ring, does not block NMDAR (Snell & Johnson, 1989). Additionally its mechanism at nAChR appears unclear; hexamethonium was classified initially, by pharmacological techniques, as a competitive inhibitor (Van Rossum, 1962), though its clear voltage dependence favoured a channel block type mechanism (Ascher et al., 1979). However, certain features, most notably a lack of "use-dependence" (Large & Sim, 1986), suggest the need for further reappraisal. Mecamylamine also deviates from these structural formulae, and displays a considerable variety of mechanisms of action (see section 4.1.2). Particular attention is focussed on its mode of action in this project.

1.5 PROJECT AIMS

Much of the mechanistic detail ascribed to nAChR function is, as will be obvious from the preceding chapter, derived from studies using the easily accessible muscle-type receptor, or the $\alpha 7$ homooligomer. The aim of this project was to build up a pharmacological profile of the

α4ß2 nAChR, and to then analyse those observations with reference to current models of receptor function.

The α4ß2 receptor subtype is the predominant one in mammalian and avian brain (see section 3.1.1), making it a good choice for characterisation. It displays some degree of similarity with the muscle nAChR, electrophysiological recordings display a similarly biphasic desensitisation profile for instance. Again in common with the muscle-type receptor, it is assumed that this process gives rise to a conformation which is able to bind agonists with high affinity (see section 3.1.1). Effectors may interact with both the functionally active and desensitised states.

The interaction of agonists and antagonists with functionally active nAChR may be investigated by various techniques, each with its own advanatges and disadvantages (see section 3.2). Receptor expression in Xenopus oocytes has proved popular in identifying active subunit combinations, whilst previous work in this laboratory has used agonist-induced radiolabelled neurotransmitter release from preloaded synaptosomes. This study made use of an agonist-induced $^{86}Rubidium^{+}$ flux into a stably transfected mouse cell line expressing α4 and ß2 subunits upon induction (see section 3.1.2). High affinity radioligand binding to both the cell line and to detergent extracts of rat brain tissue was used to determine effector interaction with the desensitised receptor.

The results are presented in two sections: the action of agonists on α4ß2 nAChR first, then the

antagonists. The final part of this report will then attempt to describe these data in the terms of the current models of receptor function, thus returning to the primary aim of the project.

Fig. 1.1 **Aspects of nAChR structure.** (A) Vertical section through the native Torpedo nAChR as visualised by helical diffraction image reconstruction (resolution 17Å; from Unwin, 1990). (B) Cross-sectional representations of Torpedo nAChRs, showing possible subunit arrangements (from Kubalek et al., 1987). Note the location of the agonist binding sites (black triangles) at the α-τ and α-δ subunit interfaces. The "α_H" and "α_L" designations refer to the proposed difference in binding affinites between the two agonist sites (see section 1.2.1). (C) Hydropathy plot of the bovine α-subunit (from Maelicke, 1988), showing the four strongly hydrophobic membrane-spanning domains (M1-M4). (D) Topographical organisation of nAChR subunits (see section 1.1.3).

A

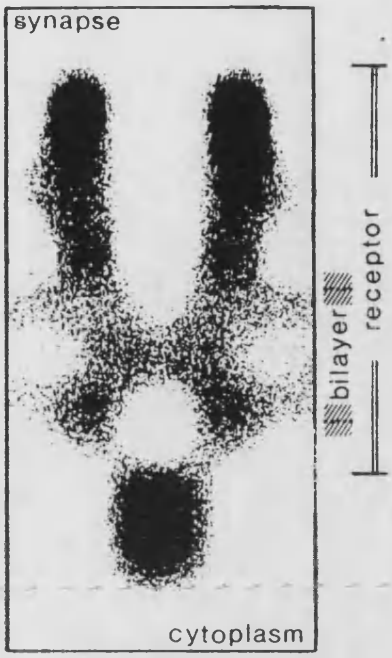
synapse
receptor
bilayer
cytoplasm

B

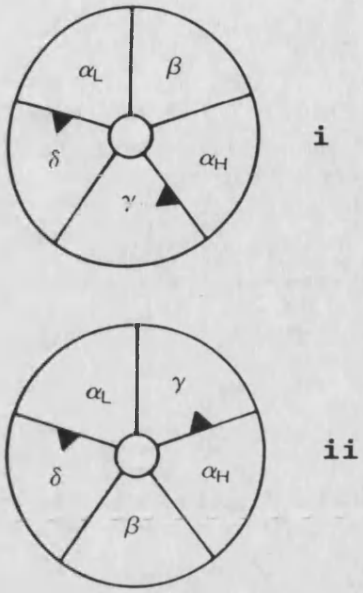
α_L
β
δ
α_H
γ
i
α_L
γ
δ
α_H
β
ii

C

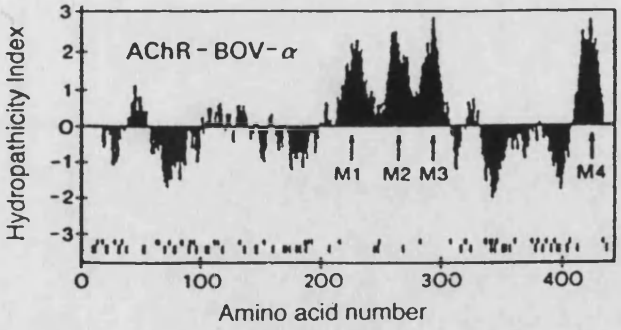
AChR - BOV - α
Hydropathicity Index
3
2
1
0
-1
-2
-3
M1
M2
M3
M4
0
100
200
300
400
Amino acid number

D

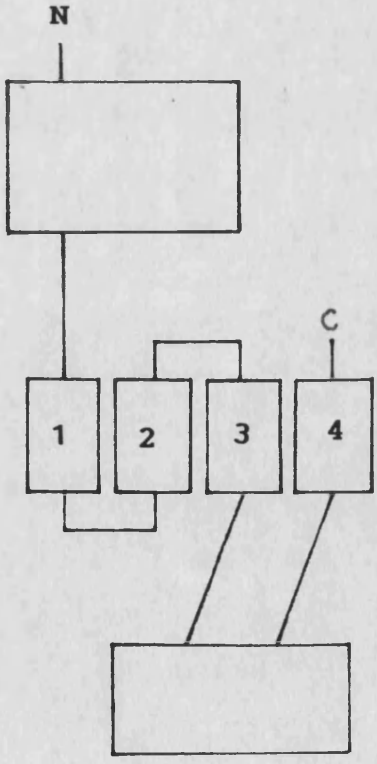
N
C
1
2
3
4

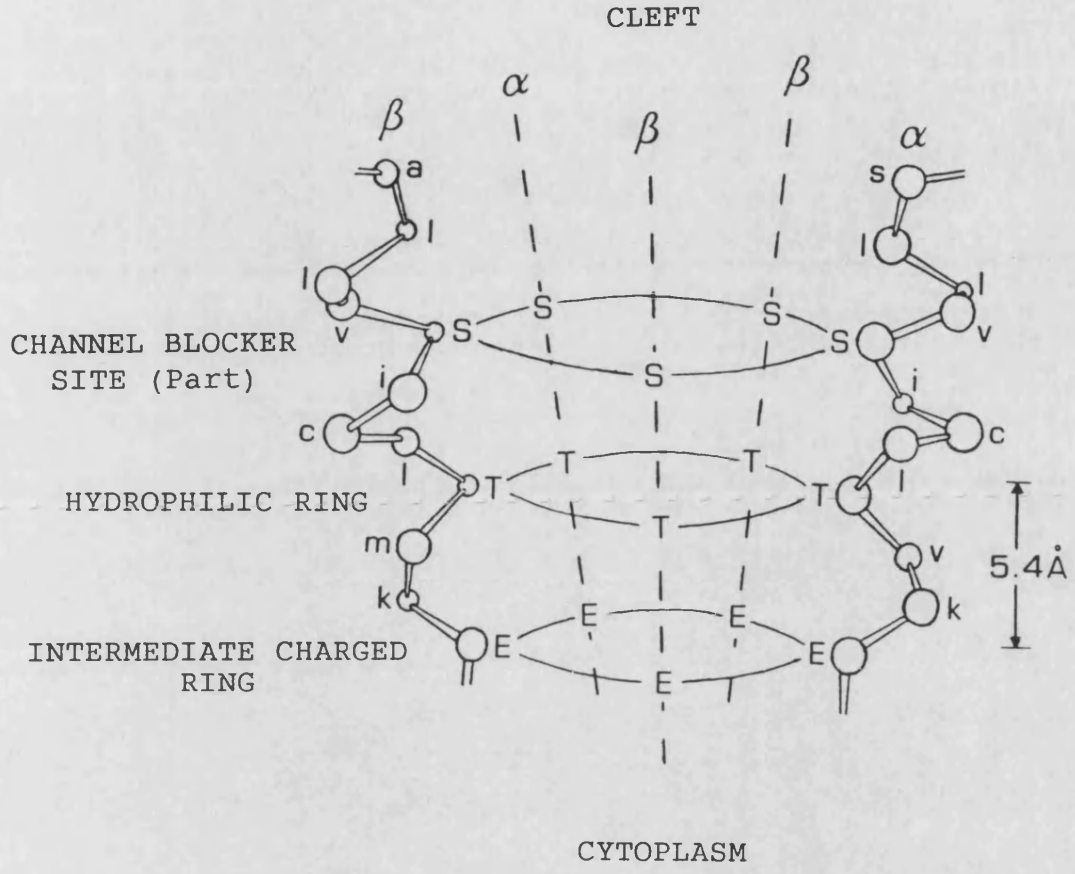

Fig. 1.2 **Model of the lower (cytoplasmic) portion of the ion channel of the α4ß2 nAChR.** The model is modified from Giraudat et al. (1989), in which the pore-lining M2 segment of the muscle-type nAChR is represented as an α-helix. A 2:3 stoichiometry of α:ß subunits is assumed (see sections 1.1.1 and 3.3.4). The single letter code is used for the amino acid residues.

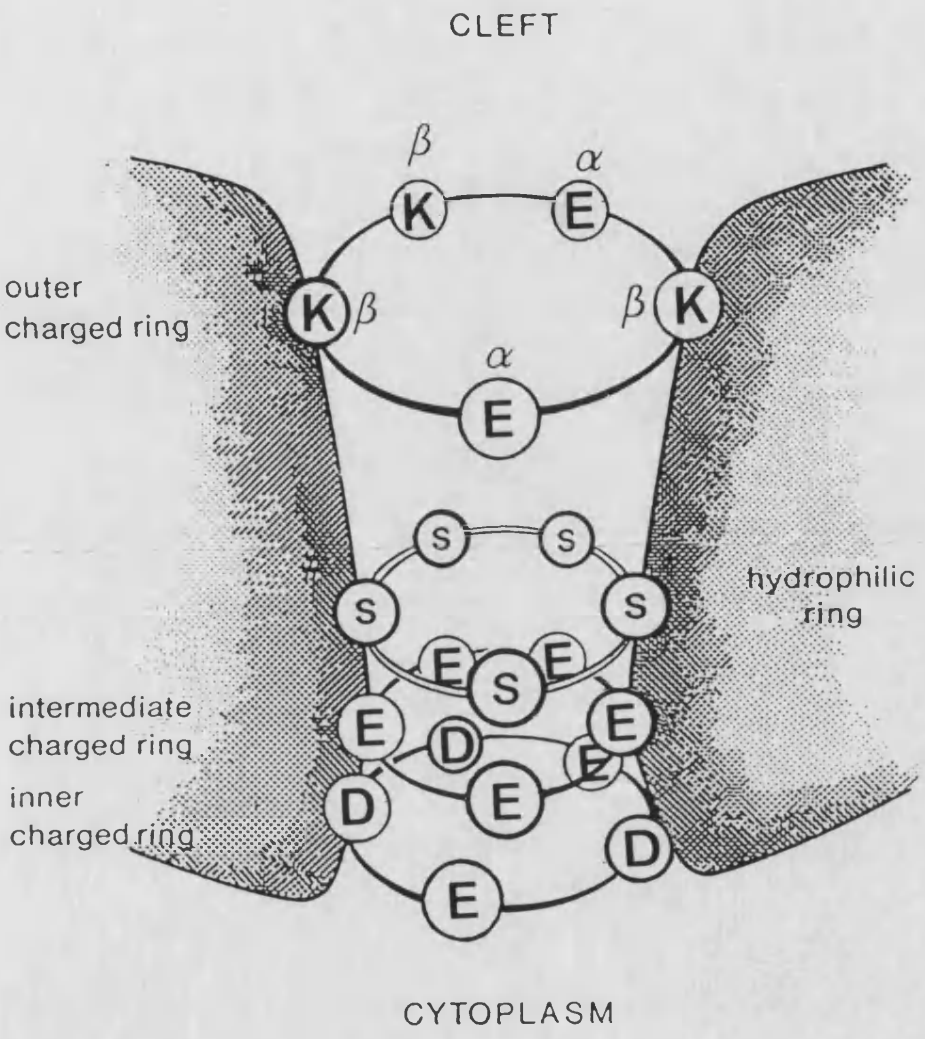

Fig. 1.3 **Schematic representation of the four superimposed rings of amino acids assumed to influence ion channel conduction in α4ß2 nAChR.** The model is modified from Changeux (1990). Previous assumptions regarding subunit stoichiometry and the conformation of the M2 domain (see Fig. 1.2) are maintained here.

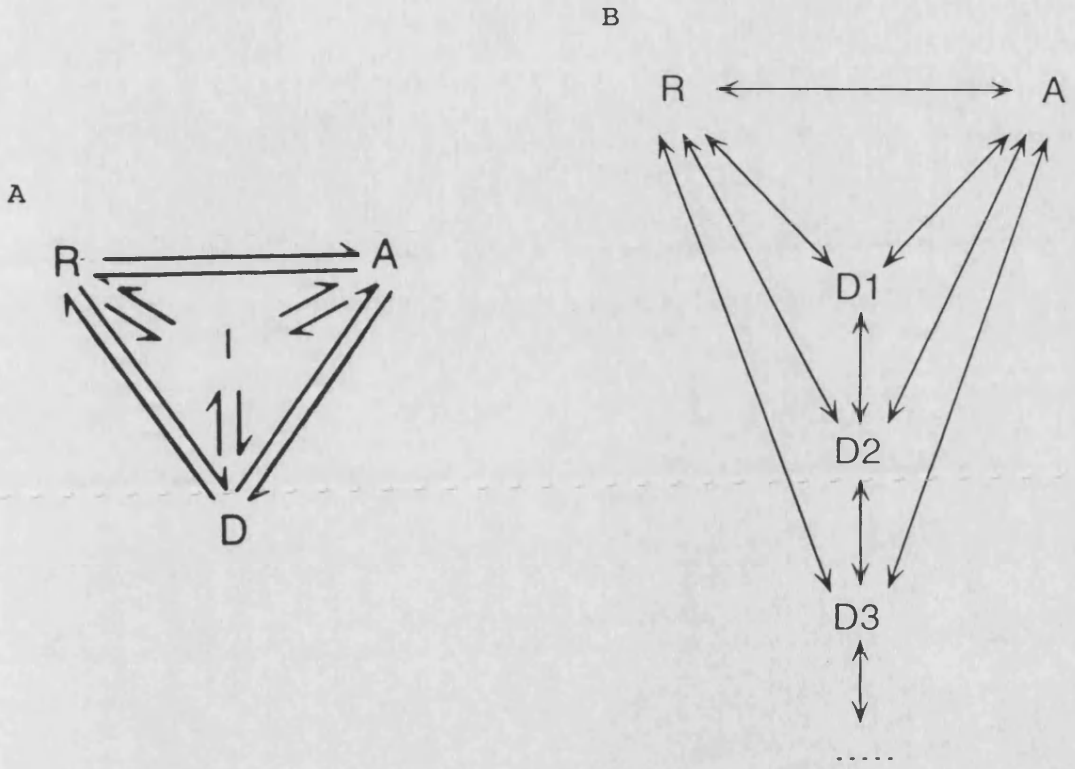

Fig. 1.4 **Models of the conformational transitions of nAChRs.** (A) The "four-state" model (from Changeux, 1990); **R** represents the resting state, and **A** the active state in which the channel is open. Both the **I** and **D** states are inactive, products of the fast and slow phases of desensitisation respectively (see section 1.3.1). (B) The modified multiple-state model (from Lena & Changeux, 1993); **D1** and **D2** are equivalent to the **I** and **D** states of the previous model, **D3** represents the additional desensitised state observed in mutated α7 nAChR (see section 1.3.2).

Fig. 1.5 **Structures of non-competitive inhibtors of nAChRs.**

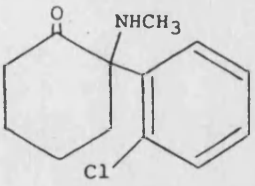

KETAMINE

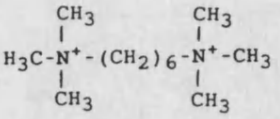

HEXAMETHONIUM

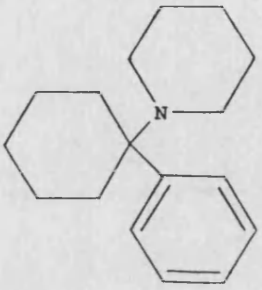

PCP

MK-801

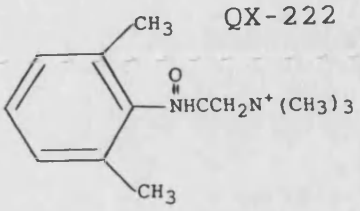

QX-222

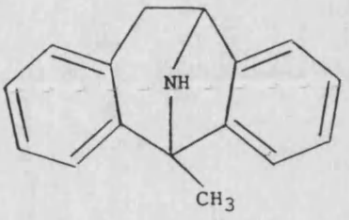

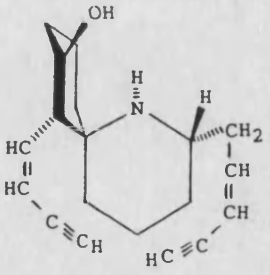

HISTRIONICOTOXIN

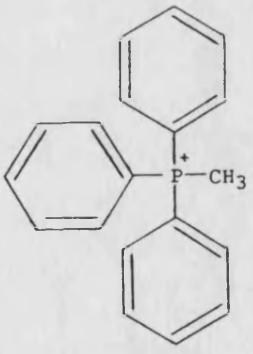

TPMP

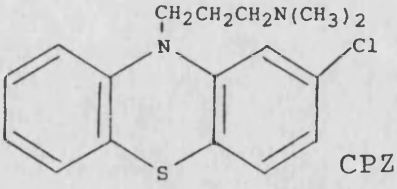

CPZ

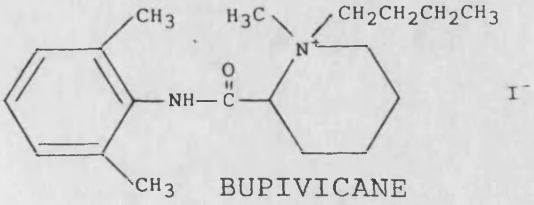

BUPIVICANE METHIODIDE

MECAMYLAMINE

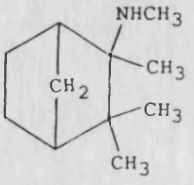

Sequence 1.1 **The putative agonist binding domain of (A) the Torpedo α subunit, and (B) representative neuronal α subunits.** The Torpedo sequence, taken from Changeux (1990b), indicates the relative positions of the three groups of residues implicated in agonist binding by affinity labelling studies. Residues marked with a large star show unambiguous labelling with DDF; other possible sites are indicated with a small star. Residues marked with a circle are labelled with MBTA, those with a triangle, lophotoxin. The neuronal sequence alignment appears courtesy of V. B. Cockcroft.

A Putative agonist binding segments: Torpedo α-subunit

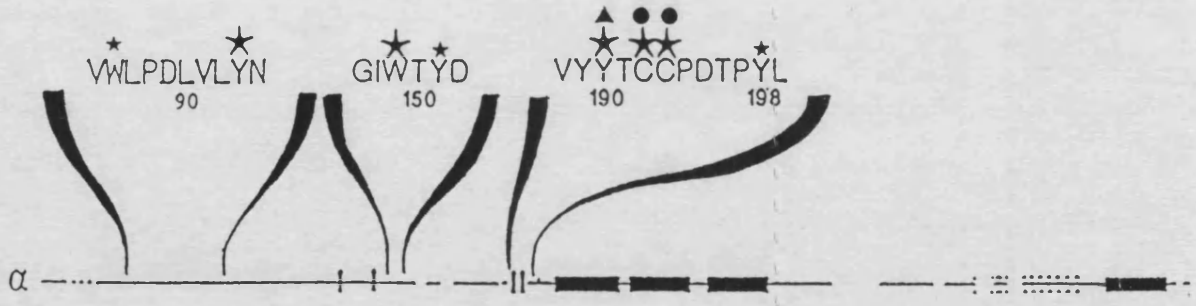

B Putative agonist binding segments: neuronal α-subunits

rat α2	IWIPDIVLYN	GSWTYD	KKYDCC-AEIYP
chick α2	IWIPDIVLYN	GSWTYD	KKYDCC-TEIYP
rat α3	IWKPDIVLYN	GSWSYD	IKYNCC-EEIYQ
chick α3	IWKPDIVLYN	GSWSYD	IKYNCC-EEIYT
rat α4	IWRPDIVLYN	GSWTYD	RKYECC-AEIYP
chick α4	IWRPDIVLYN	GSWTYD	KKYECC-TEIYP
rat α5	LWIPDIVLFD	GSWTYD	RTDSCC---WYP
chick α7	IWKPDILLYN	GSWTYG	SFYECC-KEPYP

Sequence 1.2 **The M1 and M2 regions of (A) Torpedo nAChR subunits, (B) representative neuronal nAChR α subunits and (C) representative neuronal nAChR ß subunits.** The Torpedo sequence, taken from Changeux (1990b), shows those residues affinity labelled with chlorpromazine (CPZ; circles) which constitute the high affinity channel blocker site. Also shown are the binding sites of other compounds: quinicrine azide (QA; squares) and meproadifen mustard (MM; diamonds). Small dots indicate residues mutated by Imoto et al. (1988). The neuronal sequences appear courtesy of V.B. Cockcroft.

A Torpedo nAChR subunits

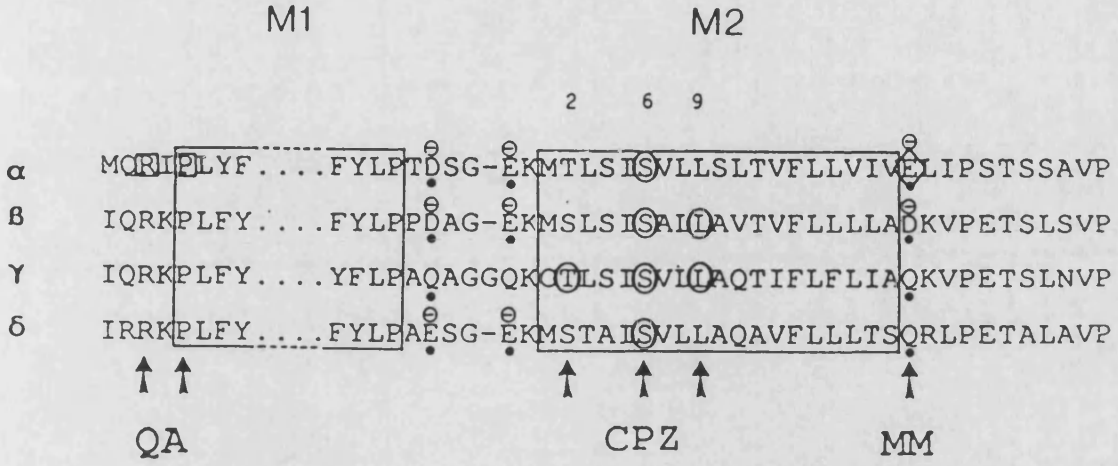

B Representative neuronal nAChR α-subunits

rat α2	IRRL	PLFY....	FYLP	SECG_EK	ITLCISVLLSLTVFLLLITE	IIPSTSLVIP
chick α2	IRRL	PLFY....	FYLP	SDCG-EK	ITLCISVLLSLTVFLLLITE	IIPSTSLVIP
rat α3	IRRL	PLFY....	FYLP	SDCG_EK	VTLCISVLLSLTVFLLVITE	TIPSTSLVIP
chick α3	IRRL	PLFY....	FYLP	SDCG_EK	VTLCISVLLSLTVFLLVITE	TIPSTSLVIP
rat α4	IRRL	PLFY....	FYLP	SECG_EK	VTLCISVLLSLTVFLLLITE	IIPSTSLVIP
chick α4	IRRL	PLFY....	FYLP	SECG_EK	ITLCISVLLSLTVFLLLITE	IIPSTSLVIP
rat α5	IKRL	PLFY....	FYLP	SNEG_EK	ISLCTSVLVSLTVFLLVIEE	IIPSSSKVIP
chick α7	MRRR	TLYY....	FLLP	ADSG_EK	ISLGITVLLSLTVFMLLVAE	IMPATSDSVP

C Representative neuronal nAChR ß-subunits

rat β2	IRRK	PLFY....	FYLP	SDCG_EK	MTLCISVLLALTVFLLLISK	IVPPTSLDVP
chick β2	IRRK	PLFY....	FYLP	SDCG_EK	MTLCISVLLALTVFLLLISK	IVPPTSLDVP
rat β3	LRRL	PLFY....	FYLP	SDEG_EK	LSLSTSVLVSLTVFLLVIEE	IIPSSSKVIP
rat β4	IKRK	PLFY....	FYLP	SDCG_EK	MTLCISVLLALTFFLLLISK	IVPPTSLDIP

2 MATERIALS AND METHODS

2.1 MATERIALS

(-) [^{3}H]Nicotine (approximately 75Ci/mmol, 15μM in 90% ethanol), (-) [^{3}H]cytisine (approximately 30Ci/mmol, 30μM in 90% ethanol) and ^{86}Rubidium chloride (approximately 4mCi/mg in 0.5M hydrochloric acid) were obtained from New England Nuclear (Stevenage, Herts., U.K.). A 10 fold molar excess of mercaptoacetic acid was added to the [^{3}H]nicotine on receipt to reduce reductive degradation of nicotine during storage (Romm et al., 1990).

Dihydro-ß-erythroidine, MK-801 and phencyclidine were gifts from Merck, Sharp & Dohme Research Laboratories (Rahwey, New Jersey, U.S.A).

The monoclonal antibodies, mAb 290 and 295 were gifts from Dr. P. Whiting (Merck, Sharp & Dohme Research Laboratories, Harlow, Essex, U.K.).

All other reagents were obtained from Aldrich (Gillingham, Dorset, U.K.), BDH (Poole, Dorset, U.K.), Gibco BRL (Paisley, Scotland, U.K.) or Sigma Chemical Company Ltd. (Poole, Dorset, U.K.).

2.2 METHODS

For ease of reference, protocols will be grouped according to tissue from which the receptor proteins were derived (ie either rat forebrain preparations or the

transfected M10 cell line).

2.2.1 **Brain tissue protocols**

2.2.1.1 Membrane preparation

Male Wistar rats (200-250g, 12 hour light and dark cycle with free access to food and water) were killed by cervical dislocation then decapitated. The brains were removed (minus cerebellum), frozen rapidly and stored at -70°C if not required immediately. (Such treatment does not significantly alter the number of measurable high affinity agonist binding sites (Benwell & Balfour, 1985)).

Membrane preparation followed the protocol of Macallan et al. (1988). Breifly, brains were homogenised (10% w/v) in 0.32M sucrose (pH 7.4, containing protease inhibitors (1mM EDTA and 0.1mM phenylmethylsulphonyl fluoride) and 0.1% (w/v) sodium azide) in a pre-cooled glass-Teflon homogeniser (clearance 0.31mm) by 2x6 up and down strokes at 300rpm. The suspension was centrifuged at 1,000xg for 10 minutes at 4°C (Sorvall RC-5B refigerated centrifuge). The supernatant, S1, was retained on ice, whilst the pellet, P1, was washed with 0.32M sucrose (5ml/g original wet weight) by resuspension then centrifugation (1,000xg, 10 minutes).

The combined supernatants were centrifuged at 12,000xg for 30 minutes to give the P2 pellet. This was washed twice by resuspension in 50mM potassium phosphate buffer (see section 2.1; pH 7.4, containing protease inhibitors as above) to give a final volume of 2.5ml/mg

original wet weight, and centrifugation (12000xg, 30 minutes), before final resuspension in 50mM phosphate buffer. Aliquots (10ml) were stored at -20°C until required.

2.2.1.2 Triton X-100 extraction of P2 membranes

P2 membranes were centrifuged at 12,000xg for 30 minutes, then resuspended up to half original volume in binding buffer (Krebs-HEPES-TRIS, see section 4.2.1). Triton X-100 (10% v/v) was added to give a final concentration of 0.5%.

After continuous stirring for 1 hour at 4°C, the suspension was centrifuged at 100,000xg for 45 minutes (Beckmann L5-50B Ultracentrifuge, SW50.1 rotor). The supernatant, termed the Triton extract, was collected, stored at 4°C, and used within a period of 3 days.

2.2.1.3 [^{3}H]Nicotine binding assays

Tritiated nicotine binding to brain preparations was first convincingly demonstrated by Romano & Goldstein (1980), using a racemic ligand and rat membranes. The protocols for both equilibrium and kinetic binding studies shown here, follow those of Lipiello & Fernandes (1986), modified for use with Triton extracts.

2.2.1.3.1 Equilibrium studies

The Triton extract was diluted with Krebs-HEPES-TRIS buffer, such that the final detergent concentation was below 0.1% (unless otherwise stated, see section 4.2.3).

Triplicate samples (0.25ml, approximately 1mg protein/ml) were incubated with [^{3}H]nicotine (final concentration 10nM for competition assays, 1 to 40nM for saturation assays unless otherwise stated) for 30 minutes at room temperature, and in the presence and absence of excess unlabelled nicotine (1mM) to determine specific binding. The samples were chilled for 1 hour at 4°C. Incubation was terminated by dilution with 3ml ice cold phosphate buffered saline (PBS; 10mM potassium phosphate (see section 2.1), pH 7.4, containing 0.14m sodium chloride and 0.01% sodium azide).This was followed by rapid filtration under vacuum on to a double thickness of Gelman GFA/E glass fibre filters presoaked overnight in 0.3% (v/v) polyethyleneimine (Bruns et al., 1983), using a Brandel 24-channel tissue harvester to separate bound and free radioactivity. The filters were further rinsed with 2x3ml PBS; filtration and washing were accomplished within 15 seconds. The radioactivity retained on the filters was measured by liquid scintillation counting (5ml Optiphase scintillant per filter), using a Packard scintillation spectrophotometer. Binding to P2 membranes was performed in a similar manner.

Where the effects of an antagonist on binding to P2 membranes were under investigation (see sections 4.3.1 and 4.3.2), the drug was first dissolved in 95% (v/v) ethanol, then 10μl added with the radiolabel at the beginning of the assay.

2.2.1.3.2 Kinetic studies

The conditions under which the kinetics of [^{3}H]nicotine binding to Triton X-100 extracts were assayed were similar to those of equilibrium assays, unless otherwise stated. Experiments were performed at 4°C. To determine the observed association rate (k_{obs}), [^{3}H]-nicotine binding (concentration usually 10nM, but see section 4.3.1.1) was determined at intervals up to 3 hours. This was later amended, and binding was measured at 1, 2, 5, 10, 15, 30 and 180 minutes, to focus on the early rapid binding phase (see section 4.3.2.1). To measure the dissociation rate (k_{-1}), extract was equilibrated with [^{3}H]nicotine for 3 hours, then excess unlabelled competing ligand (1mM (-)nicotine) was added. The radiolabel remaining bound at 1, 2, 5, 10, 15 and 30 minutes after this addition was measured.

2.2.1.4 Protein determinations

Protein concentrations were obtained by the method of Lowry et al. (1951). Standard curves were constructed using a solution of bovine serum albumin (BSA) over a concentration range of 50 to 350μg/ml.

Breifly, duplicate samples (200μl) of BSA standards or test solutions, diluted up to 1 in 2000 with distilled water, were incbated in 1ml alkaline cupric tartarate (freshly prepared by mixing 1 volume 1% (w/v) copper sulphate, 1 volume 2% (w/v) sodium tartarate and 100 volumes 2% (w/v) sodium carbonate in 0.1M sodium hydroxide)

for 10 minutes at 20°C. Folins-Ciocalteau reagent (100µl, diluted 1 in 2 with distilled water) was added and the colour allowed to develop for 40 minutes. Blanks contained distilled water in place of the protein solution. Absorbance was read at 690nm in a Titertek Multiscan spectrophotometer.

The use of Triton X-100 and Krebs-HEPES-TRIS buffer both interfered with this reaction (see section 4.2.3.2). The protocol was modified such that the detergent and buffer concentrations were the same within each sample, a similar volume then being added to each standard.

2.2.1.5 Binding data analysis

[^{3}H]Nicotine binding parmeters to Triton extracts were determined from saturation binding assays. The dissociation constant (Kd) and the number of binding sites (Bmax) were first calculated by the method of Scatchard et al. (1949). These values were then used as first estimates for an iterative, least-squares curve fitting of the binding data performed on the SIGMAPLOT 4.1 software package (Jandel Scientific, California, U.S.A.). As well as being the basis for this more sophisticated calculation of Kd and Bmax, the Scatchard transformation of the data provided information on the homogeneity (or otherwise) of the binding sites.

Competition data were analysed by the Hill transformation, to give the concentration at which the competing ligand had half-maximal effect (IC_{50}). The IC_{50}

value was used to calculate the inhibiton constant (Ki) was using the relationship of Cheng & Prusoff (1974):

$$Ki = IC_{50}/(1+[L]/Kd)$$

Where [L]/Kd is the ratio of concentration of [^{3}H]nicotine and its dissociation constant calculated from saturation assays. Data were also fitted to asigmoid curve using an iterative curve fitting routine on the SIGMAPLOT 4.1 software package.

2.2.2 **Transfected M10 cell protocols**

2.2.2.1 Cell culture

Cell stocks were routinely grown up in 175cm^2 platic culture flasks using Dulbecco's modified eagle medium (DMEM; 70ml per flask) additionally containing 10% foetal bovine serum, additional glutamine (2mM) and antibiotic agents (100U/ml streptomycin and 100μg/ml penicillin) at 37°C in a humidified atmosphere containing 4% (v/v) CO_2. Maintenance medium also contained 0.5mg/ml G418 geneticin as a selection agent (see section 3.1.4). This was replaced in promotion medium with 1μM dexamethasone, which was noted to bring about a change in cell morphology within a day of application, the cells changing from a bipolar to more trapezoid form (see Fig. 2.1).

2.2.2.2 Cell harvesting and plating

The tissue culture flasks were gently washed

twice with 10ml warmed, sterile PBS. This was removed by aspiration, and 5ml trypsin-EDTA (0.5g/l trypsin and 0.2g/l EDTA.4Na$^+$ in Hank's balanced salt solution) added for 1 minute, with agitation. DMEM (5ml) was then added, and the cells pelleted by centrifugation (500xg, 3 minutes). The pellet was resupended in 10ml DMEM. A sample (10μl) of this suspension was added to an equal volume of trypan blue (0.2% v/v in PBS), and cell numbers determined in a haemocytometer. The cells were then either plated for experimentation (see following sections) or returned to 175cm^2 flasks for continuous culture.

2.2.2.3 Immunoaffinity immobilisation

This protocol is taken from Whiting et al. (1991). Induced cells were scraped into 1ml PBS, pelleted, then resuspended in 500μl Lysis buffer (50mM TRIS, pH 7.5, 200mM sodium fluoride, 1% (v/v) Triton X-100, 5mM EDTA, 5mM EGTA, 5mM iodoacetamide, 1mM PMSF) additionally containing 5mg/ml bovine serum albumin (from a 50mg/ml stock in 1% SDS) and 10μg/ml each of antipain, leupeptin and pepstatin. After 15 minutes gentle rotation at 4°C, insoluble material was removed by centrifugation (15 minutes, 4°C). The cell extract was pre-absorbed by further rotation for 15 minutes with 30μl of goat-anti rat IgG coupled to Sepharose (Sepharose-GART). This was removed by centrifugation, and the extract rotated for 4 hours at 4°C, with 25μl of a monoclonal antibody, mAb 295, directed against the ß2 nAChR subunit, coupled to an AFC resin. The resin was pelleted,

then washed with 5 x 1ml lysis buffer, 5 x 1ml lysis buffer additionally containing 800mM sodium chloride and 2 x 1ml lysis buffer, by repeated centrifugation and resuspension.

2.2.2.4 [^{35}S]Methionine incorporation

After Whiting et al. (1991), confluent M10 cells (10cm diameter dishes, $2x10^6$ cells per dish) were induced with 1μM dexamethasone for 16 hours, washed with 3 x 5ml methionine-free DMEM, then incubated in the same, additionally containing 500μCi [^{35}S]methionine, for 6 hours at 37°C. After immunoaffinity purification (see section 2.2.2.2), nAChR were eluted from the resin by 2 x 10 minutes incubation in 50μl 50mM citrate (pH 3.0, containing 0.01% Triton X-100), followed by 2 minutes in 100μl distilled water. The eluate was neutralised with 1M Tris (pH 7.5) and concentrated using a Centicon (Amicon) to approximately 50μl. This was then diluted with 1ml distilled water, reconcentrated and finally lyophilised. The subunits were separated by SDS-PAGE. The samples were electrophoresed on a 12% (w/v) acrylamide gel in SDS at 35mA for 2 to 3 hours. The gel was then soaked in enhancer for 30 minutes, followed by a further 30 minutes in water. The gel was dried, and exposed to x-ray film at -70°C for 7 days. To calculate subunit stoichiometry (see section 3.2), the gel bands were also excised, dissolved overnight in 1ml soluene, and the radioactivity measured by liquid scintillation counting.

2.2.2.5 Radioligand binding assays

2.2.2.5.1 To immunoaffinity purified receptors

M10 cells were induced by incubation in promotion medium containing 1μM dexamethasone for 3-5 days, and the receptor proteins solublised as previously (see section 2.2.2.3). The cell extract was then rotated gently for 16 hours with sepharose-GART and mAb290 (25μl and 0.25μl respectively per 10cm dish), instead of the previous two-step process (mAb 290 has a similar specificity to mAb295, binding to the ß2 subunit). Samples were routinely pooled, and aliquots taken for binding studies.

Binding assys were performed in triplicate. Immobilised nAChR were incubated with either 150μl (-)-[^{3}H]nicotine or 50μl [^{3}H]MK-801 (final concentrations 20nM and 5μM, repectively) for 30 minutes at 20°C, washed with 3 x 1ml PBS (including 1% Triton X-100), and the bound radioactivity quantified by liquid scintillation counting. Non-specific binding was taken as that bound to an equivalent volume of sepharose-GART in the absence of the monoclonal antibody.

2.2.2.5.2 To receptors in situ

Cells were plated out (0.29x10^6 cells per well, 6-well plates) and induced with 1μM dexamethasone for 3-5 days. The medium was removed, and each well washed with 2 x 1ml PBS. Triplicate wells were incubated with [^{3}H]cytisine (1nM in competition assays, 0.1-5nM for saturation assays),

or [^{3}H]nicotine (concentration 1-30nM), dissolved in Krebs-HEPES-TRIS (1ml per well) for 2 hours at 20°C. Total and non-specific radioligand binding was determined in the absence or presence of excess unlabelled (-)nicotine, respectively. Incubation was terminated by the removal of buffer by aspiration. Each well was then rapidly washed with 4 x 1ml PBS. Washing was routinely accomplished within 5 seconds. The receptors were then solublised by application of 1ml 1M sodium hydroxide overnight. Radioactivity was measured by liquid scintillation counting (efficiency = 55%).

2.2.2.6 ^{86}Rubidium$^+$influx assays

The protocol of McGee & Liepe (1984) was followed with only minor modifications. Breifly, M10 cells were plated out ($0.29x10^6$ cells per well, 6-well plates) and induced with 1μM dexamethasone for 3-4 days. On each plate, half of the wells were used in the ion-flux assay; [^{3}H]-cytisine binding (see section 2.2.2.4.2) was measured in the other half. This allowed for the normalisation of the flux data by comparison of the levels of surface expression of α4ß2 nAChRs.

The medium was removed, and each well washed with 2 x 1ml PBS, and the cells incubated for 15 minutes in 1ml balanced salt solution (BSS; 150mM sodium chloride, 1.2mM magnesium chloride, 5mM potassium chloride, 0.8mM sodium dihydrogen orthophosphate, 10mM glucose, 1.8mM calcium chloride and 15mM HEPES). The cells were pretreated for 1

minute with sodium-free BSS (sodium chloride replaced with 300mM sucrose) additionally containing 2mM ouabain, then washed with 2 x 1ml of the same. Each well was incubated for 1 minute in 1ml sodium-free BSS additionally containing 5μCi/ml ^{86}Rubidium^{+} and the combination of agonists/ antagonists under investigation. Each well was then rapidly washed with 4 x 1ml BSS, and the contents then solublised in 1ml 1M sodium hydroxide. Radioactivity was measured by liquid scintillation counting (efficiency = 75%).

2.2.3 Chronic chlorisondamine treatment

Two groups of male Wistar rats (240-260g, but otherwise as previously; see section 2.2.1.1) were injected subcutaneously with either 2ml chlorisondamine solution (final concentration 10mg/kg; after Clarke, 1984) or saline as controls. Technical assistance was provided by members of the Animal House at the University of Bath, who held a Home Office license for this procedure. One week after injection, the animals were killed by cervical dislocation and decapitated. The brains were removed and the cortices and hippocampi rapidly dissected. Membrane preparations were produced as previously (see section 2.2.1.1).

A

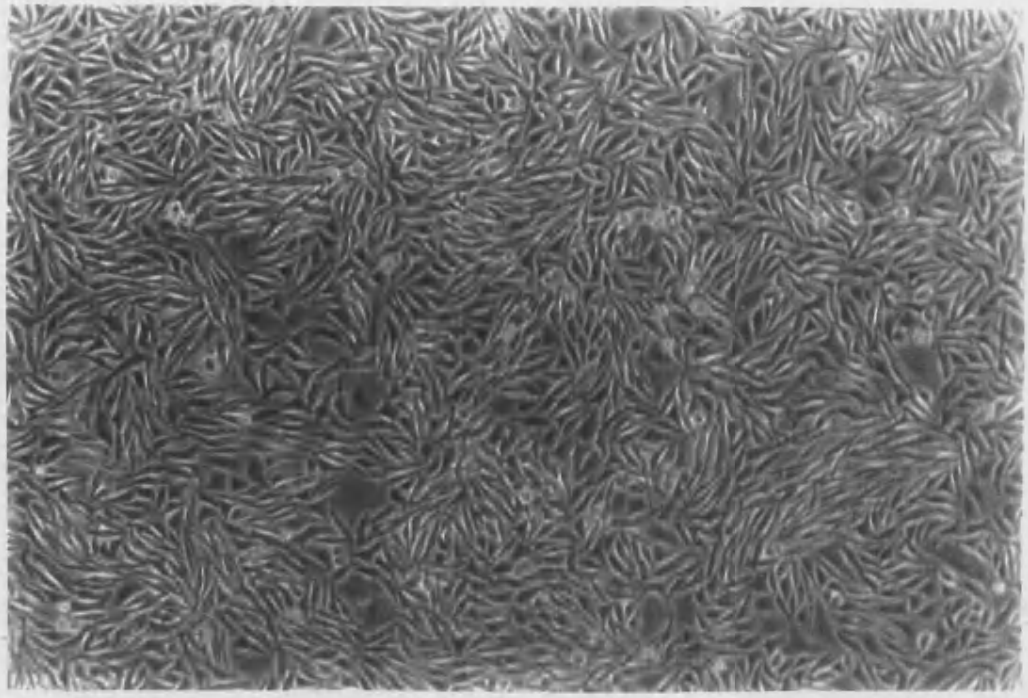

B

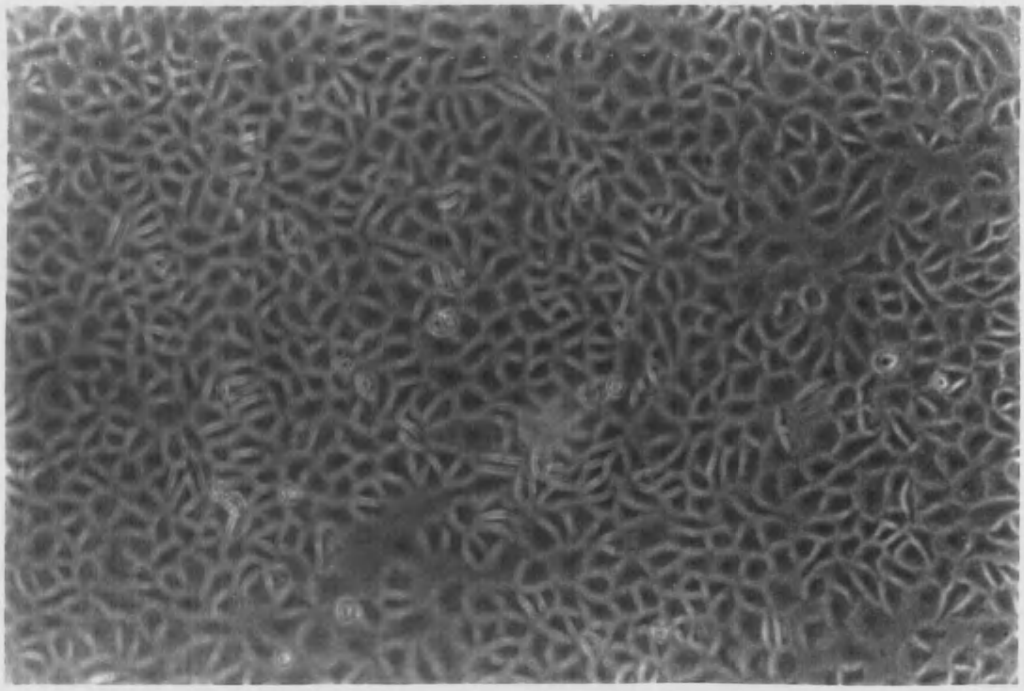

Fig. 2.1 Light photomicrographs of M10 cells showing the morphology before (A) and after (B) induction with 1μM dexamethasone. (Viewed at x100 magnification.)

3 CHARACTERISATION OF THE α4ß2 nAChR SUBTYPE

3.1 INTRODUCTION

Models of nAChR function rely on data garnered from the more accessible, hence more readily studied, muscle-type receptors. One of the more notable features of such models is the conformational switch nAChR undergo in the presence of agonists, and to some extent antagonists (see section 1.3.1). Briefly, the receptors shift from a "resting" (R) state, in which the affinity for ACh - the endogenous agonist - has been measured in the micromolar range, to a "desensitised" (D) state. This switch proceeds via a transitory "active" (A) conformation in which the channel is open. The D state is non-functional, and able to bind agonists with higher (nanomolar) affinity. It is assumed that neuronal nAChR also broadly follow this scheme (see section 1.3.2). However, each subtype appears to possess a distinctive pharmacological "fingerprint", as reflected in expression studies in Xenopus oocytes for example.

The main aim in this section of the project was to investigate the pharmacology of a defined receptor subtype - the avian α4ß2 nAChR - stably expressed in a mammalian cell line. (-)Nicotine, ACh, cytisine and (+)anatoxin-a ((+)AnTX) were chosen as representative agonists. The cell line allowed examination of the interaction of the agonists with both the R and D states of the receptor with only minimal differences in tissue preparation and reaction conditions between protocols (see sections 2.2.2.5 and

2.2.2.4.2 respectively). Agonist affinities for the R conformation were measured by their ability to elicit ^{86}Rubidium^{+} influx into the cells (see section 3.3.3). For the D state, agonist affinity was assayed by competition for equilibrium binding of [^{3}H]cytisine (see section 3.3.2.4).

Before the results are presented, brief backgrounds to both the α4ß2 nAChR subtype, and the M10 transfected cell line will be given (see sections 3.1.1 and 3.1.2 respectively). In addition, the literature relating to the chosen agonists will be reviewed (see section 3.1.3).

3.1.1 Properties of the α4ß2 nAChR subtype

The predominant nAChR immunoaffinity purified from brain was shown by amino-terminal sequence determination to be composed of subunits corresponding to α4 and ß2 (Whiting et al., 1987; Schoepfer et al., 1988). Studies of mRNA levels confirmed that α4 was the most widely expressed of the nicotinic α genes in the brain, whilst ß2 was shown to be present in all regions examined (Wada et al., 1989). Coexpression in Xenopus oocytes confirmed that this combination of subunits was indeed capable of forming functional ligand-gated ion channels (Bertrand et al., 1990). It should be noted that the rat α4 clone has been shown to give rise to electrophysiological responses when injected alone, though these were comparatively uncommon and very weak (Boulter et al., 1987). This has not been so for rat ß2 (Deneris et al., 1988), or the equivalent avian

subunits (Ballivet et al., 1988; Bertrand et al., 1990).

The rat α4 gene may be differentially spliced, giving rise to two alternative products. These proteins, α4-1 and α4-2 differing only at their carboxy-termini (Goldman et al., 1987), appear to show little difference in their distribution (Wada et al., 1989), or functional properties as observed in Xenopus oocytes (Connolly et al., 1992).

The α4ß2 subtype appears to be the major component of the high affinity agonist binding sites in the brain. The regions in which α4 and ß2 are coexpressed coincide with those in which high affinity radiolabelled agonist binding has been observed (reviewed in Deneris et al., 1991). Receptors immunoaffinity purified from chick brain using antibodies raised to Electrophorus, bound [^{3}H]nicotine with nanomolar affinity (Whiting & Lindstrom, 1986, 1987; see also section 3.2) and were found to contain the α4 subunit (Whiting et al., 1987). Similarly, [^{3}H]ACh binding to purified nAChR was almost totally depleted by preincubation with an anti-α4 monoclonal antibody (Nakayama et al. 1991). Receptors labelled with a variety of tritiated agonists were precipitated from a brain extract by antisera to both α4 and ß2, though analogous antisera against α2, α3, α5 and ß4 had no effect (Flores et al., 1991). The inactivity of the antiserum raised against α5 is of particular note; a recent report (Conroy et al., 1992) has suggested that α5 can coassemble with α4 and ß2 subunits. However, the relatively low abundance of α5 within the CNS (Wada et al., 1990) implies that, even if all α5 subunits were present

with α4 and ß2 , this would only represent a very small proportion of the α4ß2 receptor population.

3.1.2 The transfected M10 cell line

The M10 cell line stably transfected with chick α4 and ß2 subunits expresses surface nAChRs when induced by dexamethasone. It thus provides a model system in which the biochemical, pharmacological and electrophysiological properties of this subtype may all be studied. The construction and preliminary characterisation as reported by Whiting et al. (1991) are summarised here.

The cDNA clones encoding the chicken α4 and ß2 subunits (pCh26.1 and pCh23.1 respectively) were engineered to remove untranslated 5' and 3' regions, then cloned into a pMSG derived expression vector additionally including a neomycin resistance gene (see Fig 3.1). The subunits were cloned into separate constructs at the EcoR1 site, then cotransfected into mouse Ltk^- cell. Levels of nAChR expression, as measured by [^{3}H]nicotine binding to solubilised and immunoimmobilised receptors (protocol analogous to that in section 2.2.2.4.1), was found to increase rapidly for 3 days after induction with dexamethasone, then stabilise.

[^{3}H]Nicotine binding to immunoimmobilised cells was shown to be saturable, and to display an affinity similar to that of α4ß2 prepared from chicken brain (Kd = 3.2 ± 1nM compared to 3.6 ± 0.3nM respectively). Binding was

displaced from both M10 and chicken brain receptors by cholinergic agonists and antagonists with similar Ki values (see Table 3.1).

Table 3.1 Inhibition of [^{3}H]nicotine binding to α4ß2 nAChR purified from M10 cells and chicken brain (Whiting et al., 1991)

Agonists and Antagonists	Ki	
	α4ß2 from M10 cells	α4ß2 from chicken brain
Cytisine	0.14 ± 0.03nM	0.14 ± 0.04nM
(-)Nicotine	3.9 ± 2.1nM	2.4 ± 0.5nM
Carbachol	0.36 ± .13μM	0.45 ± 0.12μM
d-Tubocurarine	25 ± 14μM	7.7 ± 1.5μM
Hexamethonium	0.30 ± 0.06mM	0.16 ± 0.05mM
Mecamylamine	>1mM	>1mM

Functional data from whole cell voltage clamp measurements showed the cell line to respond to ACh (30μM) and to display a characteristic biphasic desensitisation (see Fig 3.2A), which mirrors that observed for α4ß2 nAChR expressed in Xenopus oocytes (see Fig. 3.2B). These currents were not influenced by muscarinic agonists or antagonists, but were blocked by hexamethonium, d-tubocurarine and DHßE.

3.1.3 **The agonists**

The three dimensional conformations of the four chosen agonists - ACh, (-)nicotine, cytisine and (+)anatoxin-a - are shown in Fig. 3.3. Before moving to individual agonists, it may be of value to examine the strengths and weaknesses of the experimental systems commonly encountered in the literature. It is not the practical details of each that are important in this context, rather the constraints a given system places on the results it generates. It is vital that these considerations be borne in mind when examining the data which follow.

In the widest sense, it may be argued that binding studies are of only limited value in the study of neuronal nAChR. It is fair to say that high affinity agonist binding is only of relevance to the $\alpha 4\beta 2$ subtype (see section 3.1.1), and even then relates to the non-functional D conformation (see section 1.3). However, binding studies do provide valuable information regarding receptor density, in addition to insights into the mechanisms of receptor-ligand interactions.

Functional data - that is, relating to agonist affinity for the R state - must also be treated with caution. Two questions must always be borne in mind: what is the identity of the receptor subtype present, and does the experimental system used reflect physiological conditions? For example, the expression of nAChR subunit combinations in Xenopus oocytes has proved invaluable in

the delineation of the possible functional receptor subtypes. However, the properties of these subtypes may not be identical to those *in vivo*; the membrane environment may differ considerably to that of the native receptor, whilst any necessary post-translational modification may be performed incorrectly, or not at all. In addition, functional neuronal nAChR containing more than two different subunit types have yet to be demonstrated in the *Xenopus* oocyte expression system, even though recent evidence suggests that such receptors occur *in vivo* (Conroy *et al.*, 1992; see section 3.1.1). Such considerations do not apply to preparations of neuronal tissue, such as brain slices or synaptosomes. In essence the latter are isolated, though still functional, nerve terminals, and have proved useful in the investigation of neuronal nAChR. However, overlapping subunit distributions within the brain often leads to heterogeneous receptor populations in both forms of tissue preparation; subsequent difficulties may arise in subtype identification. This potential heterogeneity may also be true of tumour-derived cell lines; the extensively used PC12 cell line has been found to contain mRNA encoding no less than 6 different nAChR subunits for example (see section 1.3.2).

3.1.3.1 Acetylcholine and (-)Nicotine

In essence, these agonists define this subclass of ligand-gated ion channels. So, whilst ACh is the endogenous ligand of all cholinergic receptors, it is the rapid

response to (-)nicotine which distinguishes the ionophores - the nAChR - from their G-protein coupled counterparts, the muscarinic receptors. Thus it seems appropriate to review the actions of these two molecules together.

It is well established that (-)[^{3}H]nicotine and [^{3}H]ACh label the same site in rodent brain (Marks et al., 1986; Martino-Barrows & Kellar, 1987), and that this site has subsequently been shown to be the α4ß2 nAChR subtype (see section 3.1.1). However, a difference between the two agonists in binding affinity is evident. Kd values for (-)-[^{3}H]nicotine have been variously reported to be between 2 and 20nM (Wonnacott, 1987), varying little over a range of species; thus, those in rat (9.3nM; Macallan et al., 1988), mouse (6nM; Grady et al., 1992) and chicken (4nM; Whiting & Lindstrom, 1987) all fall within a similar range. This high binding affinity appears enantiomer specific. In a series of studies, (+)nicotine displaced (-)[^{3}H]nicotine from brain membranes with between 17 and 180 times less potency than did the unlabelled (-)enantiomer (Wonnacott, 1987). (Thus, the use of racemic [^{3}H]nicotine in earlier studies yielded rather lower binding affinities than those quoted above; for example, Romano & Goldstein (1980), using rat membranes, reported a Kd value of 40nM.)

The affinity of ACh for the α4ß2 receptor subtype may be somewhat lower than that of (-)nicotine. Direct comparisons are few (Martino-Barrows & Kellar, (1987) reported Kd values of 3.5nM and 11nM for (-)[^{3}H]nicotine and [^{3}H]ACh binding to rat cortical membranes respectively),

though many workers have reported ACh to be some 1.5 to 8 times less potent in competing for (-)[^{3}H]nicotine binding sites than unlabelled nicotine (Wonnacott, 1987).

In light of the foregoing difference in binding affinity to the D state, functional data suggest both agonists to have a similar affinity for the R state of the α4ß2 subtype. Expression studies in Xenopus oocytes rate them as equipotent at this subtype (though not at others, see Table 3.3). Interestingly, Rapier et al. (1990) also implied that the two agonists were of equivalent potency; when applied at the same concentration, both elicited similar profiles of [^{3}H]dopamine release from rat striatal synaptosomes. Grady et al. (1992) using a similar experimental approach with mouse tissue, recently reported similar EC_{50} values for (-)nicotine and ACh (480nM and 341nM respectively). Though further confirming the similarity in potency of the two agonists at this subtype, it should be noted that the values themselves are an order of magnitude higher than that previously published by Rapier and her colleagues (3.8μM; Rapier et al., 1988)

Aside from the expression studies, data relating to other receptor subtypes is scarce. However where they do exist, they prove to be as consistent as those for the α4ß2 nAChR. Several studies have used PC12 cells, estimating the agonist affinity of the dominant receptor subtype, which may be α3ß4 (but see section 1.3.2). Lukas (1989) measuring agonist-induced ^{86}Rubidium efflux from pre-loaded cells, estimated EC_{50} values of 20μM and 40μM for (-)nicotine and

ACh respectively. As with the α4ß2 nAChR subtype, the oocyte studies have suggested that the two agonists have a similar potency at this receptor (see Table 3.2).

Table 3.3 ACh and (-)nicotine responses of neuronal nAChR as expressed in Xenopus oocytes.

nAChR subtype	ACh EC_{50} values (μM)	Relative nicotine potency (ACh = 1)
α2ß2	-	0.2[e]
α2ß4	-	0.4[e]
α3ß2	5.6[a] (354[b])	17[e]
α3ß4	158[a] (30[b])	1[e]
α4ß2	0.77[a,c]	1[c,e]
α4ß4	4.8[a]	0.3[e]
α7	115[d] (320[f])	≈0.2[d]

References: a - Couturier et al., 1990a (chicken)

b - Cachelin & Jaggi, 1991 (rat)

c - Bertrand et al., 1990 (chicken)

d - Couturier et al., 1990b (chicken)

e - Leutje & Patrick, 1991 (rat)

f - Amar et al., 1993 (chicken)

Unfortunately, the two EC_{50} values given are wildly disparate, though at least that of Cachelin & Jaggi (1991) resembles the PC12 value. Daly et al. (1991) reported an EC_{50} of 35μM for (-)nicotine, using a ^{22}Sodium influx protocol, adding further weight to the identification of α3ß4 as the main PC12 nAChR.

3.3.1.2 Cytisine

Cytisine is a rigid nicotinic agonist found in a number of plants of the leguminosae family. Immunoprecipitation studies have shown [^{3}H]cytisine to label α4ß2 nAChR (Flores et al., 1991). Furthermore, binding studies have suggested it to have a higher affinity for this subtype than [^{3}H]nicotine, displacing the latter from brain tissue with affinities ranging between 0.3 and 14nM (reviewed in Wonnacott, 1987). Recently, Pabreza et al. (1991) showed [^{3}H]cytisine to label a single class of sites with a Kd of less than 1nM. This binding was displaced by (-)nicotine, though with an affinity less than that of unlabelled cytisine (IC_{50} values of 8.9nM and 1.2nM, respectively).

How this difference in binding affinity between cytisine and nicotine relates to functional data is less clear. A recent report by Grady et al. (1992) showed cytisine and nicotine to be equipotent in eliciting [^{3}H]dopamine release from mouse striatal synaptosomes, confirming an earlier observation by Rapier et al. (1990). Conversely, Marks et al. (1993) have reported cytisine to

be very poor at inducing ^{86}Rubidium release from mouse striatal synaptosomes; the affinity was low, and the magnitude of the induced response did not match that generated by other agonists. They concluded that cytisine was a "partial agonist". Similarly, cytisine appeared to have only low potency at nAChR subtypes which included the ß2 subunit when expressed in Xenopus oocytes; the α4ß2 subtype was reported to have a 30 fold preference for nicotine (Leutje & Patrick, 1991). These data also have echoes in behavioural studies; Reavill et al. (1990) showed cytisine to be a less potent agonist than nicotine in some behavioural tests, an observation which could not be accounted for simply by differences in their pharmacokinetics. An interaction with several nAChR subtypes, or differential effects on a single subtype, were suggested to be responsible.

3.3.1.3 (+)Anatoxin-a

(+)Anatoxin-a (AnTX), derived from a freshwater alga, is a potent agonist of muscle nAChR. Functional responses were elicited at (+)AnTX concentrations between 20 and 200nM, making it almost an order of magnitude more potent than ACh (Swanson et al., 1986). Unlike most other agonists however, there is only a modest increase in affinity for (+)AnTX during the conformational shift of the receptor from the R to the D state (see section 3.3.1). Thus, in competition binding assays, (+)AnTX was found to be only some 3 fold more potent in displacing [^{125}I]α-BgTX

than ACh (Swanson et al., 1986). The receptor also demonstrated a marked stereoselectivity for the (+)enantiomer; (-)AnTX had a 500 lower affinity than (+)AnTX in the previous assay. At high, micromolar, concentrations both AnTX enantiomers behave as channel blockers at the neuromuscular junction (Kofuji et al., 1990).

AnTX also appears to be an agonist of the neuronal nAChR, though the data are less complete, and relate to a number of subtypes. The nAChR of PC12 cells (see section 1.3.2) have been shown to respond to AnTX; the reported affinity was comparatively low (IC_{50} = 4.5μM), though the racemic agonist was used (Daly et el., 1991).In competition studies (+)AnTX displaced both [^{3}H]ACh (Zhang et., 1987) and [^{3}H]nicotine (Macallan et al., 1988) from rat brain preparations with nanomolar affinities (4.5nM and 0.34nM respectively), suggesting interaction with the α4ß2 subtype. (-)AnTX was even less potent, comparatively, than at the muscle-type receptor (Ki = 0.39μM; Macallan et al., 1988). In addition, (+)AnTX was observed to cause an upregulation of [^{3}H]nicotine binding sites (Rowell & Wonnacott, 1990). Interestingly, the concentration of AnTX was 60 fold below that of (-)nicotine required to induce a similar effect. Behaviourally, Stolerman et al. (1992) have recently shown (+)AnTX to produce similar, but not identical, effects to (-)nicotine.

The α7 (α-BgTX binding) neuronal receptor subtype appears to be less sensitive to (+)AnTX than α4ß2, though

it still displays stereoselectivity (for [^{125}I]α-BgTX binding to rat brain, (+)AnTX Ki = 91nM; (-)AnTX, Ki = 21μM; Macallan et al., 1988). Primary cultures of hippocampal neurons (which probably express α7 subunits) respond functionally to (+)AnTX (EC_{50} = 3μM), where it was found to be 10 fold more potent than ACh (Alkondon et al., 1992).

3.2 RESULTS

3.3.2 Equilibrium binding studies

To measure the characteristic high affinity agonist binding of the transfected M10 cell α4ß2 nAChR (see section 3.1.1), a variety of practical techniques were tried and evaluated. Each will be described in turn, with brief practical notes where necessary, with examples of the data each generated.

3.3.2.1 High affinity [^{3}H]nicotine binding to immunoimmobilised M10 nAChR

In the preliminary characterisation of the M10 cell line, α4ß2 nAChR were solubilised, immunoaffinity immobilised, and the [^{3}H]nicotine binding parameters determined (see section 3.1.2). Following a similar protocol to that of Whiting et al. (1991; see section 2.2.2.4.1), non-specific binding, defined as that to the Sepharose-GART only, was very low (see Fig. 3.4A); Scatchard analysis and iterative curve fitting gave a single class of sites, Kd = 2.9 ± 0.1nM (mean ± range, n=2, see Fig. 3.4B). As the assays used aliquots derived from

several "pooled" plates of cells, the derived Bmax values reflect only indirectly the density of [^{3}H]nicotine binding sites (hence receptors) per cell.

3.3.2.2 High affinity [^{3}H]nicotine binding to M10 cell detergent extracts

M10 cells were extracted with Triton X-100, and assayed for [^{3}H]nicotine binding, following a modification of the protocol used routinely for rat brain membranes (see section 2.2.1.2). Briefly, confluent cells (4x10cm plates) were scraped into PBS containing protease inhibitors (5mM EDTA, 5mM EGTA, 0.1mM benzethonium chloride, 2mM benzamide and 0.1mM PMSF). The cells were pelleted by centrifugation (1000xg, 2 minutes), then resuspended in 0.7ml Krebs-HEPES-TRIS containing 0.5% (v/v) Triton X-100 and protease inhibitors as above. After continuous agitation for 1 hour at 4°C, the suspension was centrifuged at 100,000xg for 45 minutes. The supernatant was then further diluted 1 in 5 (to reduce any possible inhibition of radioligand binding by the detergent; see section 4.2.1.3.1), and assayed for [^{3}H]nicotine binding.

Initial assays demonstrated the presence of high affinity [^{3}H]nicotine binding sites within the supernatant (see Fig. 3.5). Based on the average levels of radioligand binding and estimations of the cell numbers used in each assay, it was possible to calculate an approximate number of [^{3}H]nicotine binding sites per cell. Assuming there to be two agonist sites per receptor, 18700±4500 (mean±SEM; n=3)

α4ß2 nAChR per cell were estimated to be present. However, this value is likely to be an underestimate; receptor recovery during the extraction process is unlikely to be 100%. Further experiments to define the binding parameters of the nAChR in this preparation proved inexplicably difficult; in all cases (n=3) levels of specific [^{3}H]nicotine binding was too low to analyse.

3.3.2.3 High affinity [^{3}H]nicotine binding to M10 cell membrane preparations

Membrane preparations were produced by a modification of the protocol used previously for the immunoaffinity immobilisation of the receptor (see section 2.2.2.4.1). Hence, M10 cells were scraped into solublisation buffer including protease inhibitors (1ml/35mm plate), but lacking Triton X-100. The cells were pelleted, then washed with 2x1ml PBS by centrifugation and resuspension. Each pellet was incubated in 500µl Krebs-HEPES-TRIS, containing [^{3}H]nicotine (final concentration 20nM), then washed with 3x1ml PBS. Pellets were then dissolved in 175µl Soluene and transferred to 5ml Optiphase for scintillation counting.

A large amount of specific [^{3}H]nicotine binding to each pellet was observed, though there was considerable variation between replicate samples (see Fig. 3.6). This was probably due to the compaction of the pellet and incomplete resuspension during incubation with the radioligand and subsequent washes. Therefore, a further

variation in the assay procedure was investigated.

3.3.2.4 High affinity agonist binding to intact M10 cell monolayers

Radioligand binding to monolayers of intact, confluent M10 cells was assayed by incubation with Krebs-HEPES-TRIS containing either [^{3}H]nicotine (final concentration 20nM) or [^{3}H]cytisine (final concentration 4nM) in the absence and presence of excess unlabelled (-) nicotine followed by rapid washing with PBS (see section 2.2.2.4.2). Whilst initial assays suggested this method yielded consistent and highly reproducible data between wells, there appeared to be a larger number of [^{3}H]nicotine than [^{3}H]cytisine binding sites. This was a curious observation; cell numbers were identical in each case, and both the [^{3}H]nicotine and [^{3}H]cytisine concentrations used were considered to be saturating at this cell type (see section 3.1.2). In addition, when previously uninduced M10 cells were assayed, they too seemed to have specific radioligand binding sites. Once again, more [^{3}H]nicotine sites than [^{3}H]cytisine sites were detected (19.2fmol/10^6 cells compared with 1.2fmol/10^6 cells; see Fig. 3.7).

The use of the immunoimmobilisation assay (see section 3.3.2.1) showed that there was no α4ß2 nAChR-attributable high affinity radioligand binding in M10 cells prior to treatment with dexamethasome (see Fig. 3.8), confirming the earlier observation of Whiting et al. (1991; see section 3.1.3). Thus, the source of any specific

radioligand binding to uninduced cells was something of a mystery. However a clue probably lies in the relative levels of [^{3}H]nicotine and [^{3}H]cytisine binding. During their prolonged exposure (90 minutes) to the radioligands, some passive movement into the cell might be expected. (-)-Nicotine is more lipophilic than cytisine, thus one would predict a faster rate of diffusion into the cell plasma membranes. Subsequently, higher levels of [^{3}H]nicotine would enter the cells, and be retained during the washes and counted. The apparent "specific" nature of the labelling is probably due to the method used to define the non-specific binding. Non-specific radioligand binding is that observed in the presence of a large excess of the unlabelled ligand. In such circumstances, the rate of passive diffusion of nicotine or cytisine into the cells may actually increase (as one would assume any passive mechanism to be concentration dependent). However, only a fraction of the agonist now entering the cells would be radiolabelled (unlike in measurements of "total" binding, where only radiolabelled ligand is present). Thus, a difference in "total" and "non-specific" binding is observed in the absence of α4ß2 nAChR.

Recently, it was reported that some non-neuronal cell lines, including mouse fibroblasts, displayed specific [^{125}I]α-BgTX binding (Chini et al., 1992). It was suggested that such binding was linked to the expression of the α5 nAChR subunit. To test for the presence of such subunits in the M10 cell line, [^{125}I]α-BgTX (final

concentration 1nM) binding to intact, uninduced cells was measured. No specific binding was observed on both occasions that the assay was performed (see Fig. 3.7).

Cytisine has been reported to have a higher affinity for the D-state α4ß2 nAChR (see section 3.1.1.2). This, and the small amount of non-nAChR mediated "specific" [^{3}H]cytisine binding noted above, made it the obvious radioligand for use in the further characterisation of this protocol. The monolayer binding protocol was used for this and all subsequent assays. Saturation binding revealed a single population of sites: Kd = 3nM, Bmax = 72fmol/10^6 cells (n=2; see Fig. 3.9). This Bmax value is equivalent to approximately 22000 nAChR per cell, assuming two [^{3}H]nicotine binding sites per receptor. However, this value represents only those nAChRs on the upper face of the cell monolayer and thus readily accessible to the radioligand; any receptors on the lower surface (ie in contact with the culture dish), or inside the cells, will not be labelled.

This technique was further adapted to measure the affinity of the four chosen agonists for the D-state of the α4ß2 nAChR, as assessed by their ability to displace [^{3}H]cytisine binding in competition assays. The resultant curves are shown in Fig. 3.10, whilst the derived assay parameters are summarised in Table 3.3.

Table 3.3 Agonist competition of high affinity [^{3}H]cytisine binding to intact M10 cells.

Agonist	Ki (nM)	Hill number
ACh	6.9±2.3	0.39
(-)Nicotine	3.2±1.2	0.78
Cytisine	1.4±0.9	0.72
(+)Anatoxin-a	2.7±0.6	0.95

3.3.3 AGONIST-INDUCED ^{86}RUBIDUM$^+$ FLUX INTO M10 CELLS

The affinities of the four chosen agonists for the R-state of the α4ß2 nAChR were assessed by means of a ^{86}Rubidium ion flux assay. At activating concentrations of agonist, ligand binding results in a change of conformation in the receptor protein. The nAChR transiently passes through an "active" state in which its intrinsic cation channel is open - thus permitting ion translocation across the plasma membrane - before reaching an inactive, desensitised conformation (see section 1.3). This allosteric modulation of cell permeability forms the basis of the ion flux assay. Briefly, confluent monolayers of M10 cells were incubated in the absence and presence of increasing concentrations of each agonist for one minute (see section 2.2.2.5). The replacement of the sodium ions in the incubation medium by ^{86}Rubidium$^+$, allowed direct measurement of the active state of the α4ß2 nAChR.

The protocol of McGee & Liepe (1984) was found to produce adequate results without any fundamental modification. The resultant dose-response curves were bell shaped for all four agonists (see Figs. 3.11 and 3.12). This observation may be indicative of rapid receptor inactivation at higher agonist concentrations. The rate and extent of agonist-induced receptor desensitisation is dependent upon agonist concentration (Changeux, 1990). In the flux assays described here, induced M10 cells were exposed to ^{86}Rubidium^{+} and the chosen agonist for a uniform period (1 minute), regardless of the concentration of the latter. Thus, if the mean open time of the transfected $\alpha 4\beta 2$ nAChR ion channels was reduced - and the interval between channel openings increased - by high agonist concentrations, a reduced ion uptake would be observed.

The slopes of the dose-response curves were usually steep, both in the rising and falling phases. Whilst this was the case for all of the agonists, it was especially notable for AnTX. As a result, EC_{50} values could not be calculated (there being only one, occasionally two, points between basal and maximal influx), but were estimated by eye. As a further consequence of this steepness in receptor response, minor variations in assay conditions led to shifts in the position in the peak response between experiments. This variability is illustrated in Fig. 3.11, which shows the four data sets generated for ACh-induced ^{86}Rubidium^{+} influx. Basal influx, that observed in the absence of any nicotinic agonist, was similar in all four

assays (4156, 3623, 3520 and 4578cpm/well). Peak height also showed little variability, being between 202-299% basal influx. (Peak responses most often fell into this range for all of the agonists assayed; exceptionally values as low as 185%, and as high as 600% were observed.) However, this peak response occurs between $1x10^{-6}$M and $1x10^{-5}$M. Thus when the data sets for each agonist were normalised, the overall dose-response curves are broader than those seen in individual assays (see Fig. 3.12). Derived EC_{50} values are summarised in Table 3.4.

Table 3.4 Agonist EC_{50} values in eliciting $^{86}Rb^{+}$ flux into M10 cells.

Agonist	EC_{50} (M)
ACh	$2.3 \pm 1.7x10^{-6}$ (n=4)
(-)Nicotine	$2.7 \pm 0.7x10^{-6}$ (n=5)
Cytisine	$3.7 \pm 1.1x10^{-6}$ (n=3)
(+)Anatoxin-a	$4.8 \pm 1.8x10^{-8}$ (n=4)

3.3.4 THE SUBUNIT STOICHIOMETRY OF THE AVIAN α4ß2 nAChR

SDS-PAGE and autoradiography of the [^{35}S]-methionine labelled, immunoaffinity purified nAChR from M10 cells, revealed two closely migrating doublets with apparent Mr 50,000 and 75,000 (see Fig. 3.13). These correspond to the expected sizes of α4 and ß2 subunits (Whiting et al.,

1987).

To determine the stoichiometry of receptor subunits, the bands were excised from the gel, solubilised and the radioactivity present quantified by liquid scintillation counting. With the inclusion of a correction factor to account for the dissimilarity in the numbers of methionine residues present in each subunit (α4 has 17 methionines; ß2, 13), the ratio α:ß was calculated to be 2:3.9 $\pm$ 0.2 (mean $\pm$ range, n=2). This is greater than the expected 2:3 (see section 1.1.1), though consistent with previous data from this cell line (Whiting et al., 1991), and may reflect the protocol adopted. The purification procedure was performed on whole cell detergent extracts using the antibody, mAb 295 (see section 2.2.2.1). Though raised against the whole receptor, mAb 295 is directed against the ß2 subunit. Thus, the isolation of subunits incorporated into partially assembled nAChRs may contribute to the ratios observed, as could the aberrant assembly of homooligomers, if it occurs.

Also of note was the consistent appearance of a receptor associated band in the immunopurified preparation, with an apparent Mr 43,000. This may be an unglycosylated subunit (Whiting et al., 1991), or possibly actin. However, the demonstration of the presence of the "43 kD protein" in mouse fibroblasts (Musil et al., 1989), and the close association of that protein with muscle-type nAChR (see Fig. 1.1A), may make this chance observation one of great interest.

3.4 DISCUSSION

The range of neuronal nAChR subunits thus far cloned implies the existence of multiple receptor subtypes. Whilst only partially characterised, the strong homology that neuronal subunits show with those of the muscle-type receptor suggests that the two groups share a common functional basis (see section 1.3.2). Muscle-type nAChRs are able to adopt several discrete conformational states, each of which has its own properties (see section 1.3.1). Whilst a spontaneous process, the interconversion of the receptor between these states may be modulated by a variety of small ligands; it is this which forms the basis of receptor function. Thus, when an agonist binds to the receptor, it promotes a conformational change which ultimately give rise to the desensitised state. As this shift from the R- to D-state proceeds, the nAChR may go through several transitory, intermediate states. In one of these (the A-state), the receptor's intrinsic cation channel is permeable.

The M10 cell line, expressing the transfected avian α4ß2 nAChR, has been used as a model system in the investigation of agonist potencies for this neuronal receptor subtype. The affinities of four representative agonists - ACh, (-)nicotine, cytisine and (+)anatoxin-a - for the R- and D-states of the receptor have been measured by means of a $^{86}Rubidium^{+}$ influx assay and high affinity binding studies respectively.

3.4.1 ACh and (-)nicotine

[^{3}H]Nicotine was used initially to monitor the expression of α4ß2 nAChR in the M10 cell line. Various techniques were used; whilst high-affinity binding was always detectable, it was not always possible to measure its parameters. The similarity between the [^{3}H]nicotine binding to immunoimmobilised receptors in this study and elsewhere has already been commented upon (see section 3.2.1.1). [^{3}H]Nicotine binding to the α4ß2 nAChR of intact M10 cells proved problemmatical. Large amounts of non-nAChR dependent specific binding was detected in uninduced cells (see section 3.2.1.4), and prevented the generation of any meaningful binding parameters from saturation assays (data not shown). This was not the case with [^{3}H]cytisine (see section 3.2.1.1), and may be related to the relative lipophilicity of the two radioligands. In competition studies against [^{3}H]cytisine, (-)nicotine has about a two-fold higher affinity than ACh, whilst both have a lower affinity than cytisine; this fits well with values cited in the literature (see section 3.1.1)

The affinities of ACh and (-)nicotine for the R-state, as measured in the ion flux assay, are very similar (see Table 3.4). As with the binding data, this corresponds well with the literature. In addition, the micromolar affinities are within the range of reported EC_{50} values from different experimental systems (see section 3.1.1). However, probably of greater significance is the difference in agonist affinity between the R- and D-state. Whilst the

α4ß2 nAChR has been assumed to undergo an increase in agonist affinty upon desensitisation, based upon analogy with the muscle-type receptors (see section 1.3.1), this study represents the first quantitative demonstration of this phenomenon in a single, model system.

3.4.2 **Cytisine**

In saturation binding studies to intact M10 cells, the Kd for [^{3}H]cytisine binding (3nM) was slightly higher than might have been predicted from Pabreza et al.(1991), who reported a value of less than 1nM. However, this may reflect a difference in the species from which the receptor was derived (chick versus rat), or in the assay techniques employed. In the competition binding assays, where a direct comparison of agonist affinities for the D-state were made, cytisine was found to have a higher affinity than (-)-nicotine. This difference was again lower than might have been predicted (for example, compare Table 3.1 with Table 3.3).

With regard to the functional assays, it is difficult to reconcile the data presented here with those from the literature for the action of cytisine at α4ß2 nAChR (see section 3.1.3.2). In the ion flux assays, the affinities of cytisine and (-)nicotine for the R-state were similar (see Table 3.4). More interestingly, the cytisine-induced ^{86}Rubidium$^+$ influxes were quantitatively indistinguishable from those produced by application of any of the other chosen agonists (see Fig. 3.11). The possible

molecular basis of the differences in cytisine efficacy reported here and in the literature are discussed in section 5.2.

3.4.3 **(+)Anatoxin-a**

(+)AnTX is an extremely potent agonist of the α4ß2 nAChR, with an affinity for the R-state some 50 fold higher than that of ACh and (-)nicotine (see Table 3.5). There is little in the literature relating to the potency of (+)AnTX at this nAChR subtype (see section 3.3.1.3), thus it is difficult to comment. The EC_{50} value reported here is within the range of concentrations which gave functional responses at muscle nAChR, though the relevance of this is questionable. The upregulation study of Rowell & Wonnacott (1990), which implied a 60 fold difference in the affinities of (+)AnTX and (-)nicotine, provides some indirect corroboration. Thomas et al. (1993) recently reported that (+)AnTX elicited [^{3}H]ACh release from rat hippocampal synaptosomes with an EC_{50} of $1.4x10^{-7}$M.

In competition binding studies using [^{3}H]cytisine and the M10 cells (see section 3.3.2.4), (+)AnTX was found to have an affinity greater than that of ACh and (-)-nicotine, but below that of cytisine (see Table 3.3). More interestingly, the increase in affinity associated the shift from the R- and D-states (see section 3.1) is very small; this again echoes the muscle-type nAChR data (see section 3.3.1.3). In addition, the Hill number for (+)AnTX competition was found to be higher than those of the other

agonists (see Table 3.3). Whilst the value was still below 1, the relative increase in steepness of the curve reflects that seen in the ion-flux assays; (+)AnTX-induced dose-response curves were notably steeper than those of other agonists.

The distinctive features evident in the interaction of (+)AnTX with α4ß2 nAChR - the small shift in agonist binding affinty with desensitisation, and the steep dose-response curves - may reflect a subtle variation in the mechanism of agonist-induced receptor activation. This is discussed further in section 5.2.

3.4.4 Summary

The interaction of the α4ß2 nAChR with agonists was investigated using the transfected M10 cell line as a model system. Of the four agonists used in this study, three - ACh, (-)nicotine and cytisine - were found to elicit functional responses in the ^{86}Rubidium^{+} influx assay when present in micromolar concentrations. The same agonists had nanomolar binding affinty in [^{3}H]cytisine competition assays. These data suggest that, like the muscle-type nAChR, the α4ß2 receptor subtype desensitises upon extended exposure to agonists, and that this is accompanied by an increase in agonist affinity. (+)AnTX proved to be exceptional in its potency in the functional assay system, yet displaced [^{3}H]cytisine with an affinty similar to the other agonists. This, and the steepness of the (+)AnTX-induced dose-response curves, points to a distinctive

mechanism of receptor activation by this agonist.

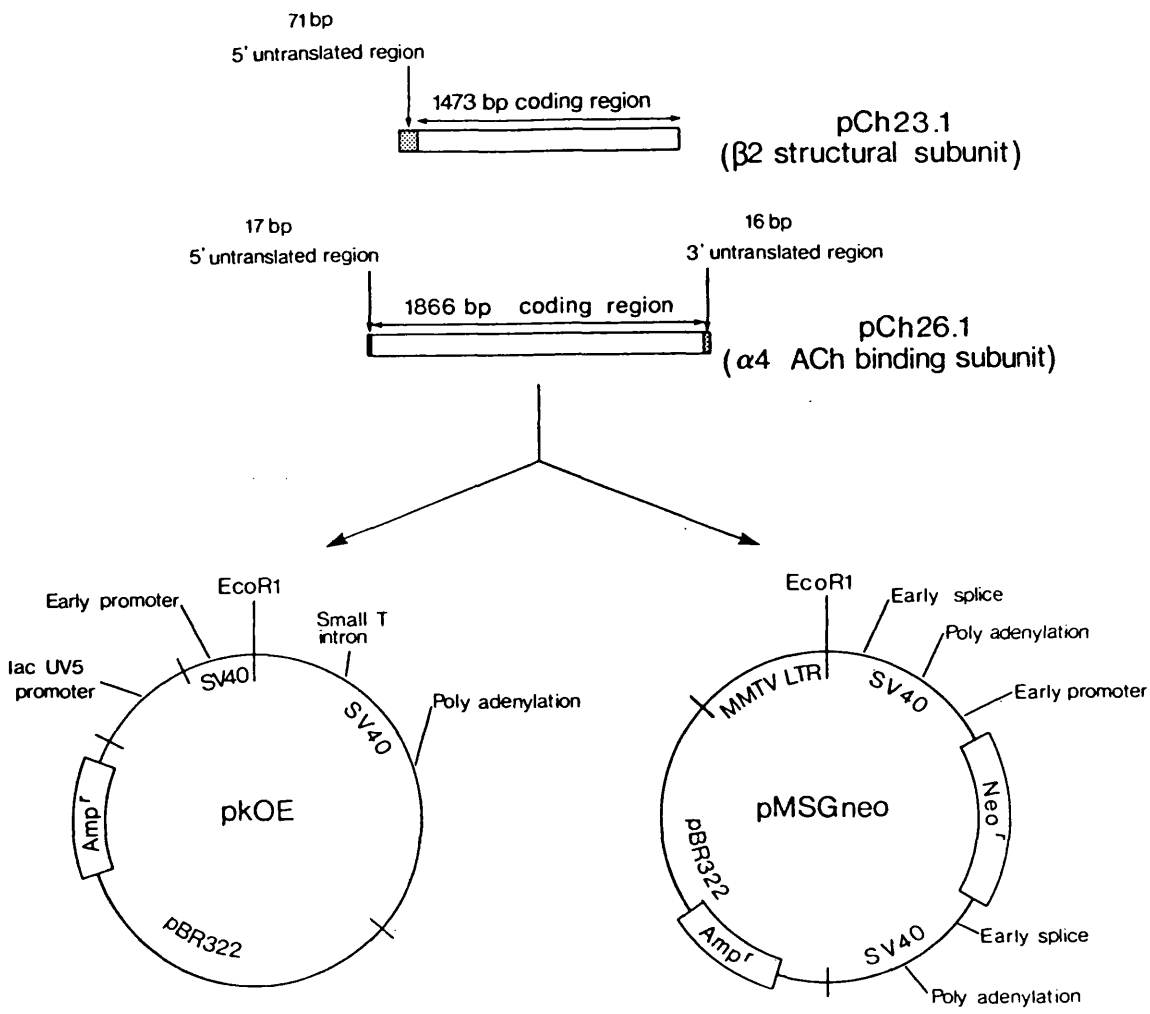

Fig. 3.1 **Transfection vectors used in the preparation of the M10 cell line** (from Whiting et al., 1991).

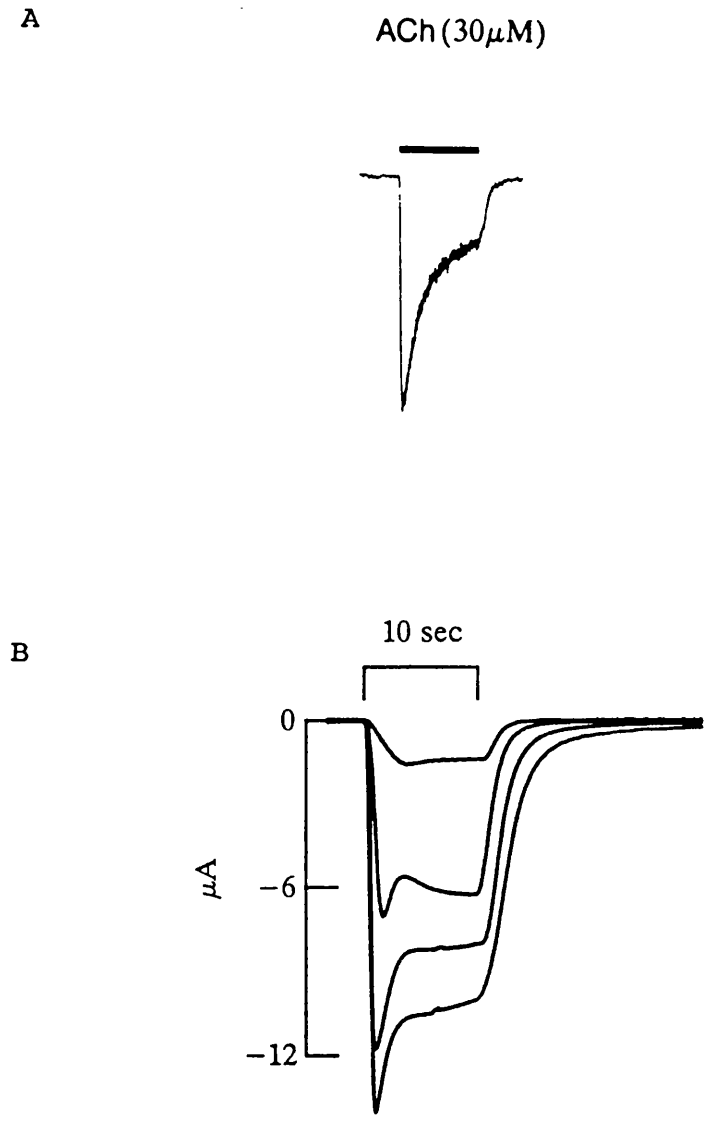

Fig. 3.2 **Comparison of agonist-induced whole cell current recordings from (A) induced M10 cells** (from Whiting et al., 1991) **and (B) Xenopus oocytes expressing chick α4ß2 nAChR** (from Bertrand et al., 1990).

Fig. 3.3 **Energy minimised structural models of (A) ACh, (B) (-)nicotine, (C) cytisine and (D) (+)anatoxin-a.** Structures were provided courtesy of P.Thomas, and were built using the HYPERCHEM modelling package (Autodesk Inc., California, U.S.A.). Individual atoms are represented as colour coded van der Waals spheres (white - hydrogen; pale blue - carbon; dark blue - nitrogen; red - oxygen).

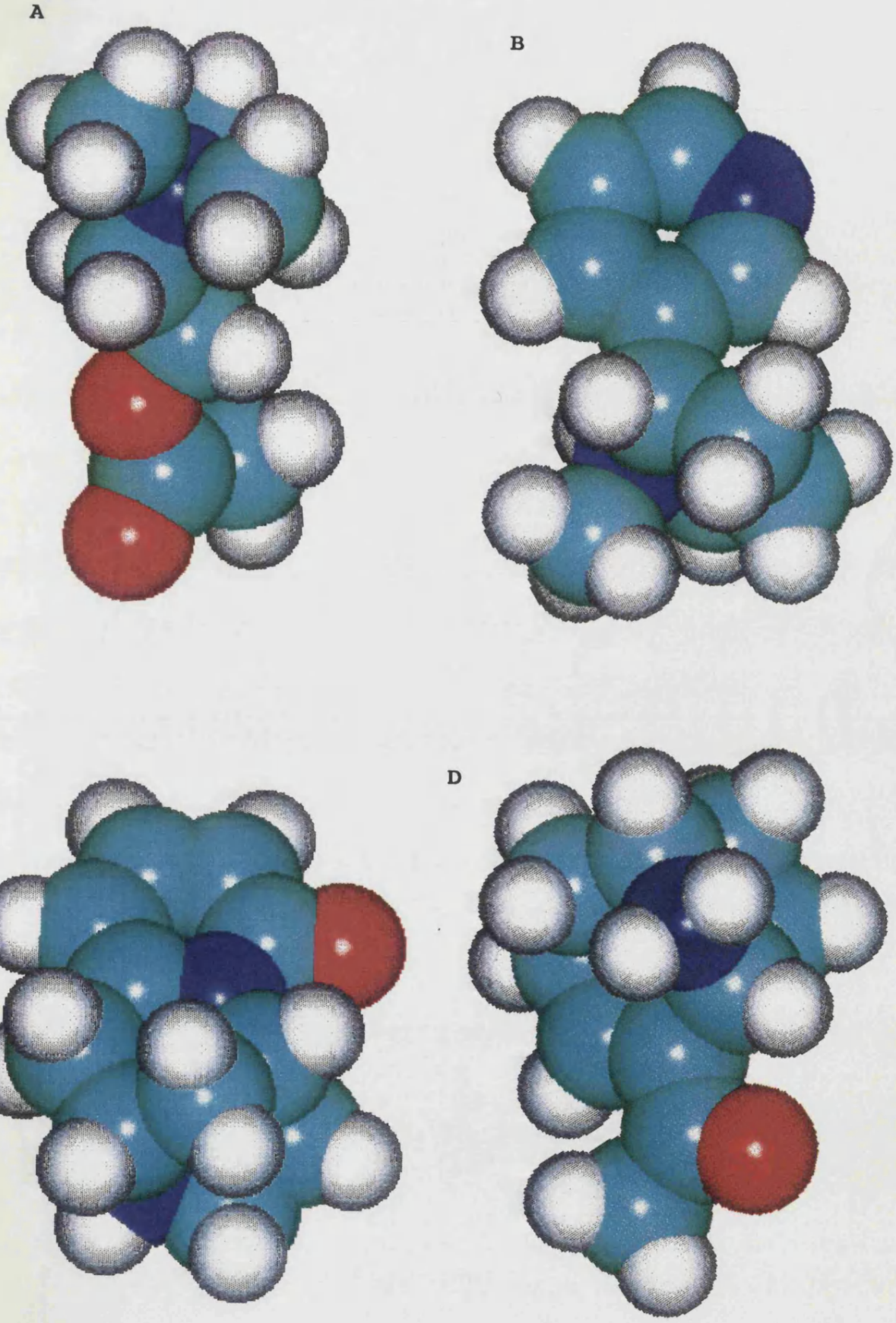
A
B
C
D

Fig. 3.4 **[^{3}H]Nicotine binding to immunoimmobilised α4ß2 nAChR from the transfected M10 cell line.** Confluent M10 cells were induced for 3 days with 1μM dexamethasome. After scraping, α4ß2 nAChR were solubilised in buffer containing Triton X-100 (1% v/v). Insoluble cell debris was removed by centrifugation, and the supernatant incubated with Sepharose-GART and mAb 290 (25μl and 0.25μl per 10cm dish respectively). The immunoimmobilised nAChR were washed by centrifugation and resuspension, then aliquoted. Aliquots were incubated with [^{3}H]nicotine (final concentration 1-20nM) to determine total binding (●). Non-specific binding (O) was taken as being that to Sepharose-GART only. Representative binding data (A) and Scatchard transformation (B) from a single experiment are shown. Each point represents the mean of duplicate samples (the standard deviation too small to show up). The Kd was calculated to be 3.0nM.

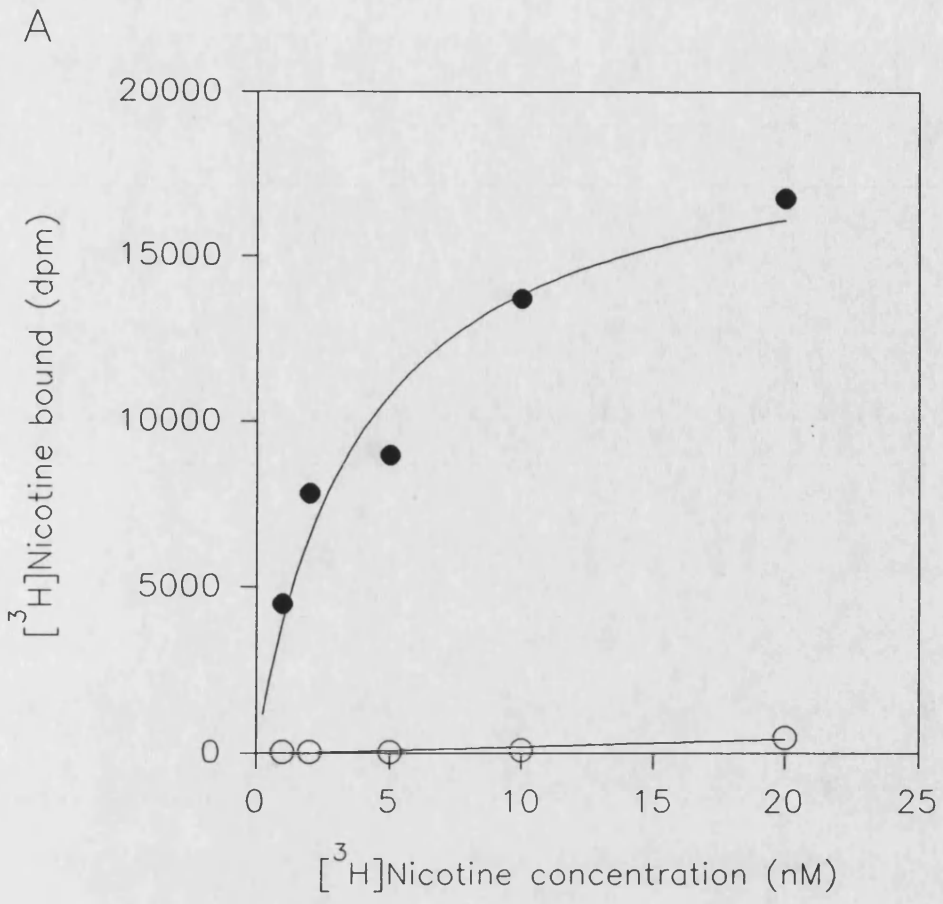
A
20000
15000
10000
5000
0
[3H]Nicotine bound (dpm)
0
5
10
15
20
25
[3H]Nicotine concentration (nM)

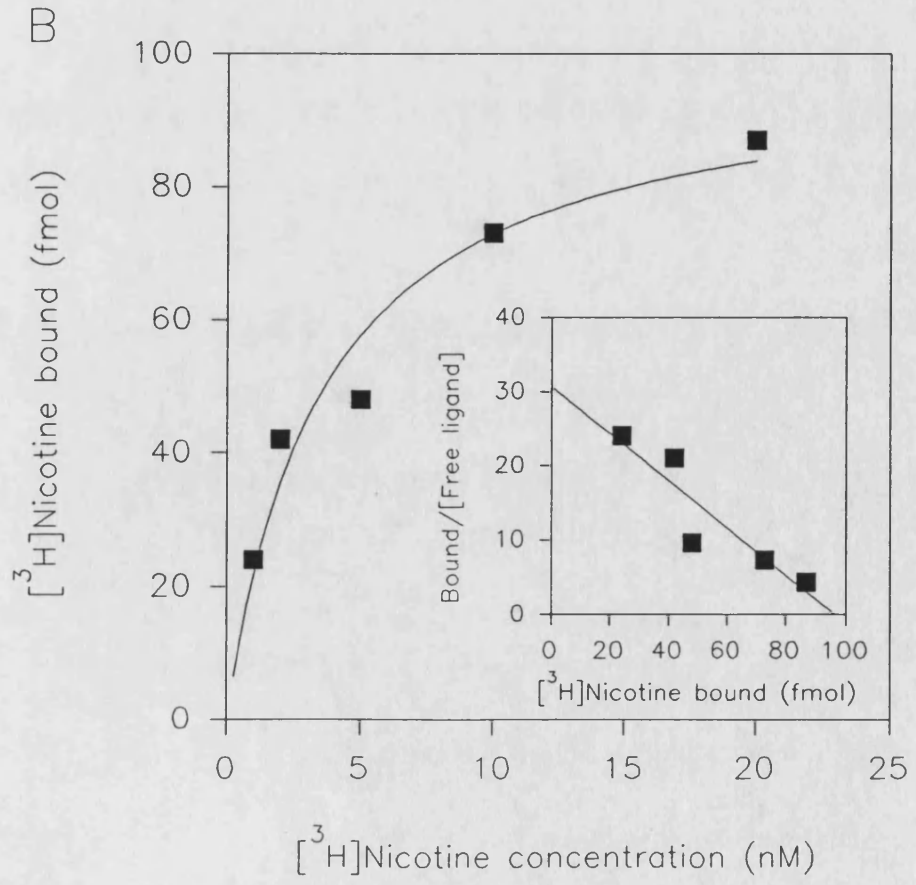
B
100
80
60
40
20
0
[3H]Nicotine bound (fmol)
0
5
10
15
20
25
[3H]Nicotine concentration (nM)
40
30
20
10
0
Bound/[Free ligand]
0
20
40
60
80
100
[3H]Nicotine bound (fmol)

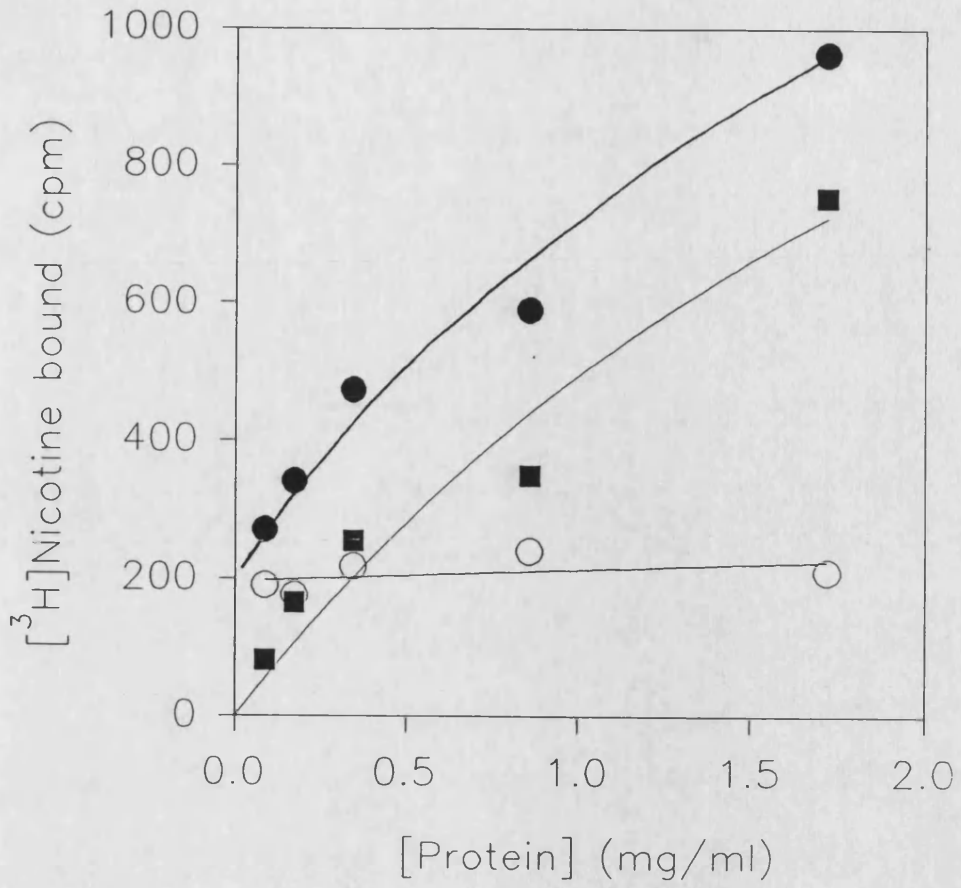

Fig. 3.5 **[^{3}H]Nicotine binding to Triton X-100 extracts of M10 cells.** Confluent M10 cells were scraped into PBS (3ml/100mm dish; $2x10^6$ cells) containing protease inhibitors, and pelleted. The cells were resuspended in Krebs-HEPES-TRIS containing 0.5% (v/v) Triton X-100. Insoluble cell debris was removed after 60 minutes by centrifugation, and the supernatant diluted 1 in 5 to reduce detergent concentration. Serially diluted samples were incubated with [^{3}H]nicotine (final concentration 20nM) in the absence and presence of excess unlabelled (-)-nicotine to determine total (●) and non-specific (○) binding respectively. Specific binding (■) was calculated as the difference between the two. Data from a single experiment are shown, each point being the mean of triplicate samples.

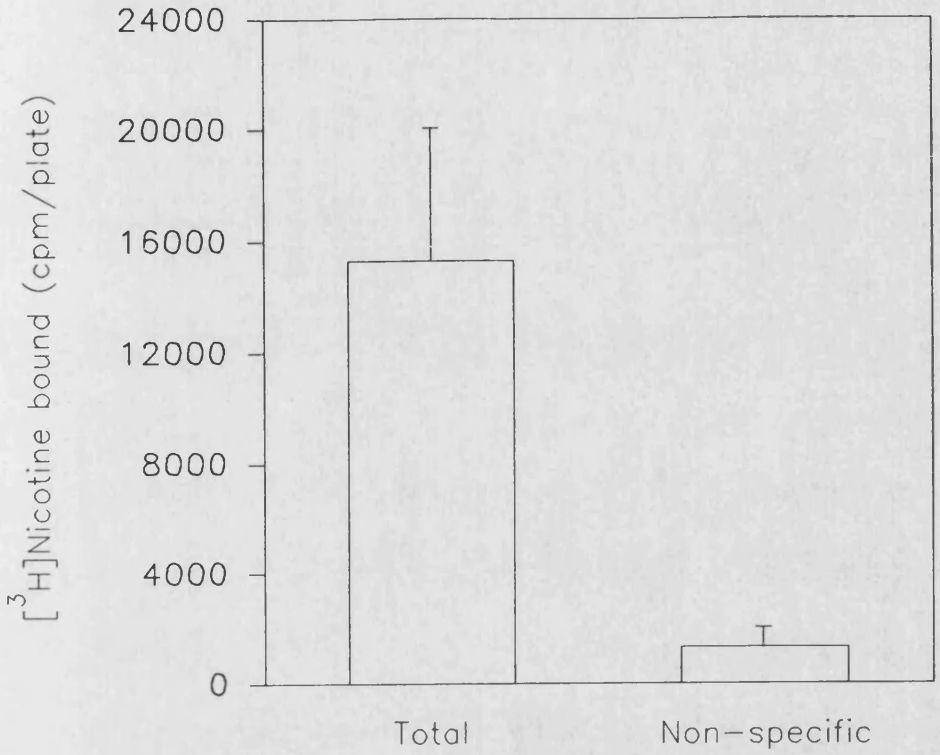

Fig. 3.6 **[^{3}H]Nicotine binding to M10 membrane preparations.** Confluent M10 cells were scraped into PBS (1ml/60mm dish; 6x10^5 cells) containing protease inhibitors, pelleted, and washed twice by centrifugation and resuspension. The membranes (500μl)were then incubated with 20nM [^{3}H]nicotine in either the absence or presence of excess (1mM) unlabelled (-)nicotine to determine total and non-specific radioligand binding. Data represent the mean ± SEM of three dishes for each condition.

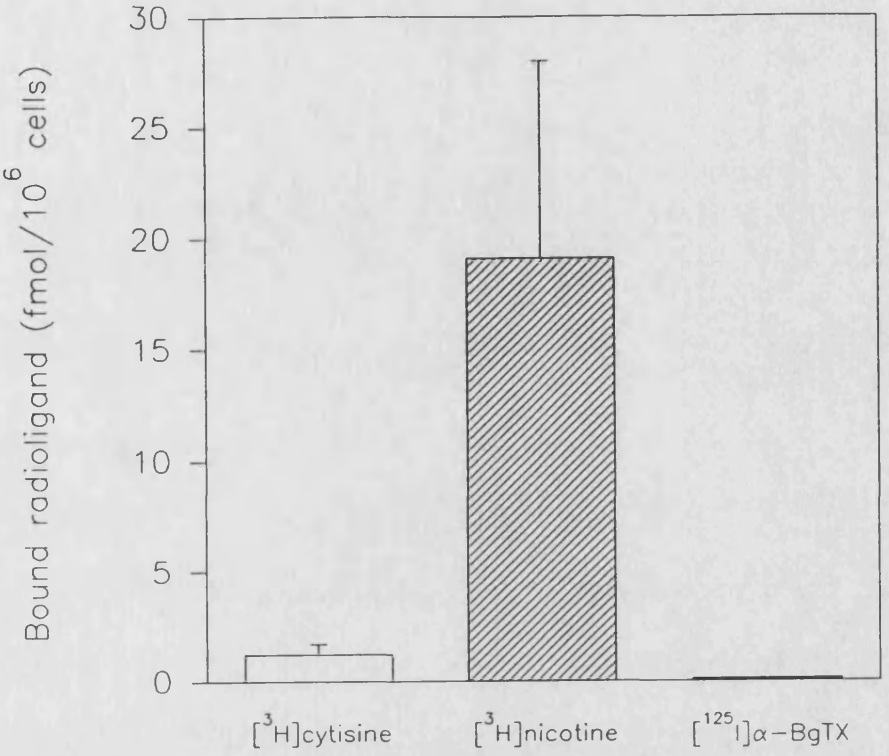

Fig. 3.7 **Radioligand binding to uninduced, intact M10 cells.** Confluent, but uninduced, M10 cell monolayers were incubated with [^{3}H]cytisine (final concentration 5nM), [^{3}H]nicotine (20nM) or [^{125}I]α-BgTX (1nM) for 90 minutes ([^{3}H]cytisine or [^{3}H]nicotine) or 180 minutes ([^{125}I]α-BgTX) in the absence or presence of excess unlabelled ligand to give total and non-specific radioligand binding respectively. Each column represents the mean ± SEM values of specific radioligand binding from four ([^{3}H]cytisine and [^{3}H]nicotine) or two ([^{125}I]α-BgTX) separate determinations.

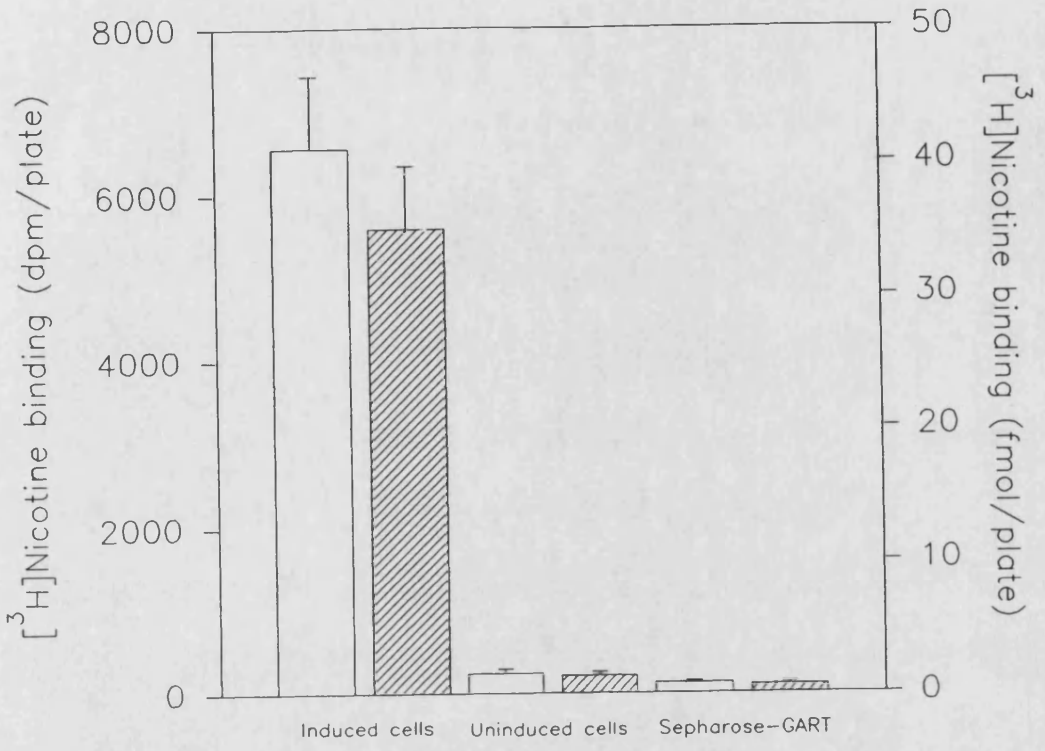

Fig. 3.8 **Comparison of specific [^{3}H]nicotine binding to mAb 290/Sepharose-GART after incubation with induced and uninduced cells.** Immunoaffinity purification and subsequent [^{3}H]nicotine binding were performed as shown previously (see Fig 3.3). Data are the mean ± range from two 60mm dishes ($7x10^5$ cells), expressed as dpm (open columns) and fmol (shaded columns) per plate. ([^{3}H]Nicotine binding to an equivalent volume of Sepharose-GART to that used in the immunoaffinty purification is also shown; this represents non-specific binding.)

Fig. 3.9 **[^{3}H]Cytisine binding to intact M10 cells.** Three days after induction with 1μM dexamethasone, M10 cells were washed with PBS (3x2ml per 35mm dish) and incubated in triplicate with [^{3}H]cytisine (final concentration 0.1-5nM) in the absence and presence of excess unlabelled (-)-nicotine to determine total (●) and non-specific (○) binding. Specific binding (■) was calculated as the difference between the two. Representative binding data (A) and Scatchard analysis (B) from a single experiment are shown (Kd = 3.1nM; Bmax = 80fmol/10^6 cells).

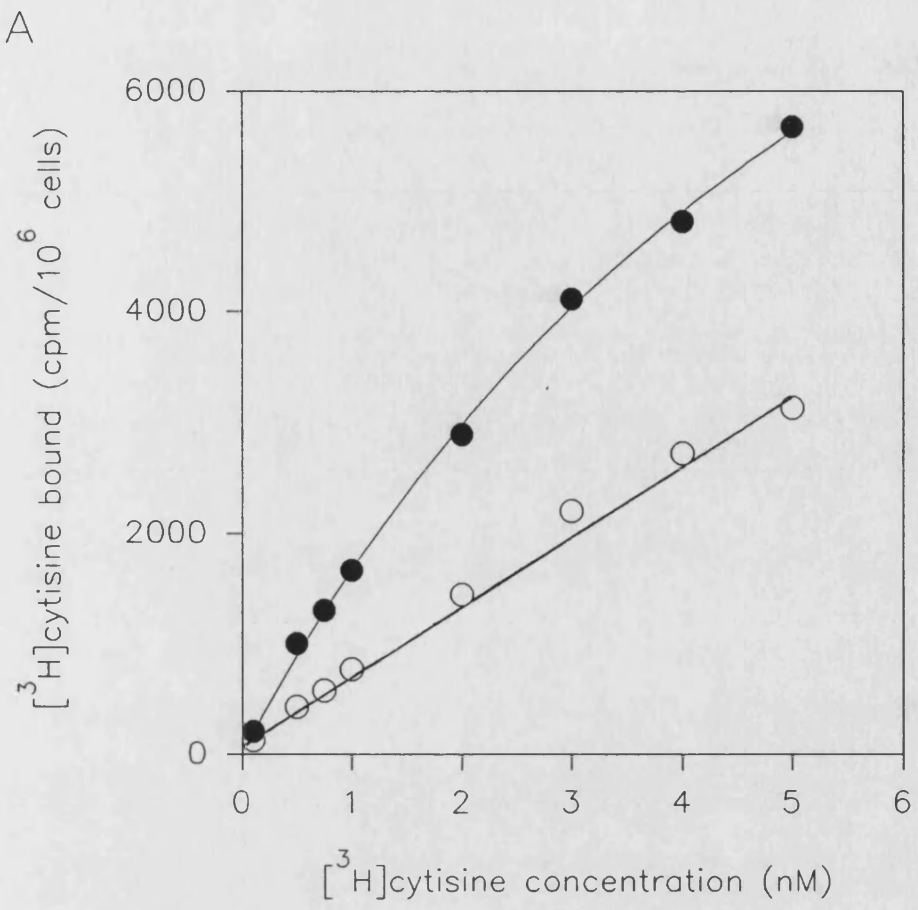
A
6000
4000
2000
0
0
1
2
3
4
5
6
[3H]cytisine bound (cpm/10^6 cells)
[3H]cytisine concentration (nM)

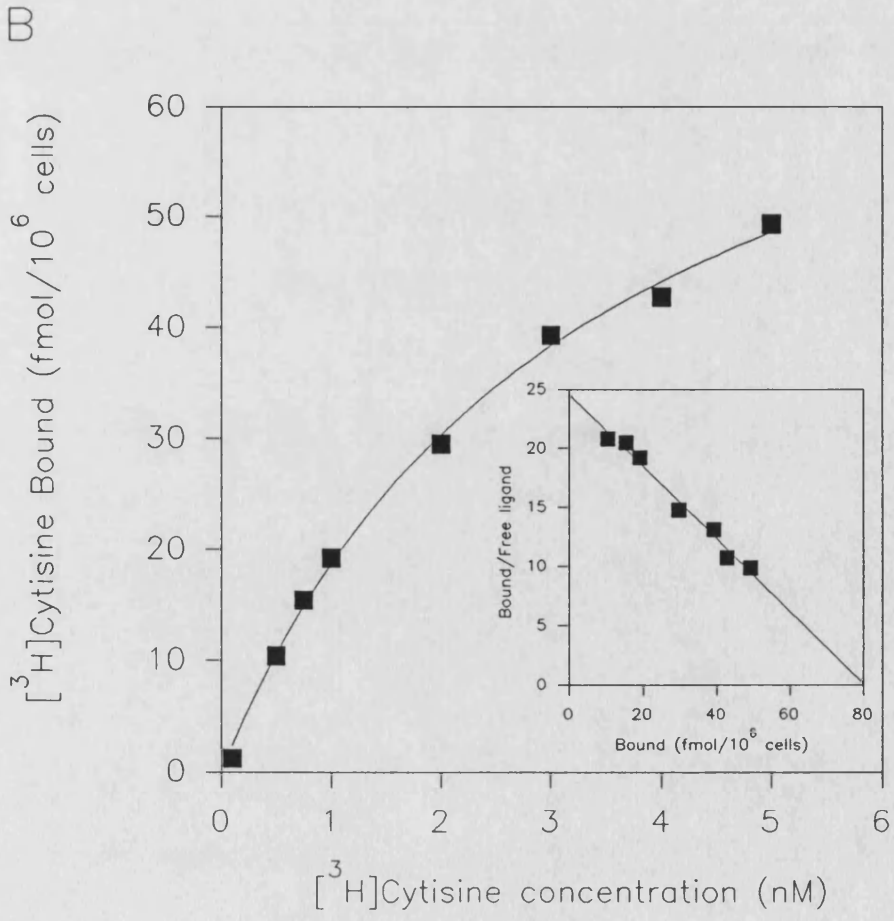
B
60
50
40
30
20
10
0
0
1
2
3
4
5
6
[3H]Cytisine Bound (fmol/10^6 cells)
[3H]Cytisine concentration (nM)
25
20
15
10
5
0
0
20
40
60
80
Bound/Free ligand
Bound (fmol/10^6 cells)

Fig. 3.10 **Competition with [^{3}H]cytisine by (A) ACh, (B) (-)nicotine, (C) cytisine and (D) (+)anatoxin-a for high affinity binding to intact M10 cells.** [^{3}H]Cytisine binding to induced M10 cells was measured in triplicate in the absence and presence of increasing concentrations of each of the agonists. Each point represents the mean ± SEM of 3 separate determinations.

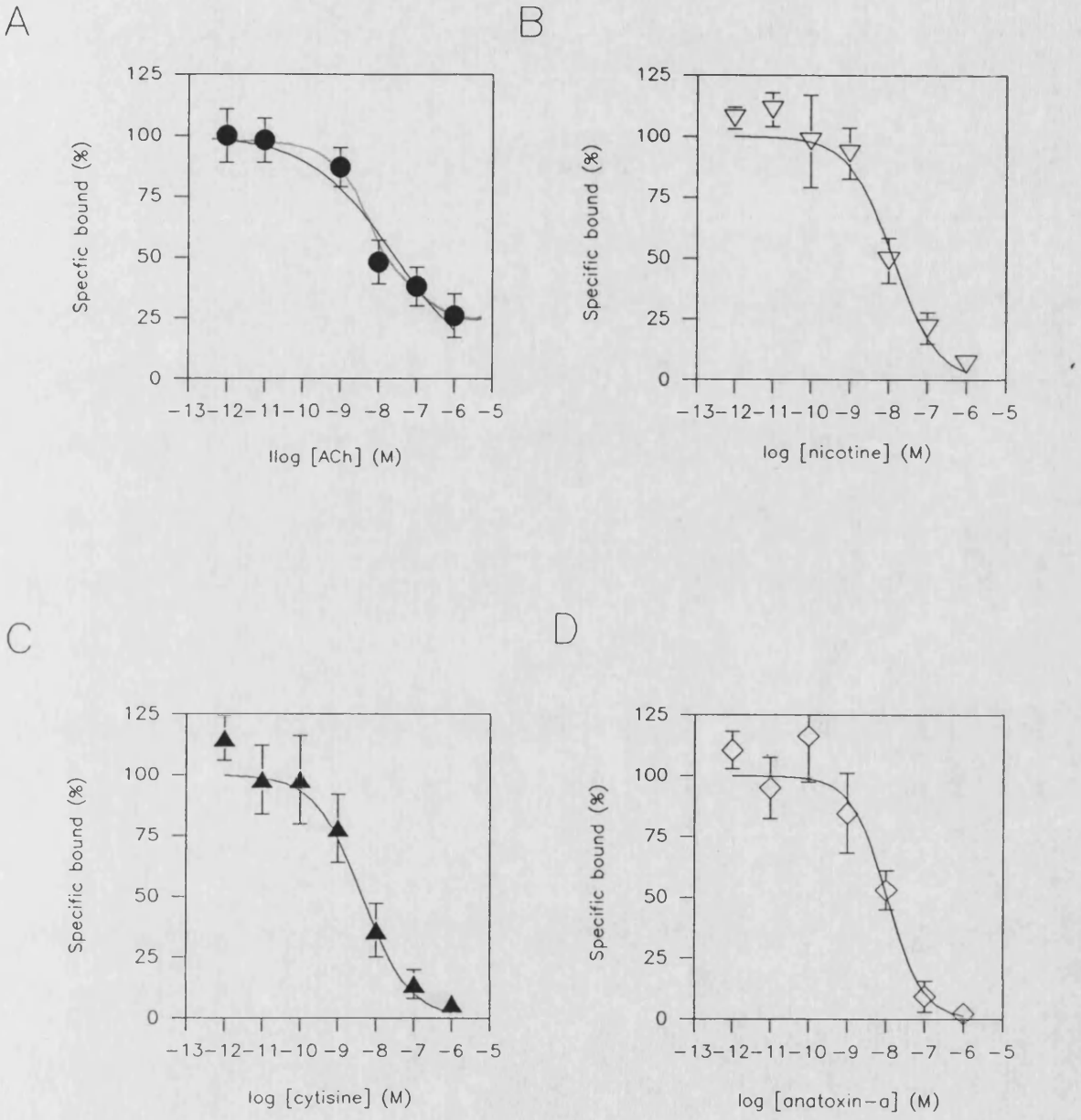
A
B
C
D
Specfic bound (%)
Specific bound (%)
125
100
75
50
25
0
−13 −12 −11 −10 −9 −8 −7 −6 −5
log [ACh] (M)
log [nicotine] (M)
log [cytisine] (M)
log [anatoxin−a] (M)

Fig. 3.11 **Acetylcholine-induced $^{86}Rb^{+}$ flux into M10 cells.** $^{86}Rb^{+}$ influx was measured in triplicate wells (35mm; $2.5x10^{5}$ cells) in the absence and presence of increasing concentrations of ACh, 3 or 4 days after induction of the M10 cells. Data were normalised by to the levels of specific [^{3}H]cytisine binding in each well. For comparative purposes, data were then adjusted such that the basal ^{86}Rubidium^{+} influx (ie that in the absence of ACh) matched the mean value of the range observed over the four individual assays (dotted lines). Data are presented in both cpm/well (left-hand column), and as a percentage of peak response (right-hand column). As each data set is from a single experiment, each point represents the mean of triplicate samples.

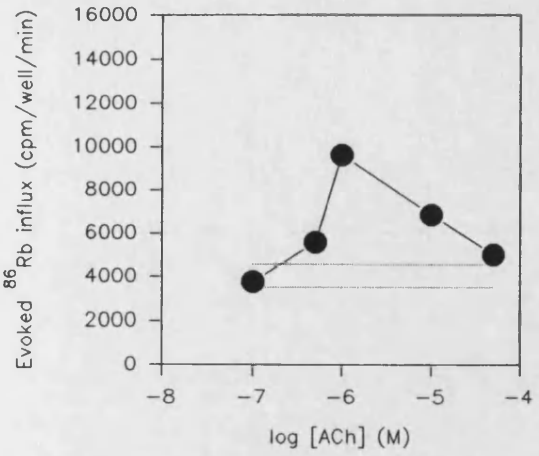
Evoked ^{86}Rb influx (cpm/well/min)
16000
14000
12000
10000
8000
6000
4000
2000
0
−8
−7
−6
−5
−4
log [ACh] (M)

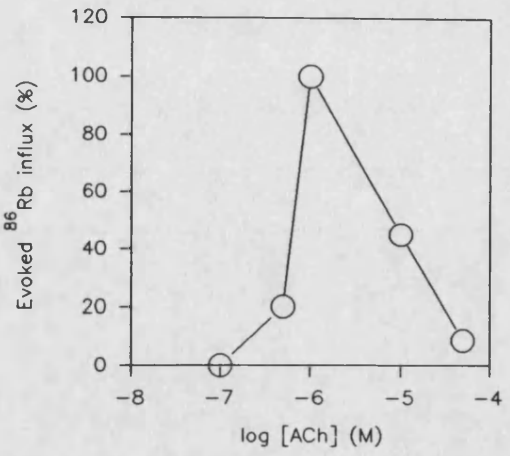
Evoked ^{86}Rb influx (%)
120
100
80
60
40
20
0
−8
−7
−6
−5
−4
log [ACh] (M)

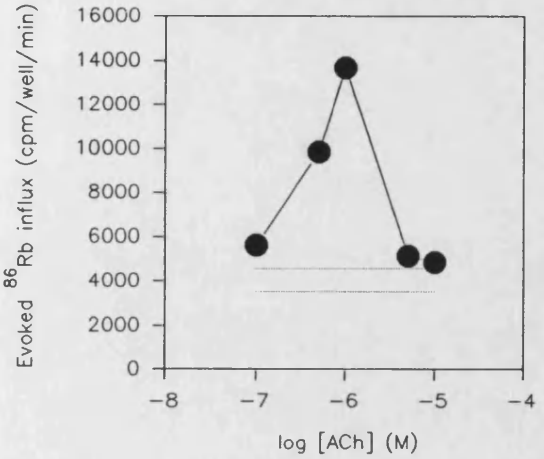
Evoked ^{86}Rb influx (cpm/well/min)
16000
14000
12000
10000
8000
6000
4000
2000
0
−8
−7
−6
−5
−4
log [ACh] (M)

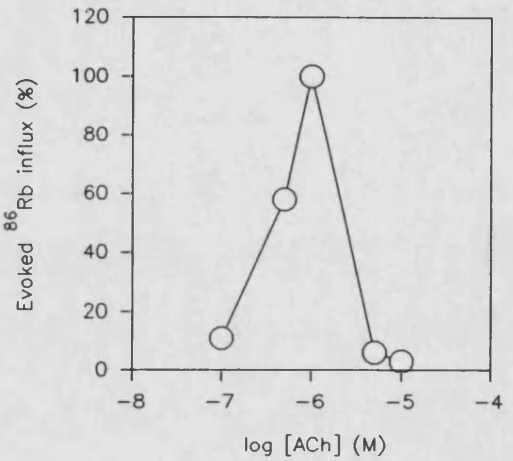
Evoked ^{86}Rb influx (%)
120
100
80
60
40
20
0
−8
−7
−6
−5
−4
log [ACh] (M)

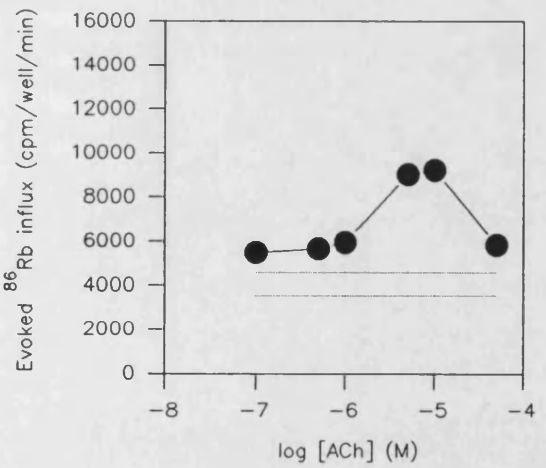
Evoked ^{86}Rb influx (cpm/well/min)
16000
14000
12000
10000
8000
6000
4000
2000
0
−8
−7
−6
−5
−4
log [ACh] (M)

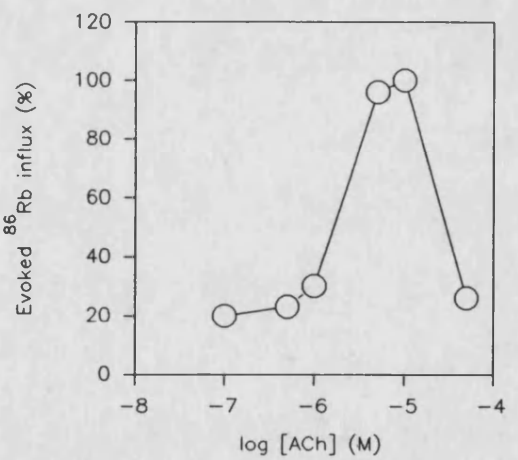
Evoked ^{86}Rb influx (%)
120
100
80
60
40
20
0
−8
−7
−6
−5
−4
log [ACh] (M)

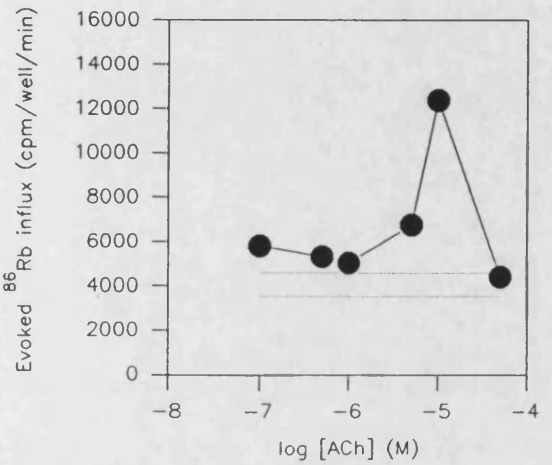
Evoked ^{86}Rb influx (cpm/well/min)
16000
14000
12000
10000
8000
6000
4000
2000
0
−8
−7
−6
−5
−4
log [ACh] (M)

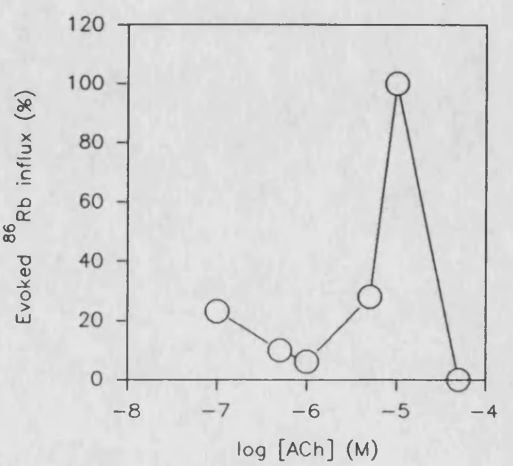
Evoked ^{86}Rb influx (%)
120
100
80
60
40
20
0
−8
−7
−6
−5
−4
log [ACh] (M)

Fig. 3.12 **Dose response curves of agonist-induced $^{86}Rb^{+}$ flux into M10 cells.** $^{86}Rb^{+}$ was measured in triplicate wells (35mm; $2.5x10^{5}$ cells) in the absence and presence of increasing concentrations of (A) (-)nicotine, (B) cytisine or (C) (+)anatoxin-a, 3 or 4 days after induction of the M10 cells. Within individual assays, data were normalised to the levels of specific [^{3}H]cytisine binding in each well. The main figure represents the meaned and normalised data for 3 or 4 separate determinations; the inset, a representative assay.

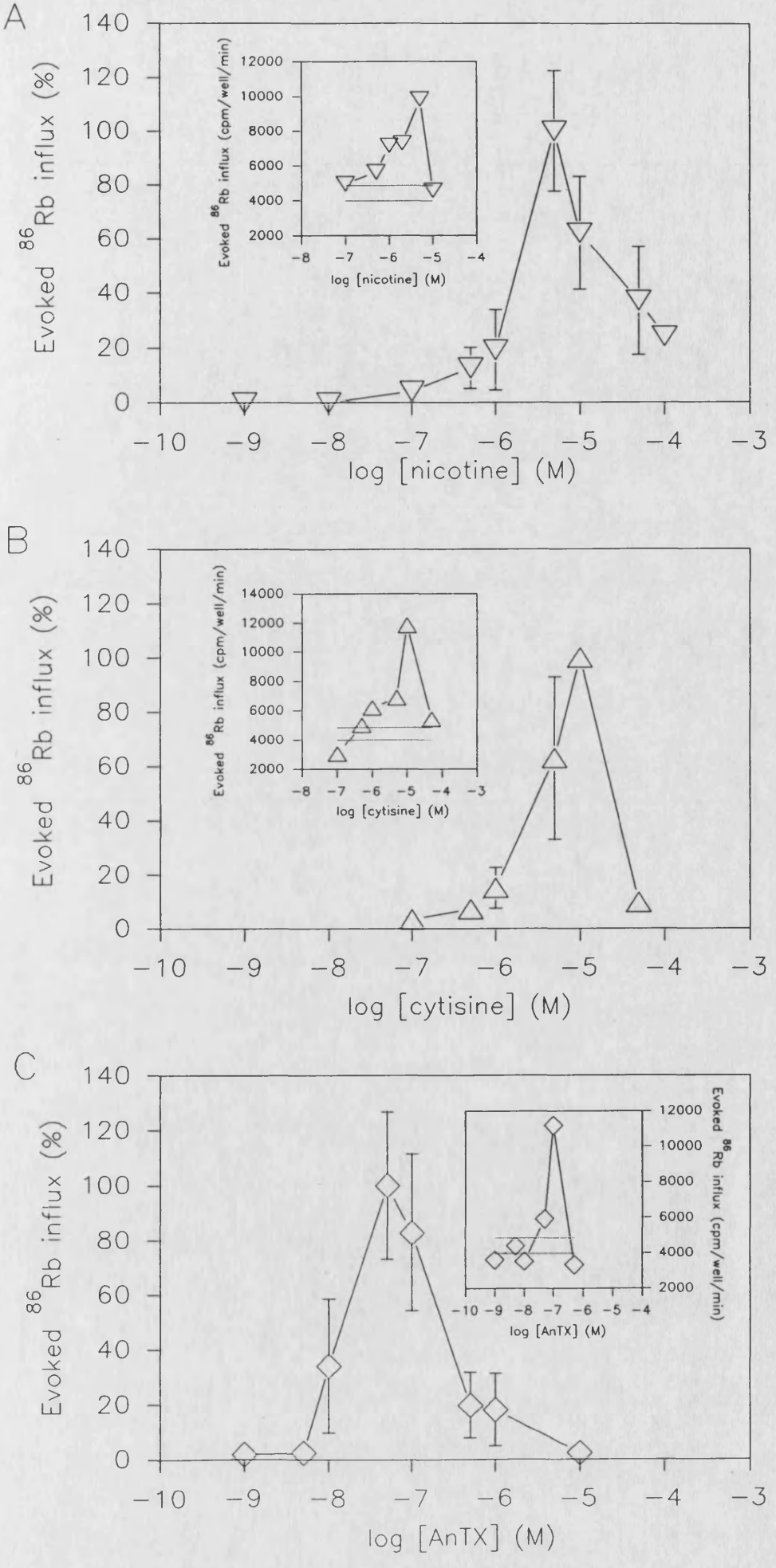
A
Evoked ^{86}Rb influx (%)
log [nicotine] (M)
Evoked ^{86}Rb influx (cpm/well/min)
log [nicotine] (M)
B
Evoked ^{86}Rb influx (%)
log [cytisine] (M)
Evoked ^{86}Rb influx (cpm/well/min)
log [cytisine] (M)
C
Evoked ^{86}Rb influx (%)
log [AnTX] (M)
Evoked ^{86}Rb influx (cpm/well/min)
log [AnTX] (M)

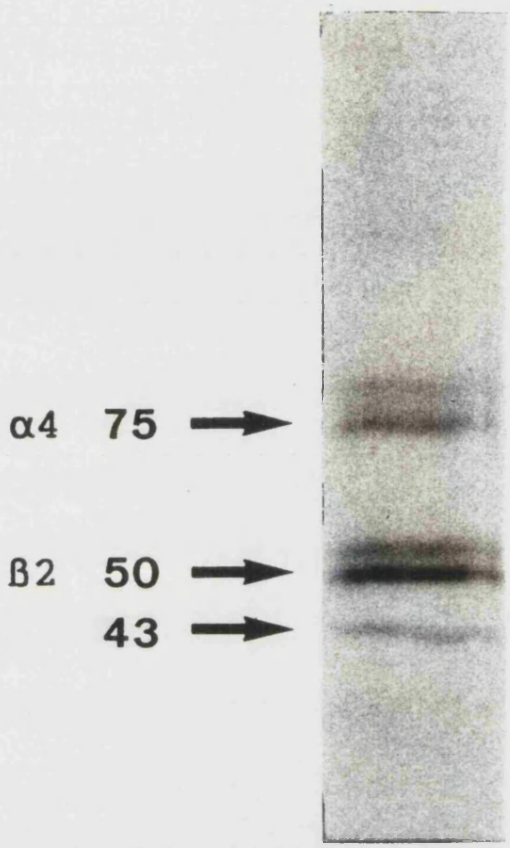

Fig. 3.13 **Subunit composition of transfected M10 cell nAChR.** Confluent M10 cells were induced for 16 hours with 1μM dexamethasone, washed and then incubated for a further 6 hours in methionine-free DMEM additionally containing [^{35}S]methionine (500μCi/10cm diameter dish). The labelled nAChR were solublised, immunoaffinity purified, then separated by SDS-PAGE (12% w/v acrylamide gel). Results were visualised by autoradiography.

4 THE INTERACTION OF NCI WITH NEURONAL nAChR

4.1 INTRODUCTION

The actions of four antagonists - one competitive (dihydro-ß-erythroidine) and three non-competitive (mecamylamine, MK-801 and chlorisondamine) - on the α4ß2 nAChR were investigated. Their effects both on high affinity [^{3}H]nicotine binding (see below), and agonist-induced ^{86}Rubidium$^+$ flux into the M10 transfected cell line were studied.

A report by Takayama et al. (1989) showed NCI to affect the binding parameters of [^{3}H]methyl-carbamylcholine (an alternative radioligand to [^{3}H]nicotine in binding assays, Boksa & Quirion, 1987) to rat brain membrane preparations, by performing saturation assays in the presence of the antagonist of interest. Such an observation emphasises the allosteric nature of the nAChR; interaction with a ligand at one site may affect other, more distant regions. Whilst the effect of agonist-induced conformational change on NCI binding is readily appreciated (for example, in exposing the channel blocker site), the reciprocal action was, until recently seldom considered. Here, these observations have been studied more thoroughly using detergent solubilised receptors from P2 membranes (see section 2.2.1.2). The removal of a large proportion of the membrane lipid prevented it from acting as an "unstirred layer" in the kinetic binding studies (see section 4.2.2.2).

The interactions of these antagonists with both

muscle- and neuronal-type nAChR as reported in the literature are reviewed first, followed by the results of this study.

4.1.1 Dihydro-ß-erythroidine

Dihydro-ß-erythroidine (DHßE) is a more active derivative of ß-erythroidine, an alkaloid isolated from the seeds of several Erythrina species. It is a secondary amine (see Fig. 4.1), and is unusual in that conversion to its salt reduces its potency as an antagonist (Wonnacott, 1987b). Early investigations established DHßE as a competitive neuromuscular blocking agent (reviewed in Wonnacott, 1987b), though more recent evidence suggests antagonism at muscle-type nAChR may include a small non-competitive element (Jones et al., 1986).

DHßE is a potent nicotinic antagonist in the central nervous system, and has been shown to attenuate receptor responses to a variety of agonists. For example, [^{3}H]dopamine release from striatal synaptosomes in response to 1μM (-)nicotine or cytisine was reduced to 30 to 40% of control values by 0.5μM DHßE (Rapier et al., 1990). At a similar concentration, DHßE was shown to shift the dose-response curve of α4ß2 nAChR expressed in Xenopus oocytes, increasing the apparent EC_{50} value of ACh over four fold (2.9μM, compared with 0.7μM in the absence of DHßE; Valera et al., 1992). This is indicative of a competitive antagonist.

DHßE, where tested, appears to act at all nAChR

subtypes, though it may do so with a gradation of potencies. Using whole cell current recordings, Alkondon and Albuquerque (1993) were able to divide a population of cultured hippocampal neurons into a number of "types" on the basis of the electrophysiological properties of their nAChRs. The majority of neurons ("type IA" currents, α7 nAChR) were affected only by DHßE at concentrations in excess of 10μM. However, a small population of cells were highly DHßE-sensitive; 100nM DHßE was found to achieve almost complete blockade. These "type II" currents were proposed to correspond α4ß2 nAChR. A (smaller) difference in DHßE affinity for the two receptor subtype is evident from high affinty binding data. Thus, Rapier et al. (1990) showed approximately a 20 fold difference in the affinty of the antagonist between [^{3}H]nicotine and [^{125}I]α-BgTx binding sites (1.3μM compared with 27μM respectively). Interestingly, [^{3}H]DHßE has been shown to bind to two populations of sites in rat cortical membranes with dissociation constants of 4nM and 22nM (Williams & Robinson, 1984). Perhaps these correspond to the two ligand binding sites examined by Rapier at al. (1990)?

In contrast, Lukas (1989) has suggested DHßE to be only a very weak, but equipotent, antagonist of both muscle and ganglionic nAChR. In ^{86}Rubidium$^+$ efflux studies using TE671 and PC12 cell lines, IC_{50} values were reported to be 2mM and 1mM, respectively.

4.1.2 **Mecamylamine**

Whilst mecamylamine has been extensively used as a central nicotinic antagonist (due to the ease with which it crosses the blood-brain barrier), the molecular basis of this action remains ill-defined. It would appear that as well as interacting with NMDAR (Snell & Johnson, 1989; see also section 1.4.2), mecamylamine exhibits different mechanisms of action according to the nAChR subtype with which it interacts. At the neuromuscular junction (where nAChR contain the α1 agonist binding subunit - but see also section 1.2.1), the mechanism of mecamylamine antagonism appeared to be voltage dependent channel block (Varanda et al., 1985). Conversely, at ganglia (which express high levels of α3, α7 and ß4 subunits (Listeraud et al., 1991)), its action has been claimed to be one of voltage independent competitive inhibition (Ascher et al., 1979). Bennet et al. (1957) showed that the effects of mecamylamine and hexamethonium at ganglia could be readily distinguished; a partial blockade by hexamethonium rapidly increased to a total one upon repetitive stimulation; this was not a feature of mecamylamine's action. This lack of "use-dependency" was confirmed electrophysiologically by Gurney & Rang (1984), and implied that mecamylamine did not act as a channel blocker. Yet in PC12 cells, mecamylamine was shown to displace [^{3}H]H_{12}-HTX (Daly et al., 1991), suggesting action at the channel blocker site (see section 1.4.1.2). The α4ß2 nAChR expressed in Xenopus oocytes was blocked by mecamylamine. Although its inhibitory action

required agonist activation, it was found to be voltage independent (Bertrand et al., 1990). These observations suggest a binding site inaccessible when the receptor is in the resting conformation, yet not deep within the ion channel itself.

4.1.3 MK-801

Originally reported as an NMDAR antagonist (Wong et al., 1986), it is now apparent that the anticonvulsant MK-801 also interacts with nAChR. Inhibition of NMDAR by MK-801 is strongly voltage dependent and effective only when MK-801 is applied with agonist (Heuttner & Bean, 1987), suggesting an open channel block mechanism. The mode of action at nAChR appears similar in all reports in which mechanism was investigated. For example, in frog neuromuscular junction, muscle twitch responses were blocked and the frequency and mean channel open time of nAChR, analysed by the patch clamp technique, reduced (Ramoa et al., 1990). A similar voltage dependent block of ACh-evoked currents was observed in bovine chromaffin cells (Halliwell et al., 1989). Presynaptic nAChR in rat hippocampus were functionally blocked by MK-801, though further delineation of the mechanism was not possible with the technique employed (Ramoa et al., 1990). Additional to these functional data, biochemical studies indicate that MK-801 is capable of displacing both [^{3}H]PCP (Kavanaugh et al., 1989) and [^{3}H]H_{12}-HTX (Ramoa et al., 1990) from Torpedo membrane preparations. As both radioligands act as open

channel blockers, they are assumed to bind to a specific site within the ion channel (see section 1.4.1.2).

4.1.4 Chlorisondamine

The molecular aspects of chlorisondamine interaction with nAChR have received little attention in studies other than those using invertebrate-based assay systems (see Lingle 1983, for example). Investigators have focussed instead on the long term antagonism of central nicotinic mechanisms observed in behavioural studies. For example, after a single intra-cerebroventricular (Clarke & Kumar, 1983; Reavil et al., 1986) or subcutaneous (Clarke, 1984) injection of chlorisondamine, significant effects were noted on different behavioural parameters for periods of up to 5 weeks. The efficacy of the latter form of administration is particularly surprising; chlorisondamine is a bis-quaternary ammonium salt (for structure, see Fig. 4.1), and as such, would not be expected to cross the blood brain barrier.

In mechanistic terms, Van Rossum (1962) viewed chlorisondamine as a "typical non-competitive ganglionic blocking agent". At frog neuromuscular junction, Neely & Lingle (1986) showed the drug to behave as an open-channel blocker, with some interesting additional features. Recovery from blockade was slow, and subsequent responses failed to match those observed before chlorisondamine treatment. This was irrespective of any changes made in agonist application or holding potential during the

recovery phase. Curiously, in binding studies using membranes prepared from Torpedo electric organ, Daly et al. (1991) showed that chlorisondamine had little ability to inhibit either [^{125}I]α-bungarotoxin or [^{3}H]H_{12}-HTX binding, suggesting no preference for either the agonist or channel-blocker binding site.

4.2 RESULTS

4.2.1 OPTIMISATION OF [^{3}H]NICOTINE BINDING TO TRITON X-100 EXTRACTS OF P2 MEMBRANES

The choice of a detergent extract instead of membrane preparation forced a re-examination of the binding assay conditions used previously, and an evaluation of their suitability in these circumstances.

4.2.1.1 Buffering system

A recent report by Romm et al. (1990) showed that the inclusion of 200mM TRIS in the incubation buffer reduced non-specific [^{3}H]nicotine binding to mouse brain membranes. TRIS, however, is incompatible with a phosphate buffer, so its adoption would necessitate a change in buffering systems. [^{3}H]Nicotine binding to Triton X-100 extracts of rat brain membranes prepared in three buffers was compared:

(i) Standard 50mM Phosphate (pH 7.4)

(ii) Krebs-HEPES (pH 7.4)

(iii) Krebs-HEPES-TRIS (as (ii), but with 200mM TRIS)

Non-specific binding, as a proportion of the total, varied between 32 to 55% in comparative assays. In all cases however (n=3), non-specific binding was reduced by approximately 25% on the inclusion of TRIS in a statistically significant fashion ($p<0.05$; see Fig. 4.2); in its absence, little difference between the levels of non-specific binding in the two buffering systems was observed. Krebs-HEPES-TRIS was therefore adopted in subsequent binding assays.

4.2.1.2 **Filters**

Lippiello & Fernandes (1986), in their use of the Brandel cell harvester, separated membrane-bound [^{3}H]-nicotine from unbound radiolabel on two thicknesses of Gelman GFA/E glass fibre filters. However, in these studies, predominantly performed on Triton X-100 extracts, this grade of filter may not have been optimal for the solubilised proteins. The retentive properties of three filter types, presoaked in 0.3% PEI (see section 2.2.1.3.1), were compared:

(i) Gelman GFA/E

(ii) Whatman GFB

(iii) Whatman GFC

(Due to a difference in thicknesses, only one layer of GFB, compared with two layers of GFA/E and GFC, was used.)

Results indicated no significant differences in the levels of specific binding retained by the three filter grades when using Triton extract (see Fig. 4.3A). However,

GFA/E filters retained the lowest values of non-specific [^{3}H]nicotine binding, both in absolute terms, and as a proportion of the total (see Fig. 4.3B). Consequently, GFA/E filters were used in all subsequent [^{3}H]nicotine binding assays to Triton extracts.

4.2.1.3 **Effects of Triton X-100**

4.2.1.3.1 On (-)[^{3}H]nicotine binding

Membrane proteins, including nAChR, were solubilised initially by treatment of P2 membranes with 1% (v/v) Triton X-100. After centrifugation (see section 2.2.2), [^{3}H]nicotine binding to both supernatant and pellet was assayed. The sum of these was much lower than the [^{3}H]-nicotine binding to a comparable, but untreated, P2 preparation (see Fig. 4.4A). However, there appeared to be a small increase in the number of binding sites in the supernatant (or, "Triton extract") upon dilution with buffer. This suggested some sort of reversible interference with radiolabel binding (it being argued that the pre-soaking of the glass fibre filters in 0.3% PEI minimised the loss of solublised labelled nAChR during washing). Triton X-100 appeared to be responsible; [^{3}H]nicotine binding to P2 membranes in the presence of increasing concentrations of detergent was reduced in a seemingly dose-dependent manner (see Fig. 4.4B). (It is likely that the lack of [^{3}H]nicotine binding reported by Whiting & Lindstrom (1986) in the preliminary stages of their purification of the chick α4ß2 nAChR was also due to a high

(2%) Triton concentration.) A similar experiment was performed using Triton extracts at a fixed protein concentration, but in the presence of increasing concentrations of Triton X-100 (see Fig. 4.5). Severe attenuation of [^{3}H]nicotine binding was again evident at the higher concentrations of detergent, although in this assay, there appeared to be little or no reduction in binding at 0.1% Triton or below. Consequently, in subsequent assays the extract was diluted such that detergent concentrations were 0.1% or less. Under these conditions, the parameters of [^{3}H]nicotine binding (most importantly, the affinity) were similar to those observed in P2 membranes (see Fig. 4.6 and section 4.2.2.1).

Although the recovery of P2 protein in the Triton extract varied (73±9%; mean±SEM, n=9), the use of 0.5% and 1% Triton were found to yield similar amounts of protein (extraction of identical membrane preparations with 0.5% and 1% Triton yielded protein recoveries of 55% and 53% respectively). Adoption of the lower concentration in all further extractions allowed the necessary dilution of the detergent, whilst retaining the protein concentrations which earlier experiments with membrane preparations showed to be optimal in binding studies (1-2mg/ml, data not shown).

4.2.1.3.2 <u>On protein determinations</u>

Triton X-100 and HEPES both give positive reactions with Lowry reagents in the absence of protein.

This causes an over estimation of protein concentration if the standard protocol is followed. As a consequence, this leads to errors in the interpretation of binding data. This is exemplified in Fig. 4.7 in which a BSA standard curve was assayed by the Lowry method in the presence and absence of Krebs-HEPES-TRIS and Triton. At the lower end of the scale (comparable with tissue samples) the presence of buffer and detergent increased readings by 25-50%. Modification of the assay (ie standardising buffer/detergent concentrations in samples and BSA standards; see section 2.2.4) eliminated this source of error.

4.2.1.4 Effect of ethanol on [^{3}H]nicotine binding

All the antagonists tested for an effect on [^{3}H]-nicotine binding were first dissolved in ethanol (see section 2.2.3). To examine any possible interaction of the solvent itself with nAChR, [^{3}H]nicotine binding at a range of concentrations (1, 15 and 40nM) and in the presence and absence of 10μl 95% (approximately 100mM) ethanol was assayed. No significant differences in radioligand binding were observed between paired experiments at each nicotine concentration (see Fig. 4.8).

4.2.2 EFFECTS OF NCI ON [^{3}H]NICOTINE BINDING TO TRITON EXTRACTS OF P2 MEMBRANES

4.2.2.1 Equilibrium binding studies

Having selected assay conditions comprising of a

final Triton X-100 concentration of less than 0.1%, and a protein concentration in the range of 1-2mg/ml in Krebs-HEPES-TRIS buffer, saturation binding studies were performed on detergent extracts to determine [^{3}H]nicotine binding parameters. Data analysis was performed as shown in section 2.2.1.5. Briefly, the dissociation constant (Kd) and site density (Bmax) were first calculated by the method of Scatchard et al. (1949), these values were then used as "first estimates" for an iterative least-squares curve fitting of the binding data performed on SIGMAPLOT 4.1 software package. Binding was found to be to a single class of sites, Kd = 16±2nM, Bmax = 104±12fmol/mg (mean ± SEM, n=13). Typical data are shown in Fig. 4.9.

The four antagonists were assayed for competition with [^{3}H]nicotine using the radioligand close to its Kd (10nM). Saturation binding assays in the presence and absence of each of the antagonists were then performed. These experiments were to provide information about the antagonists' interactions with the labelled nAChR, by showing which of radioligand's binding parameters were affected in their presence.

4.2.2.1.1 Dihydro-ß-erythroidine

DHßE was found to be an efficient inhibitor of [^{3}H]nicotine binding (IC_{50} = 5.3±2.6μM; see Fig. 4.10). In the presence of 5μM DHßE, the Kd was significantly reduced in comparison to control (control Kd = 18±3nM; with DHßE,

Kd = 63±10nM, p>0.01; see Fig. 4.11) whereas there was no significant difference in the number of sites (control Bmax = 88±15fmol/mg; with DHßE, Bmax = 113±11fmol/mg). Such observations would be predicted for a truly competitive antagonist (see section 5.2).

4.2.2.1.2 Mecamylamine

Mecamylamine did not compete strongly with [^{3}H]-nicotine for agonist binding sites (IC_{50}>1mM; see Fig. 4.10), its effect appearing to be rather similar to that of chlorisondamine (see section 4.2.2.1.4). Saturation studies suggested the interaction of agonist, NCI and receptor to be more complex. Initial analyses revealed that at 180μM, mecamylamine induced curvilinearity (concave downwards) in the Scatchard analyses of saturation binding, the data best fitting a second order regression (n=3; see Fig. 4.12A). This pattern was repeated at both lower (60μM; n=2), and higher (600μM; n=2), concentrations of mecamylamine (see Fig. 4.12B).

This curvilinear response suggests that at lower radioligand concentrations (up to approximately 10nM), nicotine binding was inhibited to a greater extent by mecamylamine than at higher concentrations. Consequently, some characteristics of [^{3}H]nicotine binding at a representative "low" concentration (2nM) of radioligand in the presence and absence of mecamylamine were investigated. Thus, [^{3}H]nicotine binding in the presence of mecamylamine (180μM) appeared to reach equilibrium much faster than in

controls as measured by the time taken to reach half maximal levels of binding ($t_{½}$). Non-linear curve fitting indicated a six fold difference in the $t_{½}$ values in the presence and absence of the antagonist (2.7 compared with 18.8 minutes respectively, see Fig. 4.13). If the association rate is assumed to partially reflect the change from a predominantly R to D state within the receptor population, then the reductions of $t_{½}$ are consistent with an increase in the rate of nAChR desensitisation in the presence of NCIs (see section 1.4.1).

Even though equilibrium was reached more quickly in the presence of NCI, the amount of [^{3}H]nicotine bound under such conditions was lower than controls (2.5fmol/mg in the presence of mecamylamine compared with a control value of 5.2fmol/mg). Competition assays, using [^{3}H]nicotine at 2nM, instead of 10nM, showed mecamylamine to inhibit agonist binding more strongly at this lower radioligand concentration; the IC_{50} value calculated from these data being at least 2 orders of magnitude higher than earlier estimates (against 10nM nicotine, IC_{50}>1mM; against 2nM, IC_{50} = 89±37μM, see Fig 4.14). From these data, one would anticipate a 60-70% decrease from a control value in the binding of 2nM [^{3}H]nicotine in the presence of 180μM mecamylamine. This compares favourably with saturation binding data in which a 66% reduction was noted at this radioligand concentration (control binding 11.4±1.4fmol/mg, with mecamylamine 3.7±1.7fmol/mg; n=3).

4.2.2.1.3 MK-801

4.2.2.1.3A Effects on [^{3}H]nicotine binding to Triton X-100 extract

The presence of 50μM MK-801 in saturation binding experiments had no effect on [^{3}H]nicotine binding parameters (data not shown); this observation is wholly consistent with competition assay data in which the IC_{50} was found to be greater than 1mM (see Fig. 4.10). However a qualitative difference between this and the other NCI was apparent. Whereas mecamylamine and chlorisondamine appeared to reduce [^{3}H]nicotine binding gradually from 10μM, MK-801 had no effect at concentrations up to approximately 100μM; greater than this, inhibition was marked. The mechanism by which this reduction was achieved was investigated by measuring the effect of 500μM MK-801 on [^{3}H]nicotine binding parameters (see Fig. 4.15). At this concentration of MK-801, the data hinted at an effect on [^{3}H]nicotine affinity for solubilised nAChR, although this was not statistically significant (Kd = 29±8nM; control Kd = 13±2nM, n=3; $p<0.1$). No significant difference was observed between the number of sites in the presence or absence of MK-801 (with MK-801, Bmax = 105±39fmol/mg; control, Bmax = 83±32fmol/mg).

In contrast to mecamylamine, the concentration of [^{3}H]nicotine used in competition binding assays had no effect on the ability of MK-801 to inhibit radioligand binding; IC_{50}>1mM at both 2nM and 10nM [^{3}H]nicotine (see Figs. 4.10 and 4.14). However, the $t_{½}$ of radioligand association in the presence of 500μM MK-801 at 2nM [^{3}H]-

nicotine was reduced (3.8 minutes compared with 18.8 minutes in controls).

4.2.2.1.3B[^{3}H]MK-801 binding

In order to further characterise the relationship of the MK-801 and agonist binding sites, some preliminary binding studies using [^{3}H]MK-801 were performed, taking advantage of the defined and homogeneous nAChR expressed by the M10 cell line. [^{3}H]MK-801 (final concentration 5μM) was found to bind specifically to immunoimmobilised α4ß2 receptors (see Fig. 4.16). At this concentration, total [^{3}H]MK-801 binding was between 55-61fmol/immunoimmobilised 10cm diameter plate of cells; non-specific binding (as defined as that to an equvalent volume of Sepharose-GART) varied between 50-60% of the total. Comparison of the amounts of [^{3}H]nicotine (20nM) and [^{3}H]MK-801 (5μM) bound to identical samples gave a stoichiometry in the region of 4:1, respectively. [^{3}H]MK-801 binding was found to be unaffected by the inclusion of 10μM unlabelled (-)nicotine, but was displaced by 10μM PCP, in contrast to [^{3}H]nicotine binding.

4.2.2.1.4 Chlorisondamine

4.2.2.1.4AEffects on [^{3}H]nicotine binding to Triton X-100 extract

In competition assays against [^{3}H]nicotine, chlorisondamine was quantitatively similar to both mecamylamine and MK-801 (IC_{50}>1mM; see Fig. 4.10), though

qualitatively its affect more closley resembled that of mecamylamine. Saturation binding assays in the presence of 20μM chlorisondamine led to a significantly lower estimation of Bmax than that in controls (79±9fmol/mg, compared with 145±16fmol/mg; n=3; $p<0.02$). The data also suggested a reduction in the affintiy of the receptor for [^{3}H]nicotine in the presence of the antagonist, though the difference was not statistically significant (Kd = 30±11nM compared with 20±5nM in controls; $p<0.1$). Typical binding curves and Scatchard plots are shown in Fig. 4.17.

4.2.2.1.4B<u>Effects of in vivo administration of chlorisondamine on [^{3}H]nicotine binding</u>

One of the most interesting features of chlorisondamine action is the extended time period over which it appears to be effective as a central nicotinic antagonist (see section 4.1.4). To investigate this phenomenon, groups of six rats received subcutaneous injections of chlorisondamine, such that the final concentration was 10mg/kg (after Clarke, 1984), or saline as controls (see section 2.2.3). A week after the injections, the animals were killed, and [^{3}H]nicotine (40nM) binding to cortical and hippocampal membrane preparations was examined in both groups.

The binding data are summarised in table 4.1

Table 4.1 Effects of <u>in vivo</u> chlorisondamine administration on [^{3}H]nicotine binding to cortical and hippocampal membrane preparations (n=6).

Injection	Cortex	Hippocampus
Saline	82±4 fmol/mg	12±3 fmol/mg
Chlorisondamine	106±15 fmol/mg	15±2 fmol/mg

In the cortex, chlorisondamine treated animals showed a 25% increase in [^{3}H]nicotine binding sited compared with controls, but this was not statistically significant ($p>0.1$), reflecting the considerable variance in this group, as depicted in a scatter plot of the individual values (see Fig. 4.18). Interestingly, the controls display considerably less variability. A lack of effect by chlorisondamine is supported by the data for hippocampus. These data suggest that whatever the mechanism by which chlorisondamine achieves its long term blockade, it does not appear to lead to a change in the number of [^{3}H]-nicotine (thus α4ß2 nAChR) binding sites in the cortex or hippocampus.

4.2.2.2 **Kinetic binding studies**

Kinetic studies were used to further investigate the unusual effects that mecamylamine was observed to have on [^{3}H]nicotine binding, and particularly the dissocaition constant (see section 4.2.2.1.2). For a given ligand, the

Kd can be defined as the ratio of dissociation rate (k_{-1}) and association rate (k_{+1}) constants, thus:

$$Kd = k_{-1}/k_{+1} \quad --- \quad (1)$$

Although k_{-1} can be directly measured in binding assays, k_{+1} cannot. However, a related term, the pseudo - first order "observed" association rate (k_{obs}), may be derived experimentally. This, in combination with k_{-1}, allows calculation of Kd, either with or without the use of equilibrium binding data (see section 4.2.2.2.3).

4.2.2.2.1 Association kinetics in rat brain detergent extracts

The time course of association was followed by measuring the amount of [^{3}H]nicotine bound to detergent extract as a function of time (see section 2.2.3.2). Initial experiments were performed over a period of 3 hours, and showed binding to be hyperbolic, with a $t_{½}$ = 3.5 minutes (see Fig 4.19). Subsequent analyses, both in control and test cases, focussed on the initial, rapid binding phase; binding was assayed at intervals up to 30 minutes and at 3 hours (taken as equilibrium). The reaction was found to have a mean k_{obs} = 0.084nM^{-1}min^{-1} (see Fig. 4.20A; SEM shown in Table 4.3). Whilst these data concur quantitatively with those of Lipiello & Fernandes (1986; k_{obs} = 0.08nM^{-1}min^{-1}), it should be noted that the k_{obs} is only constant under fixed conditions and the similarity of

little consequence.

Interestingly, [^{3}H]nicotine association to rat brain membranes was reported to be a biphasic function, rather than the hyperbolic one shown here. McCarthy & Moore (1992) have shown that the lipid environment affects receptor conformation; thus, the process of receptor solublisation may be responsible for this subtle difference in mechanism.

4.2.2.2.2 Dissociation kinetics in rat brain detergent extracts

Given the similarity between the [^{3}H]nicotine association kinetics observed in membrane-bound and solubilised nAChR (see section 4.2.2.2.1), it seemed likely that the first order dissociation reported by Lipiello & Fernandes (1986; k_{-1} = 0.04min^{-1}) would hold for detergent extracts. Thus, a full time course was not measured, rather, binding was assayed at equilibrium, then intervals up to 30 minutes after isotopic dilution of the radioligand with unlabelled nicotine (see section 2.2.3.2). Under these conditions, k_{-1} = 0.059min^{-1} (see Fig. 4.21A). This suggests that [^{3}H]nicotine dissociation from solublised nAChR to be more rapid than that from membrane-bound receptors; the significance of this however is unclear.

4.2.2.2.3 Effects of NCI on association/dissociation kinetics

The presence of mecamylamine (180μM) has already

been shown to increase the observed association rate of [^{3}H]nicotine binding to Triton extracts at a radioligand concentration of 2nM (see section 4.2.2.1.2). However, this effect was reversed when a [^{3}H]nicotine concentration of 10nM was used; mecamylamine actually appeared to reduce the association rate under these conditions (k_{obs} = 0.066nM^{-1} min^{-1}, see Fig. 4.20B). However, mecamylamine was not unique in its seemingly contradictory actions on [^{3}H]nicotine association. Thus, MK-801 (500μM) was found to apparently increase the rate of radioligand association at 2nM [^{3}H]nicotine (k_{obs} = 0.302nM^{-1}min^{-1}), and decrease it at 10nM [^{3}H]nicotine (k_{obs} = 0.061nM^{-1}min^{-1}).

Such deviations of the k_{obs} from controls are reflected in the calculated $t_{½}$ values for [^{3}H]nicotine binding to Triton extracts. Thus, whilst the effect of mecamylamine on 2nM radioligand association is quite pronounced (see Fig. 4.13), the presence of either antagonist has only a minor effect on the $t_{½}$ of 10nM [^{3}H]nicotine association (see Fig. 4.22). All the $t_{½}$ values are summarised in Table 4.2

The increases in k_{obs} observed at low radioligand concentrations as a result of coincubation with the two antagonsits were found to be statistically significant ($p<0.02$). The reductions from control values at 10nM [^{3}H]-nicotine, whilst routinely observed, were not statisically significant; this probably being due to the wide variations in the [^{3}H]nicotine binding values seen between experiments.

Dissociation rates were too rapid to be resolved

with any confidence at 2nM [^{3}H]nicotine. However, the presence of either antagonist seemingly had little effect on radioligand dissociation at 10nM [^{3}H]nicotine, with values closely resembling controls (with mecamylamine, k_{-1} = 0.056min^{-1}; with MK-801, k_{-1} = 0.055min^{-1}). Data are illustrated in Figs. 4.21B and 4.21C.

Table 4.2 The half times for [^{3}H]nicotine (2nM and 10nM) association in the presence and absence of NCI

[^{3}H]Nicotine concentration	$t_{½}$ (minutes)		
	Control	+ 500μM MK-801	+ 180μM mecamylamine
10nM	3.5	6.1	8.8
2nM	18.8	3.8	2.7

4.2.2.2.4 Calculation of Kd values from kinetic data

The association rate constant, k_{+1}, cannot be directly measured in this type of assay. The amount of ligand bound at a given time depends simultaneously on association and dissociation mechanisms. These are related to k_{obs} such that:

$$k_{obs} = k_{+1}.[L] + k_{-1}$$

[L] = ligand concentration

By rearranging these terms, k_{+1} is found to be equal to:

$$k_{+1} = (k_{obs} - k_{-1}) / [L] \quad --- \quad (2)$$

Substituting equation (2) into equation (1) (see section 4.3.2) gives:

$$Kd = k_{-1}.[L] / (k_{obs} - k_{-1}) \quad --- \quad (3)$$

It is also possible to express k_{+1} in terms of formation of the receptor-ligand complex. The second order equation this approach yields may be simplified by assuming [L] is constant throughout; an assumption made acceptable by the great excess of ligand when compared with the actual number of specific binding sites available (nano- compared with picomolar).

From this basis it can be shown that:

$$k_{+1} = k_{obs}.[Be] / [L].Bmax \quad --- \quad (4)$$

[Be] = concentration of ligand bound at equilibrium

Bmax = Number of binding sites

Substituting equation (4) into equation (1):

$$Kd = k_{-1}.[L].Bmax/k_{obs}.Be \quad --- \quad (5)$$

This provides two expressions ((3) and (5)) from which it is possible to derive Kd values; one independent of equilibrium data, the other requiring an estimation of the number of binding sites. Both were used here. The values calculated (control, and in the presence of MK-801 or mecamylamine), as well as the kinetic data from which they are calculated, are summarised in Table 4.3.

Drug	k_{obs}	k_{-1}	Calculated Kd (nM)	
			From (3)	From (5)
Control	0.084 ± 0.024 (n=6)	0.059 ± 0.003 (n=6)	24	29
+ mecamylamine (180μM)	0.066 ± 0.019 (n=4)	0.056 ± 0.003 (n=4)	56	29
+ MK-801 (500μM)	0.061 ± 0.019 (n=4)	0.055 ± 0.004 (n=4)	92	60

Table 4.3 On- and off-rates of [^{3}H]nicotine binding to Triton extracts in the presence and absence of mecamylamine and MK-801, and the subsequent changes in radioligand affinity as calculated from those data.

4.2.3 THE ACTION OF NCI ON α4ß2 nAChR FUNCTION

The effects of the antagonists at functional α4ß2 nAChR were investigated by means of a ^{86}Rubidium^{+} influx assay using the M10 cell line (see section 2.2.2.5). Dose response curves were constructed by measuring the ion flux in response to 1μM (-)nicotine for one minute in the presence of increasing concentrations of each of the antagonists and comparing with the response seen in their absence. Dose-response curves for mecamylamine and MK-801 are shown in Fig. 4.23. Curves for chlorisondamine blockade were incomplete over the range of antagonist concentrations used. However, there did not appear to be any agonist-induced ^{86}Rubidium^{+} influx at chlorisondamine concentration greater than $1x10^{-8}$M. This suggests that chlorisondamine is an extremely potent antagonist. In addition, no curve was obtained for DHßE, experimental data proving to be highly variable. The only consistent feature was the failure of the antagonist to achieve complete blockade of the receptor-mediated influx, even at high (1μM) concentrations. A possible explanation may stem from recent observations of Alkondon & Albuquerque (1993). In their measurement of whole cell currents from hippocampal neuronal cultures, they noted that the interaction of DHBE with nAChR was slower than that with their agonist, ACh. Consequently, if the two were applied simultaneously, receptor activation proceeded too quickly to be inhibited by DHßE. The IC_{50} values are summarised in Table 4.4.

Table 4.4 Antagonism of agonist-induced ^{86}Rubidium ion flux in M10 cells (N.D. = not determined)

Antagonist	IC_{50} (M)
DHßE	N.D.
Mecamylamine	$1.0x10^{-6}$ (n=3)
MK-801	$1.1x10^{-4}$ (n=3)
Chlorisondamine	$<1.0x10^{-8}$ (n=2)

4.3 DISCUSSION

Non-competitive inhibitors (NCIs) may interact with three distinct categories of saturable binding sites on nAChR: a single, high affinity site, a population of lower affinity sites, and, at high concentrations, the two agonist binding sites (see section 1.4). The high affinity site is conventionally equated with the site labelled within the ion channel by CPZ and TPMP (see section 1.4.1.2); the low affinity sites are less well defined. NCIs are able to shift nAChR from the resting, R, state to a desensitised, D, state (see section 1.4). This may not be an identical structural conformation to that induced by extended exposure to agonists. The NCI has a higher affinity for the D state, and binds to the small proportion of nAChR always present in this state. The distribution of conformations within the receptor population is then

pulled, essentially completely, towards the D state by mass action. This stabilisation of the D state by the antagonist may be achieved by interaction with either the high or low affinity binding sites.

4.3.1 Dihydro-ß-erythroidine

DHßE has been reported to be a simple competitive antagonist (see section 4.1.4); the data presented here confirm this. In competition assays with [^{3}H]nicotine, DHßE inhibited binding with a greater potency than the other antagonists (IC_{50} = 5.3μM). This inhibition was due a significant reduction in the affinity of [^{3}H]nicotine binding to Triton extracts (see Fig. 4.11), as would be expected for a competitive inhibitor. The affinity of DHßE for the functional, R-state nAChR proved more difficult to measure. Previous studies suggested an affinity in the micromolar range (see section 4.1.4); a similarity in affinity for both R- and D-states is also characteristic of competitive antagonists (see section 5.1). However the antagonist appeared ineffectual in the ^{86}Rubidium$^+$ influx assay, even at high concentrations. This lack of efficacy may stem from a difference in the association kinetics of agonist and antagonist, as suggested by Alkondon & Albuquerque (1993); (-)nicotine was able to bind to, and activate, the receptor more quickly than DHßE could have its effect. This could be tested quite readily by examining the effect of preincubation of the M10 cells with DHßE upon ion flux.

4.3.2 **Mecamylamine**

In contrast to the apparent confusion concerning the mechanism of mecamylamine interaction with nAChR (see section 4.1.2), there is a surprising degree of consistency to the concentrations of mecamylamine reported to elicit functional receptor blockade. Thus, the IC_{50} value reported here for mecamylamine at M10 cell $\alpha 4\beta 2$ nAChR (1μM; see section 4.2.3) compares favourably with the inhibition of [^{3}H]dopamine release from striatal synaptosomes (Rapier et al.,1990). A 50% blockade of the putative $\alpha 4\beta 2$ nAChR in the latter system was achieved at 5μM mecamylamine. When expressed in Xenopus oocytes, 100nM mecamylamine inhibited $\alpha 4\beta 2$ nAChR-derived currents (Bertrand et al.,1990). Unfortunately, the percentage blockade at this concentration was not recorded. At ganglia, 25-100nM mecamylamine attenuated nicotinic responses (Ascher et al., 1979), whilst Lukas (1989) reported an affinity of 0.2μM in PC12 cells. The antagonist may be less potent at muscle-type nAChR; in TE671 cells IC_{50} = 30μM (Lukas, 1989), though 10μM was sufficient to completely depress evoked frog muscle twitches (Varanda èt al., 1985).

Saturation [^{3}H]nicotine binding studies in the presence of mecamylamine gave rise to curvilinear Scatchard transforms (see Fig. 4.12). The shape, concave downwards, is believed to be indicative of positive cooperativity (De Lean & Robard, 1979), though the underlying mechanism in such an instance is unclear. It is possible that the effect may be artifactual; reproducibility at various

concentrations suggests this is not the case. Kermode (1989) suggested several possible causes of such artifacts in Scatchard analyses. However, all appear equally applicable to assays both in the presence and absence of mecamylamine (which were conducted in parallel), or, are of no relevance to a detergent extract. Interestingly, Takayama et al. (1989) reported no curvilinearity when performing a similar assay in the presence of 600μM mecamylamine. It is possible that the use of membrane-bound nAChRs in this study prevented whatever underlies the observation; the lipid environment is known to effect receptor conformation (McCarthy & Moore, 1992). Nevertheless, the effect is peculiar to mecamylamine, and was not seen when the other antagonists were examined. One possible interpretation of the binding data is that under certain assay conditions, the receptor population is no longer solely in a single desensitised state, but two structurally distinct conformations. This concept is explored further in section 5.2.

4.3.3 **MK-801**

The effects of MK-801 on [^{3}H]nicotine binding to Triton X-100 extracts, and what those data imply about the drug's mode of antagonism, are fully discussed in section 5.2. The potency of MK-801 in attenuating ^{86}Rubidium$^+$ flux into M10 cells is less than might have been predicted from Ramoa et al. (1990), in which 25μM was reported as sufficient to inhibit (-)nicotine-evoked τ-amino[2,3-

[^{3}H]butyric acid release from hippocamapal synaptosomes.

The sensitivity of [^{3}H]MK-801 binding to PCP confirms the identification of the antagonist as a channel blocker in neuronal nAChR. However, no increase in [^{3}H]MK-801 was evident on addition of agonist. One possible explanation is that the binding of the receptor oligomer by the monoclonal antibody used in the purification procedure "locks" the nAChR into a more rigid, though still desensitised, state. It should be noted that Ramoa et al. (1990) saw no increase in binding to muscle-type receptors, thus the effect of the antibody may be negligible. If MK-801 follows the pattern of PCP and H_{12}-HTX (both of which it can displace; see section 4.1.2), and is, in allosteric terms, a "non-exclusive effector" (Rubin & Changeux, 1966), then its affinity for the channel blocker site is only marginally greater in the presence of an agonist than in its absence in any case.

4.3.4 **Chlorisondamine**

Chlorisondamine produces a long-lasting central nicotinic blockade, though its mechanism of action is poorly characterised (see section 4.1.4). The ion flux dose-response curve for chlorisondamine suggests it to be a highly potent antagonist of nAChR function, almost totally attenuating ^{86}Rubidium$^+$ when present in concentrations greater than $1x10^{-8}$M (see section 4.2.3). If a slow rate of metabolism is assumed for the drug, one might envisage a situation in which the chlorisondamine

concentration *in vivo* remains in excess of that required for nAChR blockade for some considerable time.

Chronic *in vivo* exposure to (-)nicotine and other agonists leads to an increased density ("upregulation") of [^{3}H]nicotine binding sites (reviewed in Wonnacott, 1990). It has been suggested that a prolonged, agonist-induced desensitisation underlies these observations, and consequently treatment with antagonists should yield similar results. In this study, there was no statistically significant increase in the mean [^{3}H]nicotine binding density in chlorisondamine-treated animals, compared to controls. Binding data from the cortices of treated animals showed a particularly wide scatter (see Fig. 4.18); half of the subjects had greatly elevated levels of binding, whilst the other half were similar to controls. The concentration of chlorisondamine used was that reported to be effective by Clarke *et al*. (1984), thus one must presume that the drug crossed the blood-brain barrier. The relationship between treatment time and the rate of the mechanisms involved in any possible upregulation of nAChR is crucial. Thus, whilst all subjects received the same dose of chlorisondamine and all were killed one week later, the different levels of response to the drug treatment may be due to variability in the rate of chlorisondamine metabolism between individuals.

Chlorisondamine appeared to reduce [^{3}H]nicotine binding to Triton extracts in competition assays from concentrations of $1x10^{-5}$M. This attenuation of binding

seemed to stem from reductions in both the number and affinity of binding sites (see Fig. 4.17), though only the reduction in the former was statistically significant. These observations imply that chlorisondamine may act as both a competitive and allosteric inhibitor. Interestingly, Daly et al. (1991) reported that, in PC12 cells at least, the affinities of chlorisondamine for the agonist and channel blocker binding sites were very similar. The mechanism of action is obviously a complex one; for further discussion, see section 5.2.

4.3.5 Summary

The interactions of a number of antagonists with the neuronal α4ß2 nAChR subtype have been examined. Whilst all were able to attenuate $^{86}Rubidium^{+}$ influx, each of the four antagonists - DHßE, mecamylamine, MK-801 and chlorisondamine - had different effects on high affinity agonsit binding to Triton X-100 extracts of rat brain P2 membrane preparations. The possible mechanisms behind these observations are examined in sections 5.1 and 5.2.

Fig. 4.1 **Energy minimised structural models of (A) DHßE, (B) mecamylamine, (C) MK-801 and (D) chlorisondamine.** Structures were provided courtesy of P. Thomas, and were built using the HYPERCHEM modelling package (Autodesk Inc., California, U.S.A.). Individual atoms are represented as colour coded van der Waals spheres (white - oxygen; pale blue - carbon; dark blue - nitrogen; red - oxygen; green - chlorine).

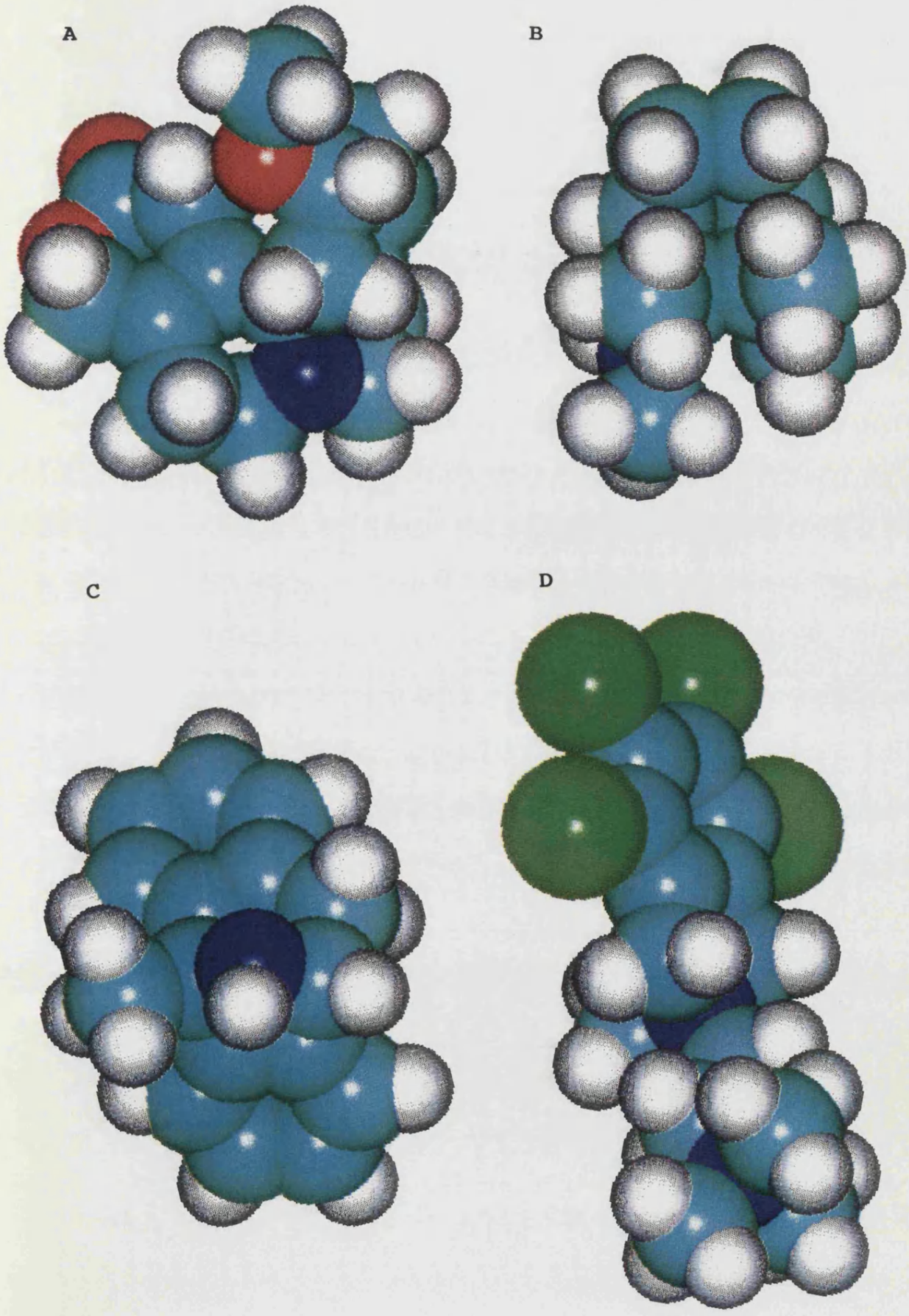
A
B
C
D

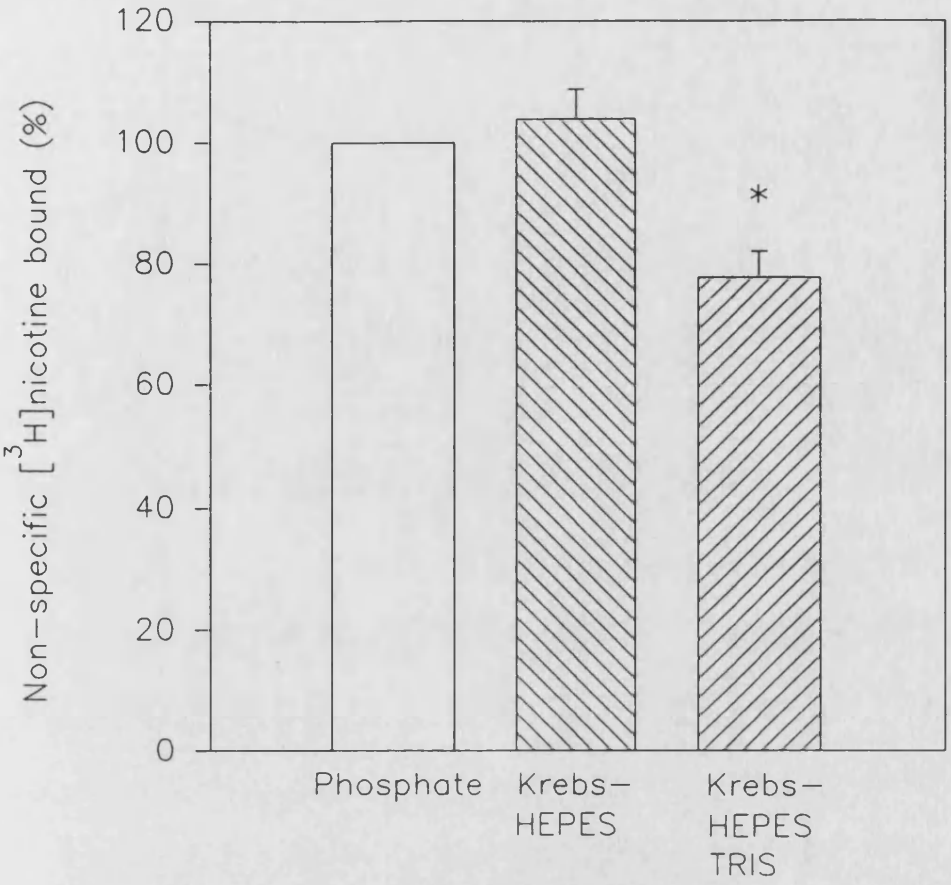

Fig. 4.2 **Comparison of non-specific [^{3}H]nicotine binding to Triton extracts in different buffering systems.** P2 membranes were extracted with 0.5% (v/v) Triton X-100 in a series of different buffers (50mM Phosphate, Krebs-HEPES, and Krebs-HEPES additionally containing 200mM TRIS). [^{3}H]-Nicotine binding (final concentration 20nM) was assayed by standard techniques (see section 2.2.1.3.1). In each assay, non-specific binding, measured in the presence of unlabelled nicotine, was calculated as a percentage of the total in each buffer. Each column represents the mean±SEM of three separate determinations. For comparison, each set of data was then standardised against the non-specific [^{3}H]nicotine binding in the phosphate buffer (which was taken as 100%). * Significantly different from phosphate buffer ($p<0.05$).

Fig. 4.3 **Comparison of the properties of different glass-fibre filter grades with respect to (A) specific and (B) non-specific [^{3}H]nicotine binding to Triton extracts.** [^{3}H]Nicotine binding (final concentration 20nM) to identical detergent extract samples in Krebs-HEPES-TRIS buffer was assayed as previously. Bound and free radioligand were separated from unbound by filtration on GFA/E, GFB and GFC glass-fibre filters. Bound radioactivity was calculated as fmol [^{3}H]nicotine/mg protein (open columns) or % total binding (shaded columns). Each column represents the mean± SEM of three separate determinations.

A

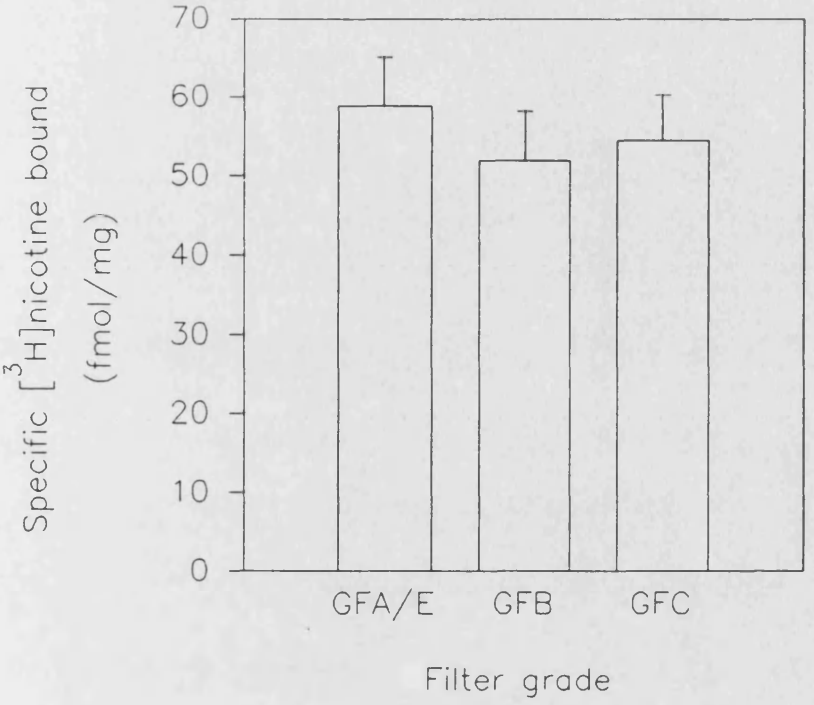
Specific [3H]nicotine bound
(fmol/mg)
70
60
50
40
30
20
10
0
GFA/E
GFB
GFC
Filter grade

B

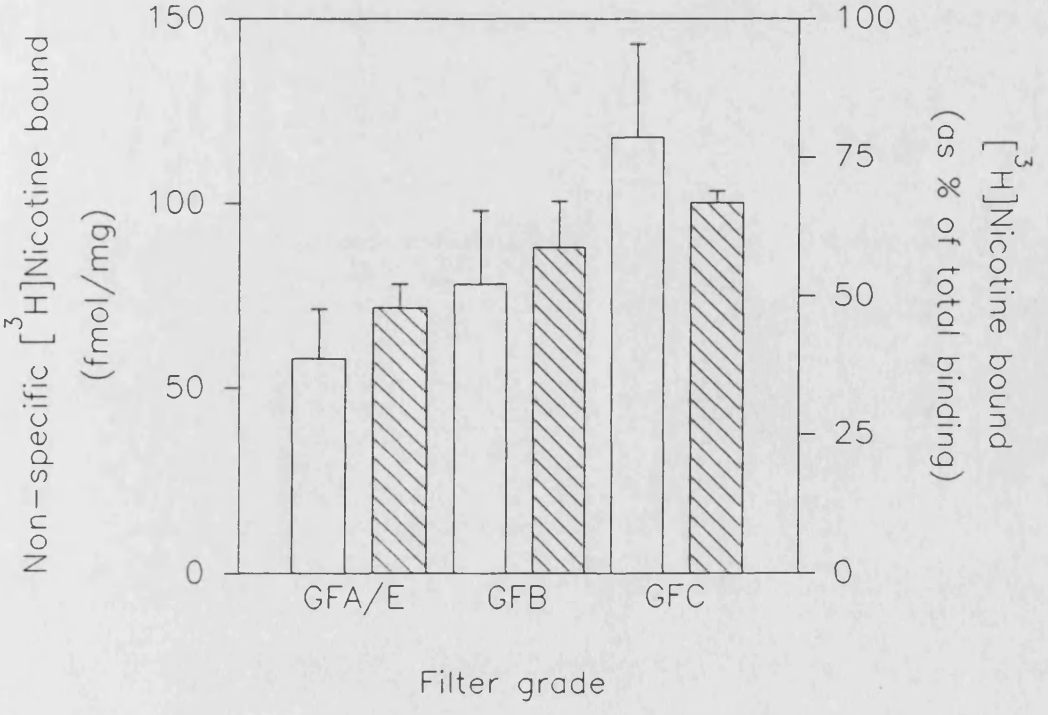
Non-specific [3H]Nicotine bound
(fmol/mg)
150
100
50
0
100
75
50
25
0
[3H]Nicotine bound
(as % of total binding)
GFA/E
GFB
GFC
Filter grade

Fig. 4.4 **The effects of Triton X-100 on [^{3}H]nicotine binding (I).** (A) [^{3}H]Nicotine binding (20nM) to Triton X-100 extract (supernatant) and residual pellet expressed as a percentage of the original P2. (B) Effect of increasing Triton X-100 concentration on [^{3}H]nicotine binding to P2 membranes.

A

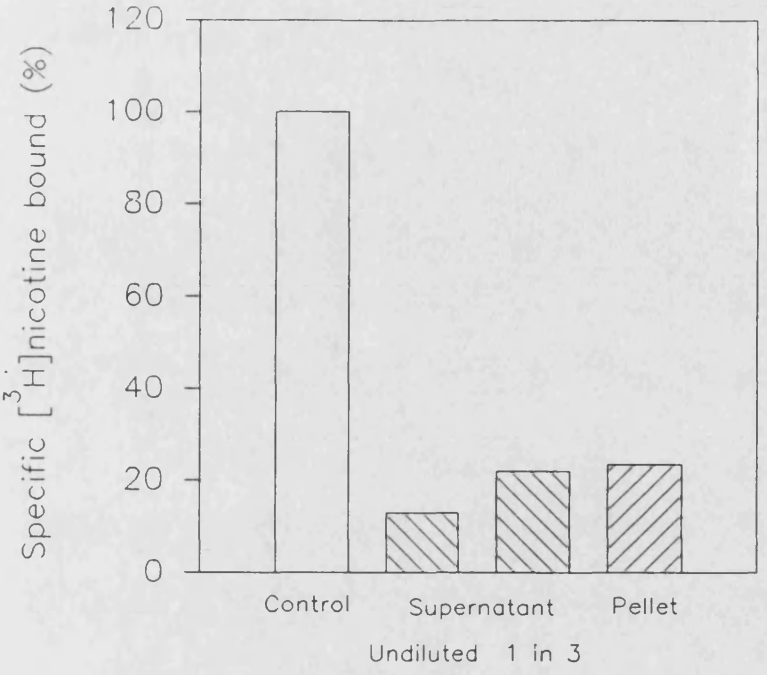
Specific [3H]nicotine bound (%)
120
100
80
60
40
20
0
Control
Supernatant
Pellet
Undiluted
1 in 3

B

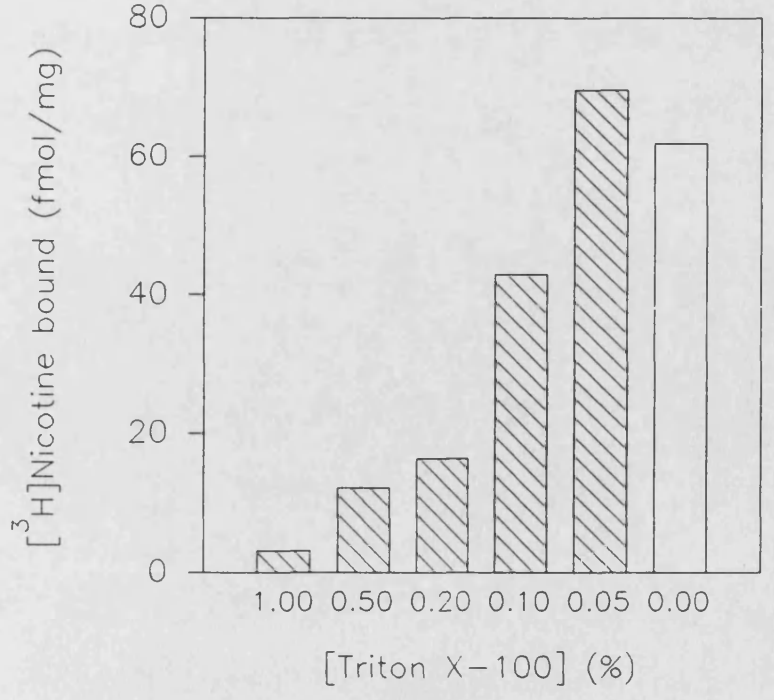
[3H]Nicotine bound (fmol/mg)
80
60
40
20
0
1.00
0.50
0.20
0.10
0.05
0.00
[Triton X-100] (%)

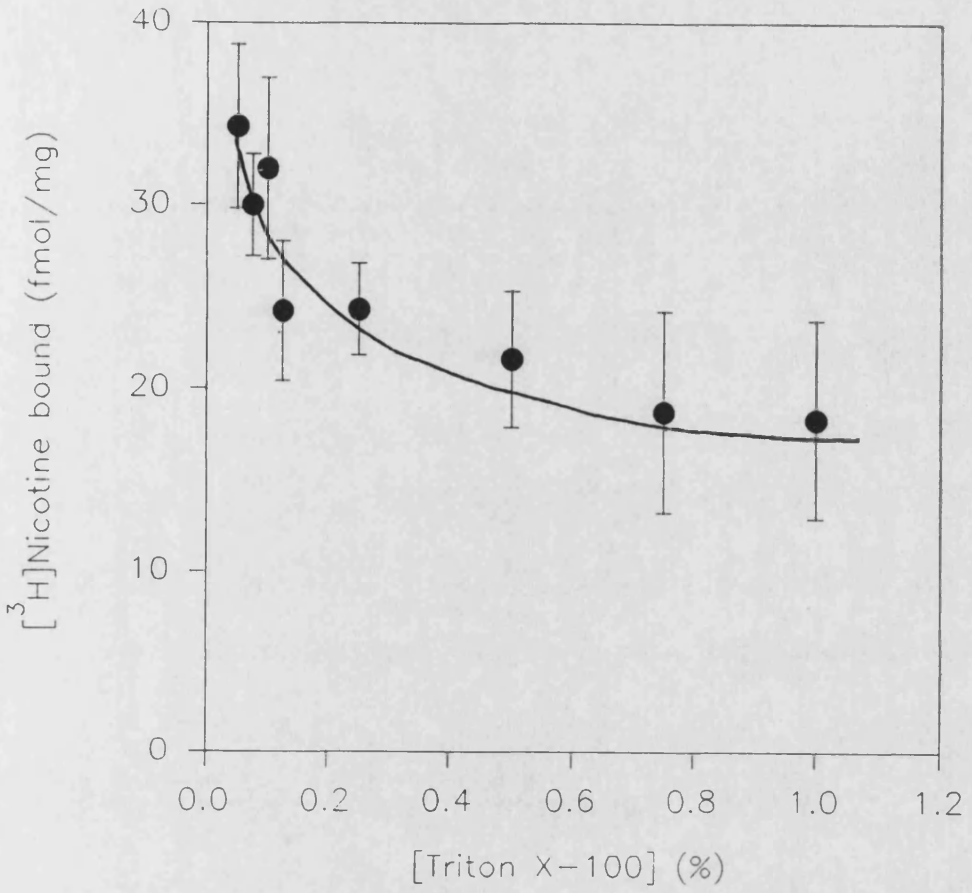

Fig. 4.5 **The effects of Triton X-100 on [^{3}H]nicotine binding (II).** [^{3}H]Nicotine binding (20nM) to detergent extracts was assayed at a constant protein concentration in the presence of increasing concentrations of Triton X-100. Each point is the mean ± SEM of 3 determinations.

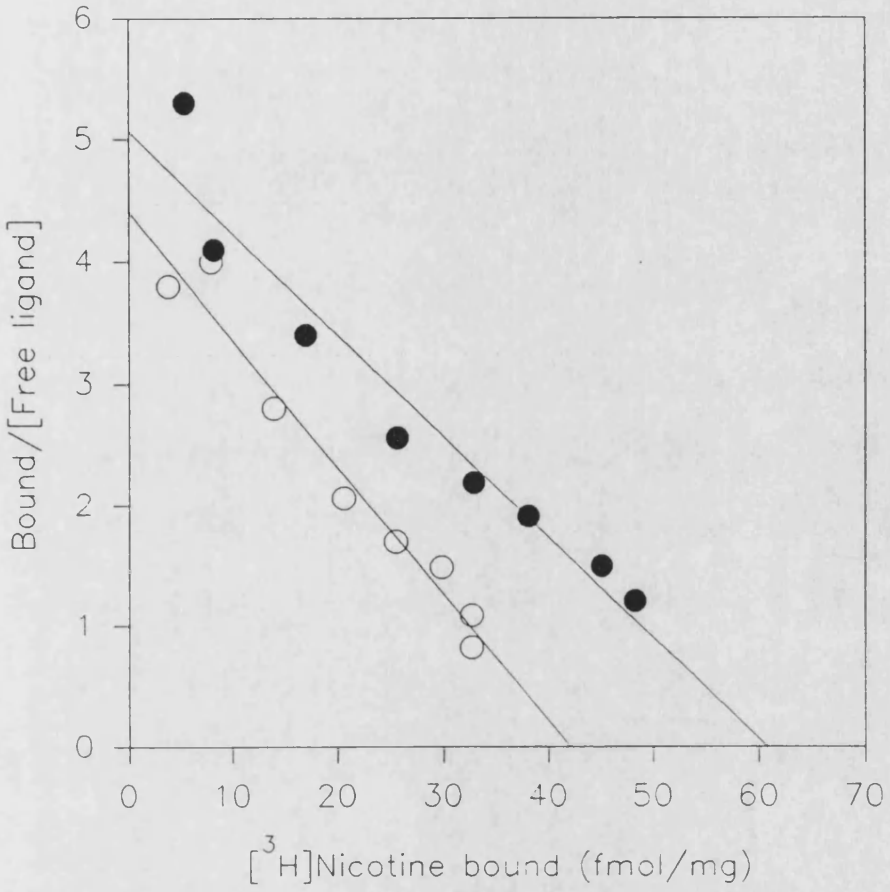

Fig. 4.6 **Comparison of [^{3}H]nicotine binding to P2 membranes and Triton extracts.** Scatchard analyses of [^{3}H]nicotine saturation assays performed in parallel on a P2 membrane preparation (●), and a Triton extract prepared from it (O) are shown. The data are from a single representative experiment performed as previously, using triplicate samples. The binding parameters were calculated as: Kd: P2 = 11nM, extract = 9nM; Bmax: P2 = 62fmol/mg, extract = 43fmol/mg.

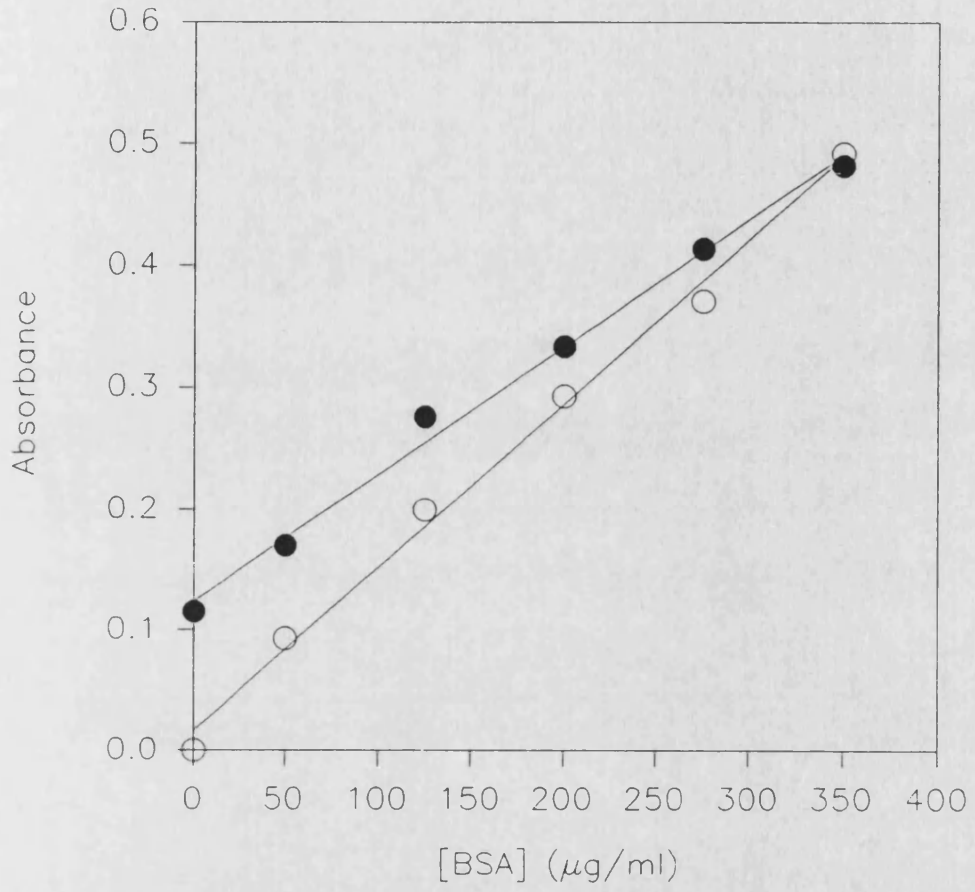

Fig. 4.7 **The effect of Triton X-100 on protein determinations.** Concentrations of BSA standards were determined by the Lowry method (Lowry et al., 1954) in the absence (O) and presence (●) of 10μl Krebs-TRIS-HEPES buffer additionally containing 0.5% (v/v) Triton X-100. The data shown are from a single representative experiment, each point representing the mean of triplicate samples.

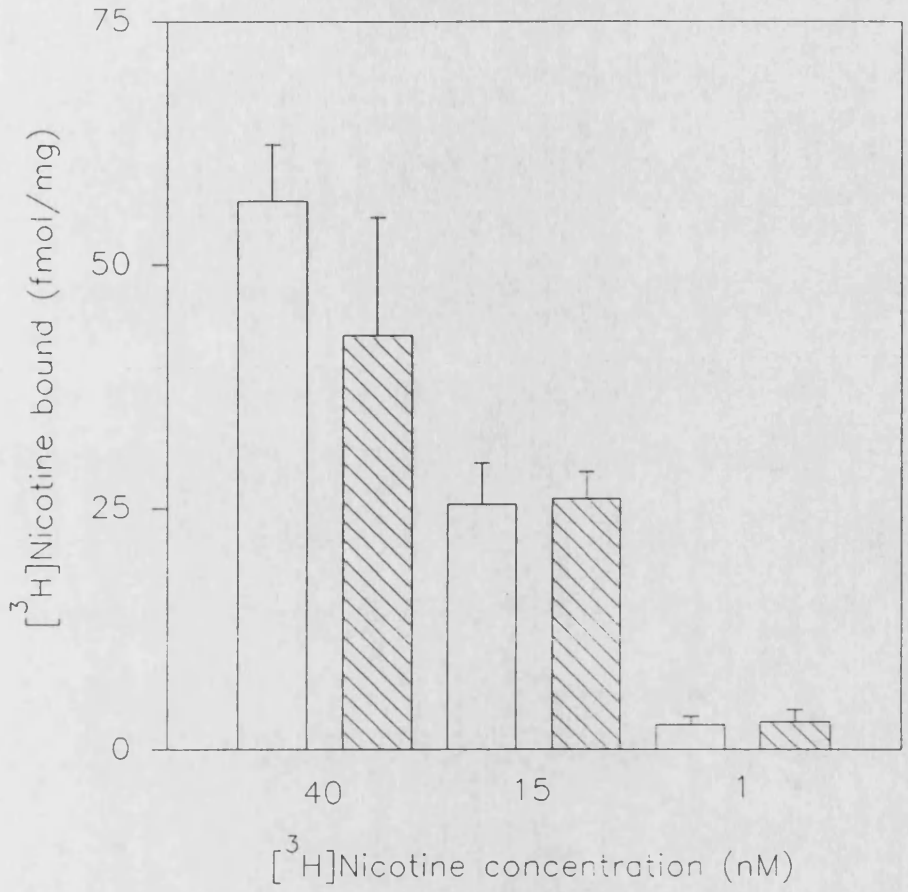

Fig. 4.8 **The effect of ethanol on [^{3}H]nicotine binding.** [^{3}H]Nicotine binding to Triton extracts was assayed at three radioligand concentrations (1nM, 15nM and 40nM) in the presence (shaded columns) and absence (open columns) of 10μl 95% (v/v) ethanol. Each column represents the mean ± SEM of three determinations.

Fig. 4.9 **Typical [^{3}H]nicotine binding parameters in Triton X-100 extracts.** [^{3}H]Nicotine saturation binding to Triton extracts typically gave hyperbolic specific binding curves. Specific [^{3}H]nicotine binding was calculated as the difference between radioligand binding to Triton extracts assayed in the absence (TOTAL BINDING) and presence (NON-SPECIFIC BINDING) of excess (1μM) unlabelled (-)nicotine (see section 2.2.1.3.1). Representative data (A) and Scatchard transformation (B) from a single experiment are shown. In this experiment Kd = 11nM, Bmax = 135fmol/mg (regression coefficient = -0.98).

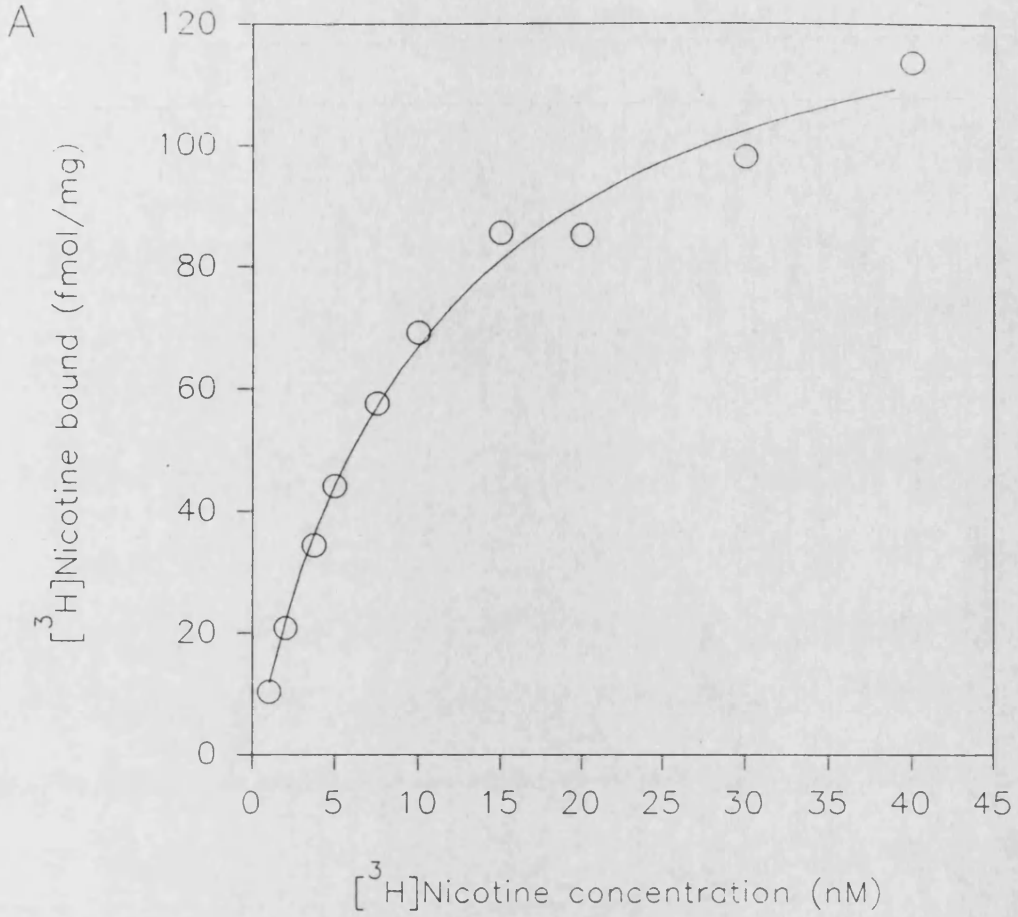
A
120
100
80
60
40
20
0
[3H]Nicotine bound (fmol/mg)
0
5
10
15
20
25
30
35
40
45
[3H]Nicotine concentration (nM)

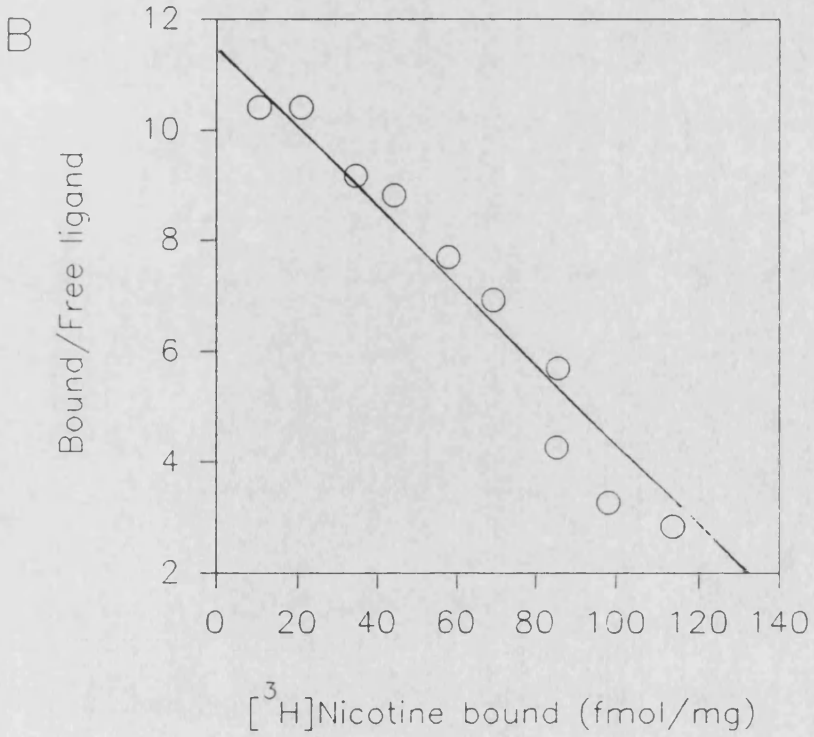
B
12
10
8
6
4
2
Bound/Free ligand
0
20
40
60
80
100
120
140
[3H]Nicotine bound (fmol/mg)

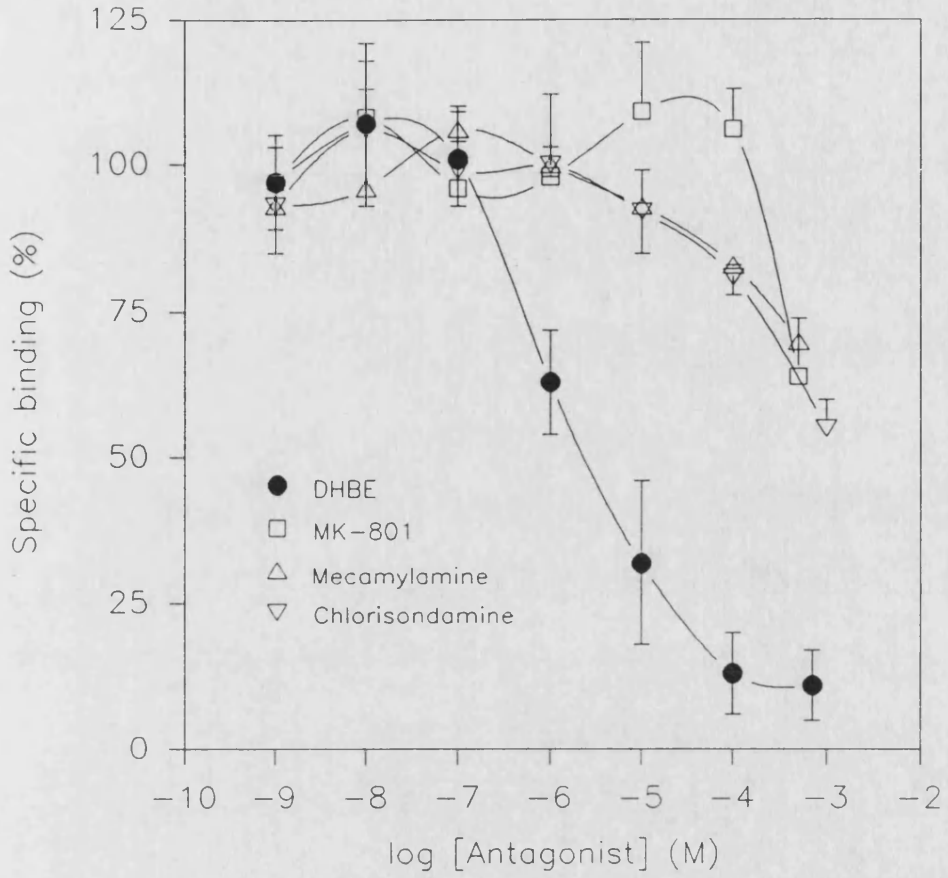

Fig. 4.10 **The effects of DHßE, mecamylamine, MK-801 and chlorisondamine on [^{3}H]nicotine binding to Triton X-100 extracts.** Specific [^{3}H]nicotine binding (triplicate samples, final concentration 10nM) to Triton extracts was assayed in the presence of increasing concentrations of each of the four antagonists. The data were expressed as a percentage of the binding observed in the absence of the drugs. Each point represents the mean ± SEM of three separate determinations.

Fig. 4.11 **The effect of DHßE on [^{3}H]nicotine binding parameters in Triton X-100 extracts.** Saturation binding of [^{3}H]nicotine to Triton extracts was measured in the presence (●) and absence (O) of 5μM DHßE. A representative specific binding curve (A), and Scatchard transformation of the data (B), are shown. In this experiment control, Kd = 20nM and Bmax = 92 fmol/mg; in the presence of DHßE, Kd = 48nM and Bmax = 94fmol/mg.

A

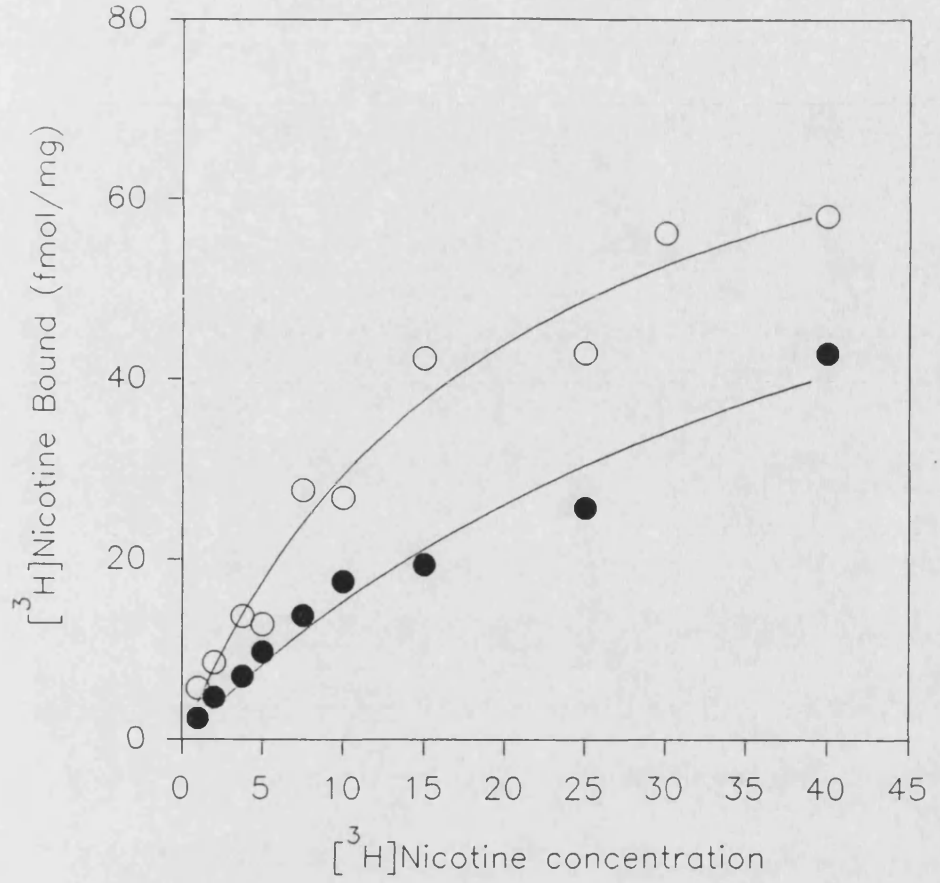
80
60
40
20
0
[3H]Nicotine Bound (fmol/mg)
0
5
10
15
20
25
30
35
40
45
[3H]Nicotine concentration

B

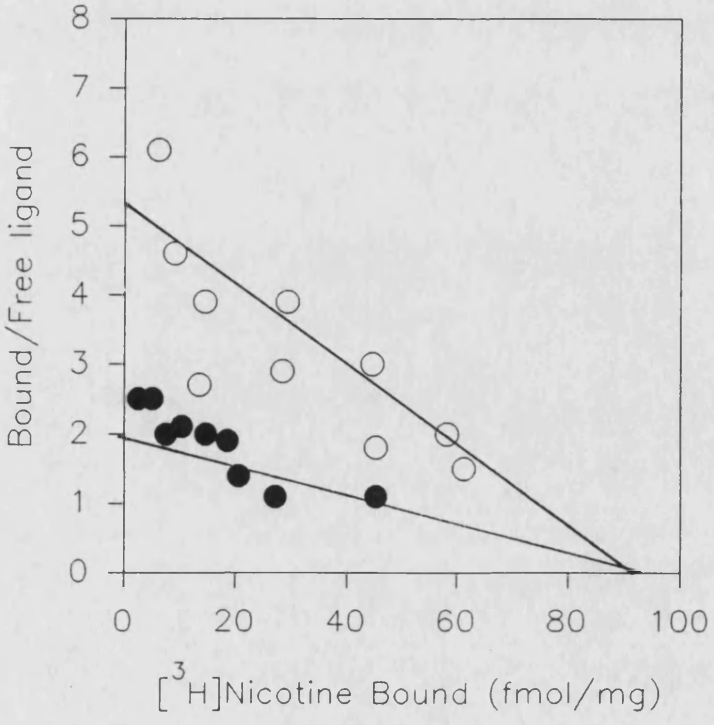
8
7
6
5
4
3
2
1
0
Bound/Free ligand
0
20
40
60
80
100
[3H]Nicotine Bound (fmol/mg)

Fig. 4.12 **The effect of mecamylamine on [^{3}H]nicotine binding parameters in Triton X-100 extracts.** (A) Representative experiment of saturation binding to Triton extracts was measured in the presence (▲) and absence (O) of 180μM mecamylamine. Representative Scatchard transformations of the data are shown. In this experiment, control Kd = 15nM, Bmax = 88fmol/mg. Scatchard data in the presence of mecamylamine best fitted a second order regression (r = 0.89); Kd was not determinable, Bmax was estimated at 86fmol/mg. (B) Scatchard analyses of another experiment of [^{3}H]nicotine binding in the presence of 600μM (◊) and 60μM (♦) mecamylamine. (Control Kd=16nM, Bmax=143fol/mg; data not shown.)

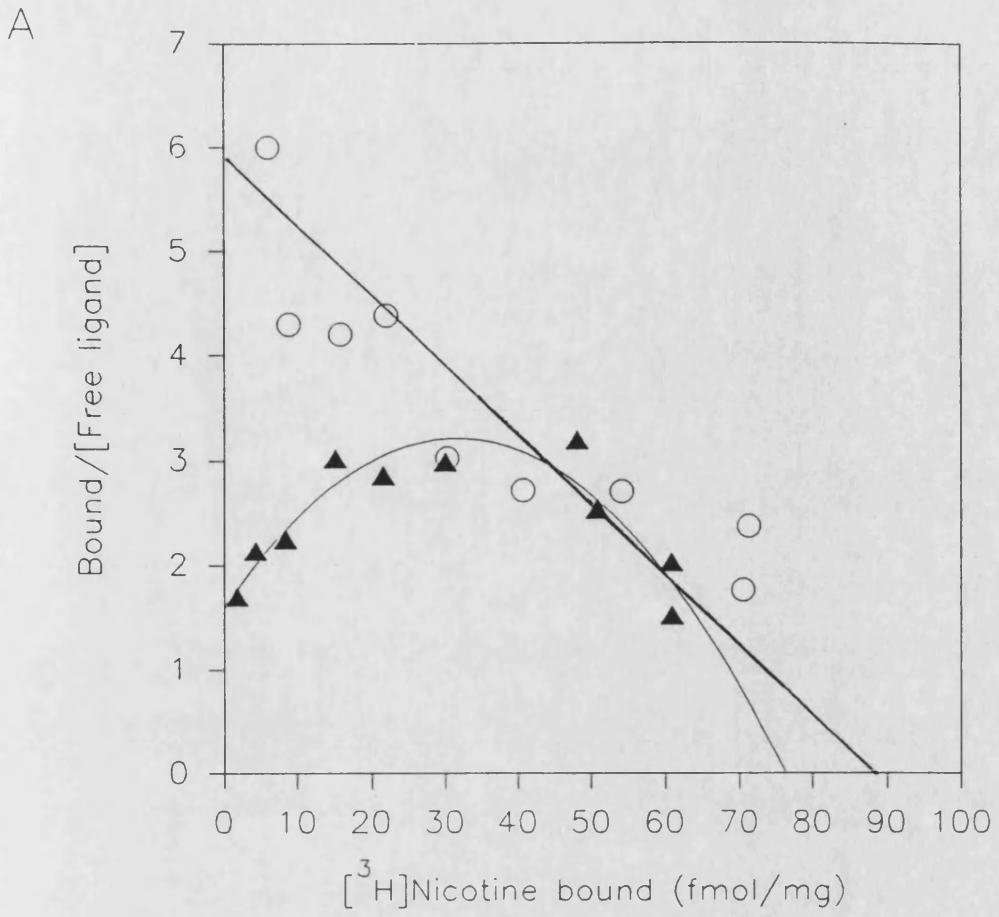
A
Bound/[Free ligand]
0
1
2
3
4
5
6
7
0 10 20 30 40 50 60 70 80 90 100
[3H]Nicotine bound (fmol/mg)

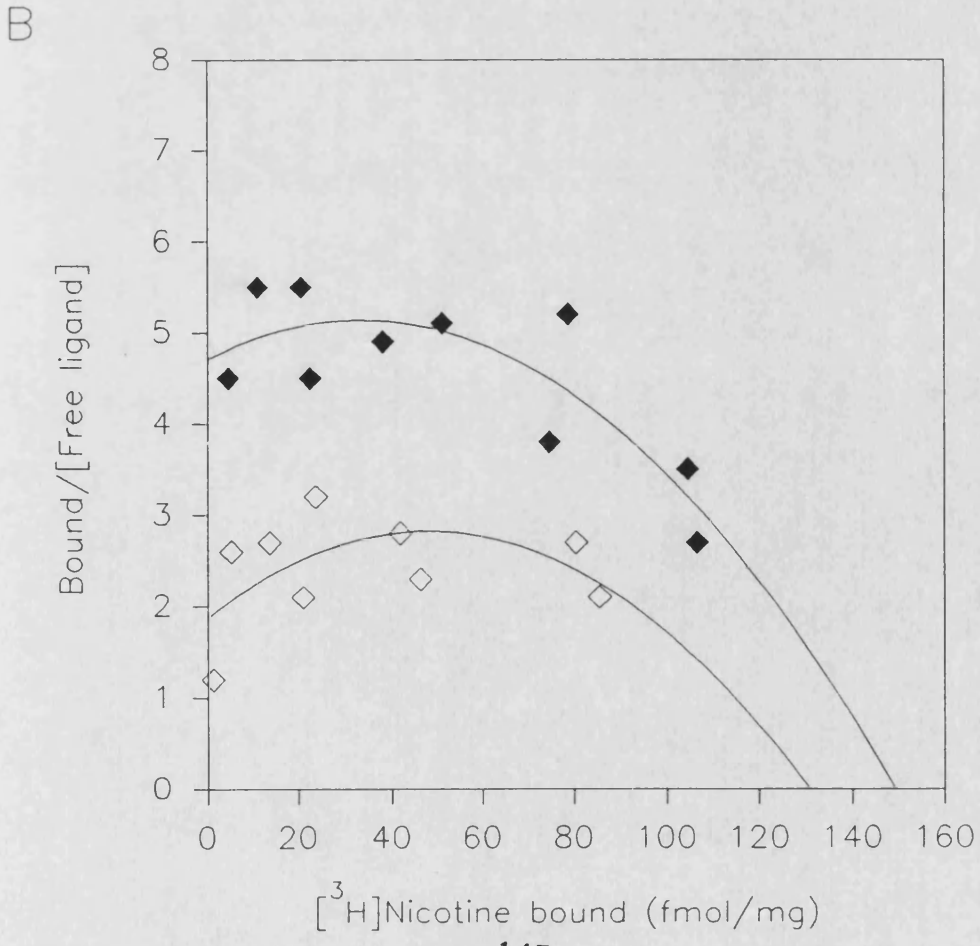
B
Bound/[Free ligand]
0
1
2
3
4
5
6
7
8
0 20 40 60 80 100 120 140 160
[3H]Nicotine bound (fmol/mg)

Fig. 4.13 **The time course of 2nM [^{3}H]nicotine binding in the absence (A) and presence (B) of mecamylamine.** The association of 2nM [^{3}H]nicotine with Triton extracts as a function of time was examined by determination of the amount of radioligand bound at intervals up to 180 minutes (which was taken as equilibrium). In controls (A), the time at which half-maximal saturation occurred ($t_{½}$) was found, by a non-linear iterative curve fitting, to be 32 minutes. Each point represents the mean ± SEM of at least 4 determinations performed in duplicate. In the presence of 180μM mecamylamine (B), a similar analysis gave a $t_{½}$ = 2.7 minutes. Each point represents the mean ± the range of at least 2 determinations.

A

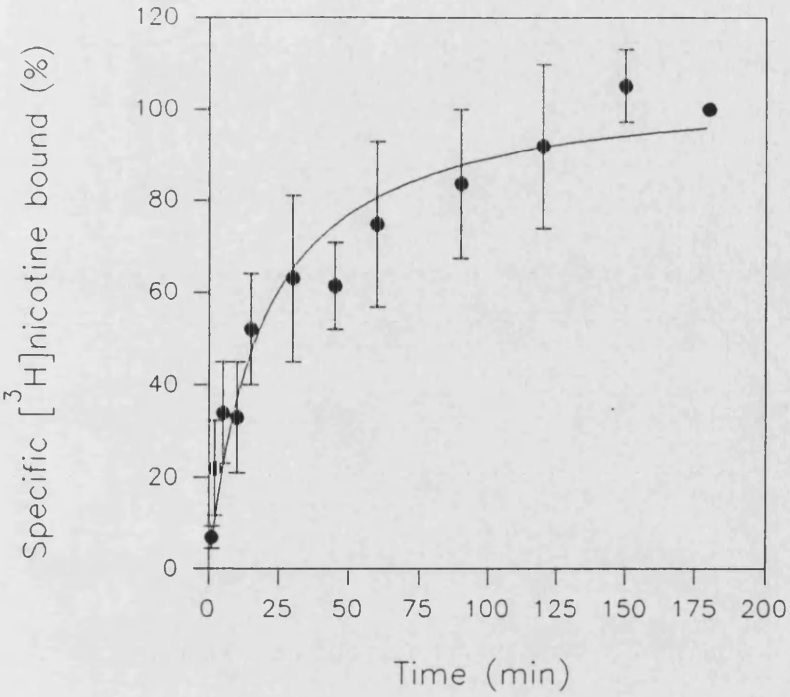
Specific [3H]nicotine bound (%)
120
100
80
60
40
20
0
0
25
50
75
100
125
150
175
200
Time (min)

B

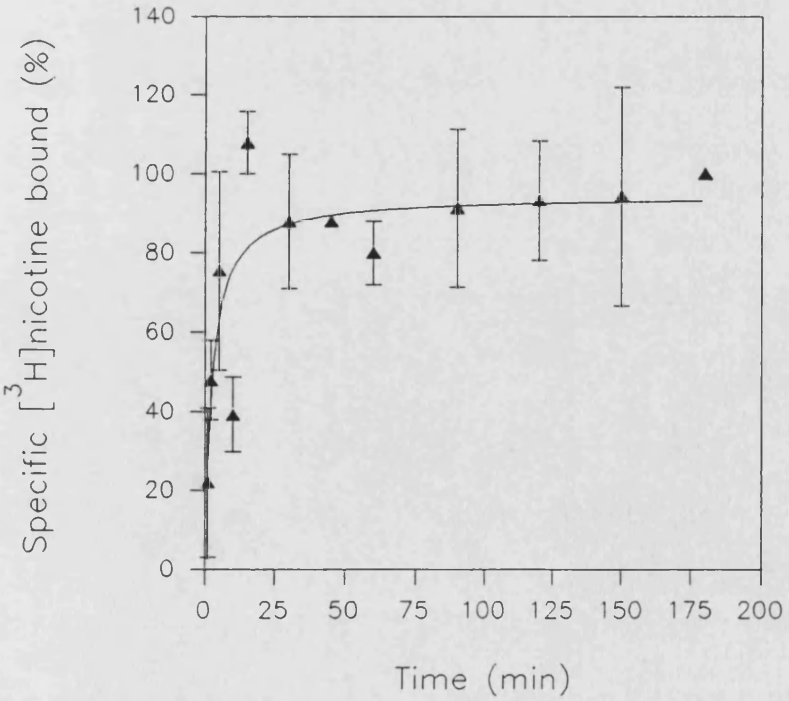
Specific [3H]nicotine bound (%)
140
120
100
80
60
40
20
0
0
25
50
75
100
125
150
175
200
Time (min)

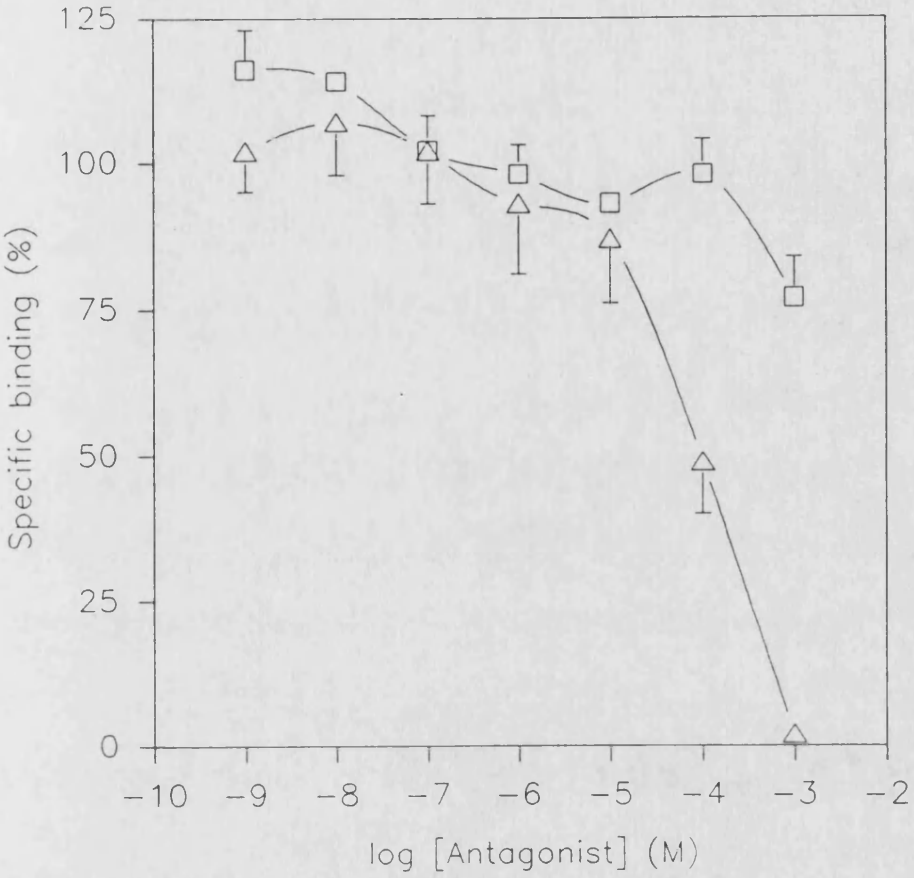

Fig. 4.14 **The effects of mecamylamine and MK-801 on [^{3}H]-nicotine binding to Triton extracts at low radioligand concentrations.** Competition binding assays were performed as before (see Fig. 4.10), except that the [^{3}H]nicotine concentration was reduced from 10nM to 2nM. For mecamylamine (180μM; $\triangle$), each point represents the mean ± SEM of 3 separate determinations, for MK-801 (500μM; $\square$), each point represents the mean ± the range of 2 determinations.

Fig. 4.15 **The effect of MK-801 on [^{3}H]nicotine binding parameters in Triton X-100 extracts.** Saturation binding of [^{3}H]nicotine to Triton extracts was measured in the presence (□) and absence (○) of 500μM MK-801. Representative specific binding curves (A) and Scatchard transformations of the data (B) are shown. In this experiment, Kd and Bmax values were: control Kd = 20nM, Bmax = 81fmol/mg; with MK-801 Kd = 53nM, Bmax = 99fmol/mg.

A

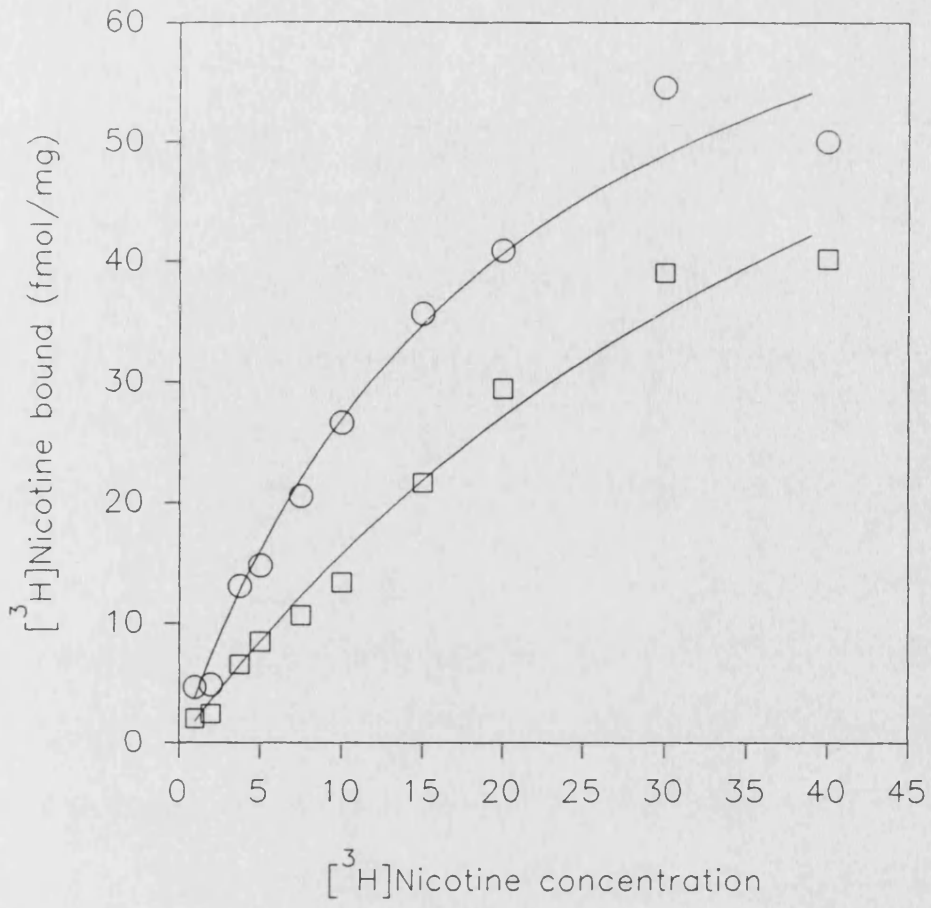
60
50
40
30
20
10
0
0 5 10 15 20 25 30 35 40 45
[3H]Nicotine bound (fmol/mg)
[3H]Nicotine concentration

B

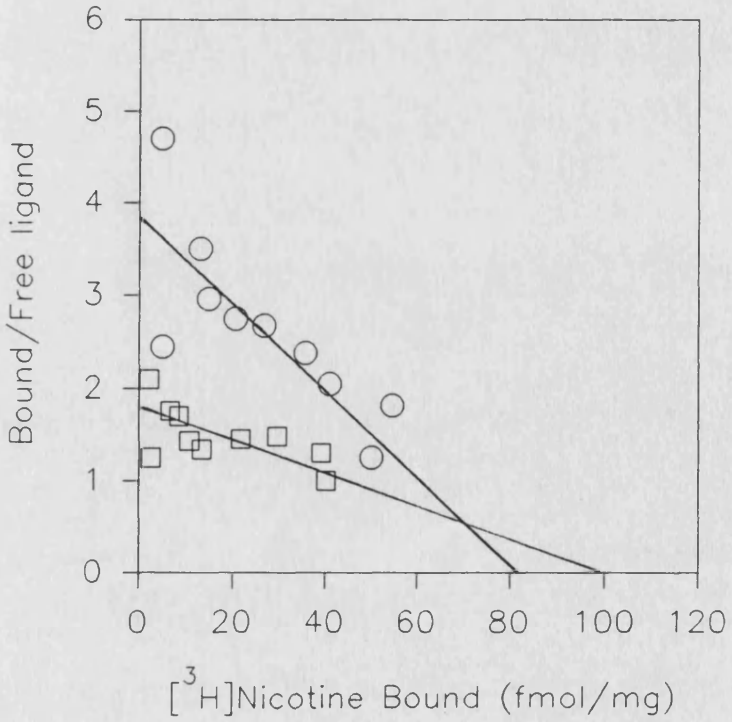
6
5
4
3
2
1
0
0 20 40 60 80 100 120
Bound/Free ligand
[3H]Nicotine Bound (fmol/mg)

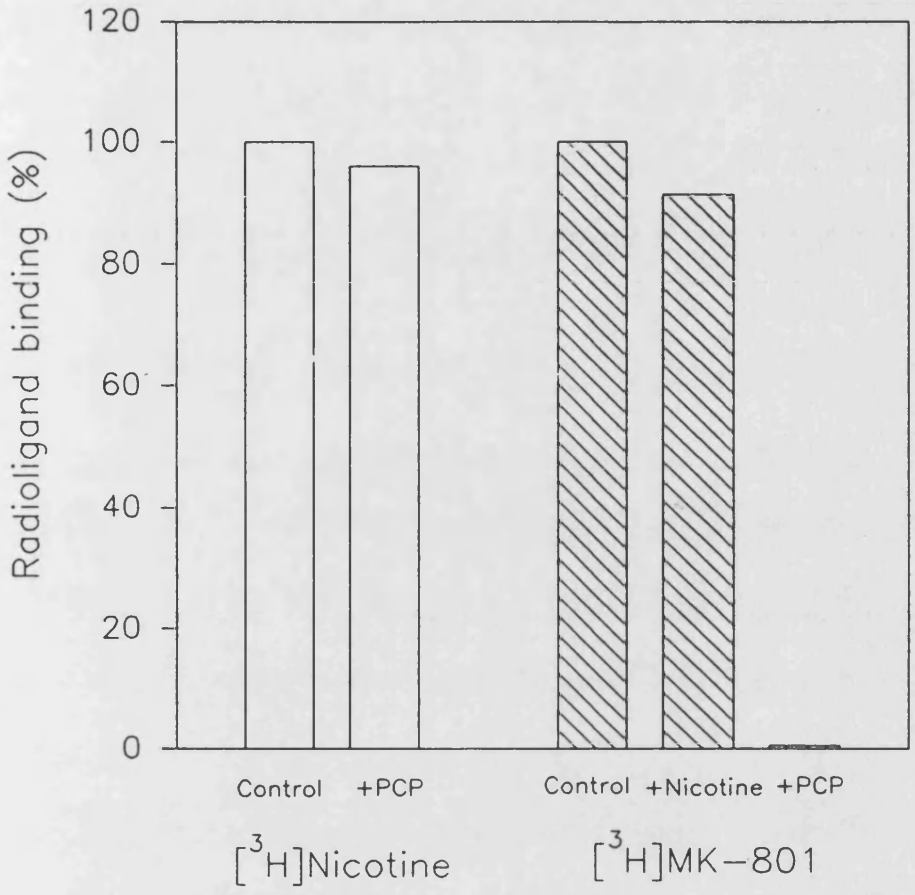

Fig. 4.16 **Comparison of [^{3}H]nicotine and [^{3}H]MK-801 binding to immunoimmobilised α4ß2 nAChR.** Three days after induction by 1μM dexamethasone, α4ß2 nAChR were solublised from M10 cells, and [^{3}H]nicotine (20nM) and [^{3}H]MK-801 (5μM) binding to the immunoimmobilised receptors was determined. Non-specific radioligand binding was defined as that to an equivalent volume (25μl) of Sepharose-GART. Control values of radioligand binding were: 99-103fmol and 55-61fmol/10cm diameter dish for [^{3}H]nicotine and [^{3}H]MK-801 binding respectively.

Fig. 4.17 **The effect of chlorisondamine on the [^{3}H]nicotine binding to Triton extracts.** Saturation binding of [^{3}H]nicotine to Triton extracts was measured in the presence (▽) and absence (○) of 20μM chlorisondamine. Representative specific binding curve (A) and Scatchard transformations of the data (B) are shown. In this experiment Kd and Bmax values were: control Kd = 19nM, Bmax = 115fmol/mg; with chlorisondamine Kd = 25nM, Bmax = 73 fmol/mg.

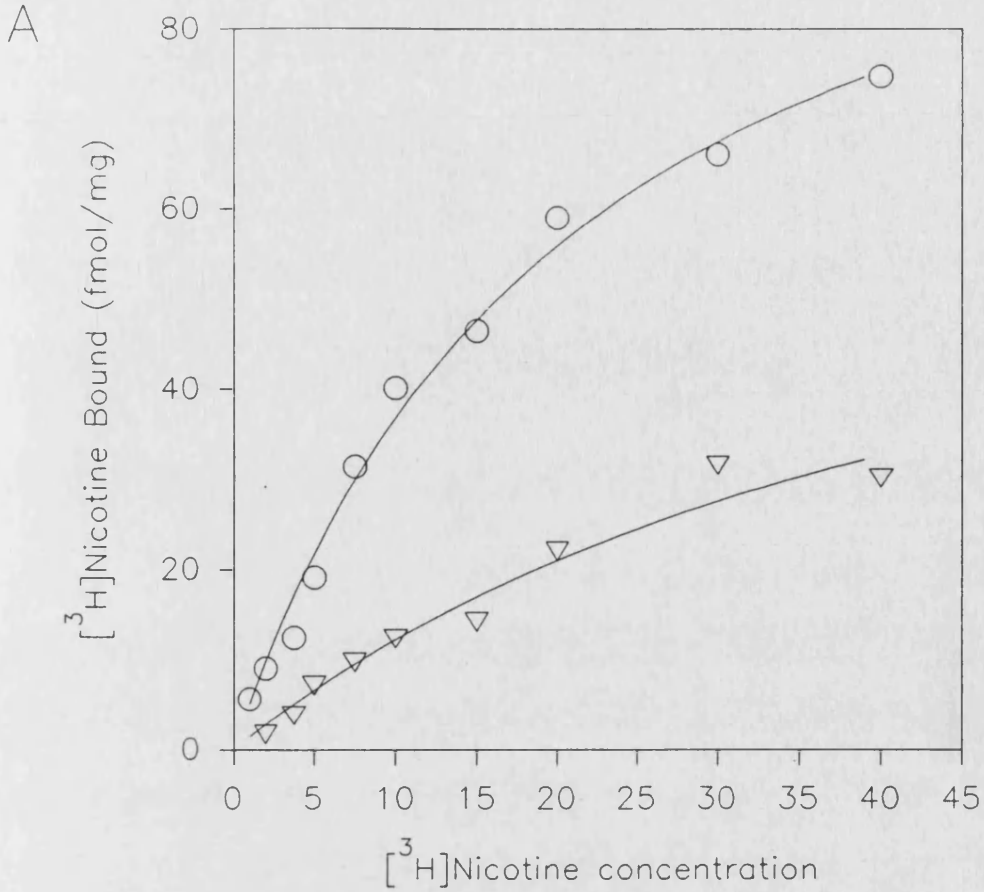
A
80
60
40
20
0
[3H]Nicotine Bound (fmol/mg)
0
5
10
15
20
25
30
35
40
45
[3H]Nicotine concentration

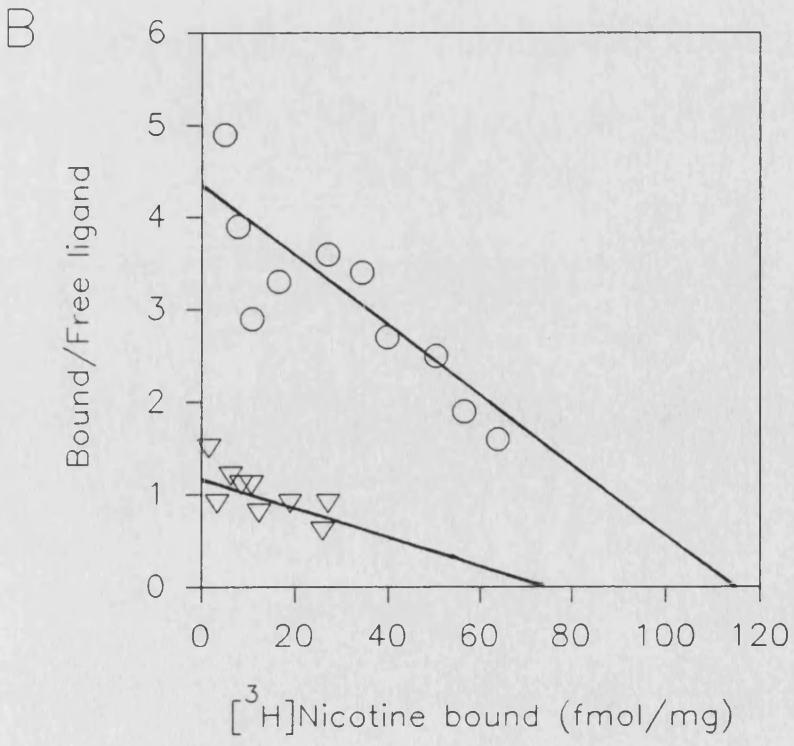
B
6
5
4
3
2
1
0
Bound/Free ligand
0
20
40
60
80
100
120
[3H]Nicotine bound (fmol/mg)

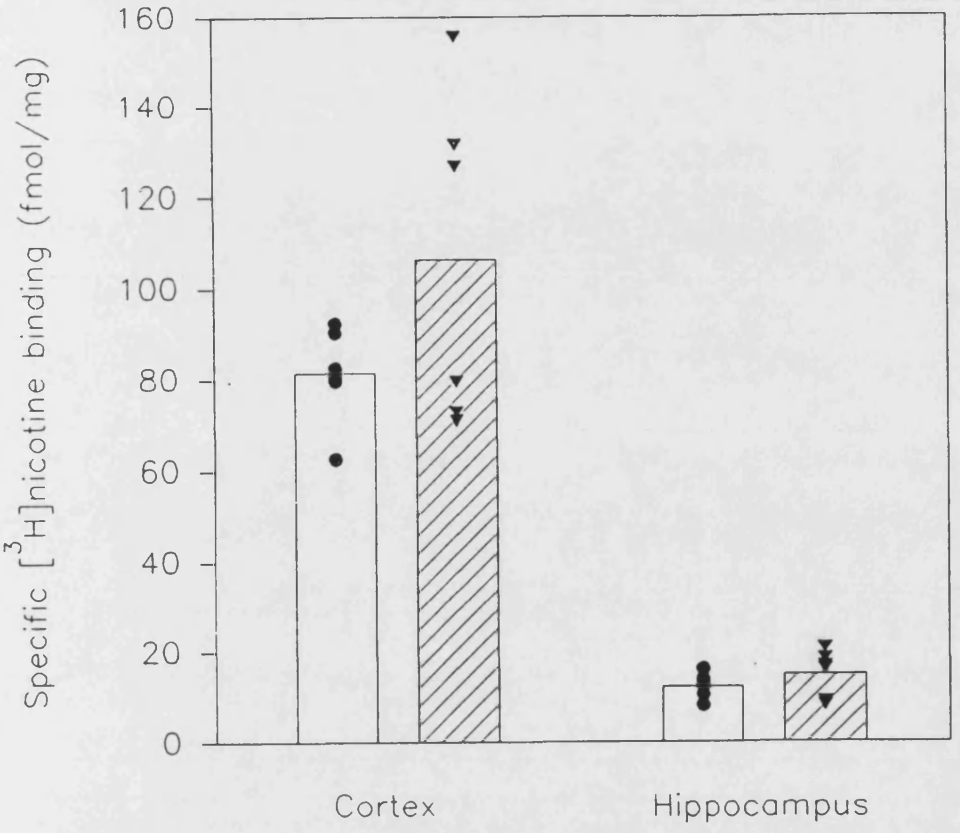

Fig. 4.18 **The effect of <u>in vivo</u> administration of chlorisondamine on [^{3}H]nicotine binding to rat cortical and hippocampal membrane preparations.** Two groups of six rats were treated with either chlorisondamine (10mg/kg; shaded columns) or saline (controls; open columns). After one week the animals were killed, and cortical and hippocampal membrane preparations were prepared from each individual brain. These were assayed for [^{3}H]nicotine (40nM) binding. The columns represent the mean specific binding (n=6); the scatter plots show the individual data points.

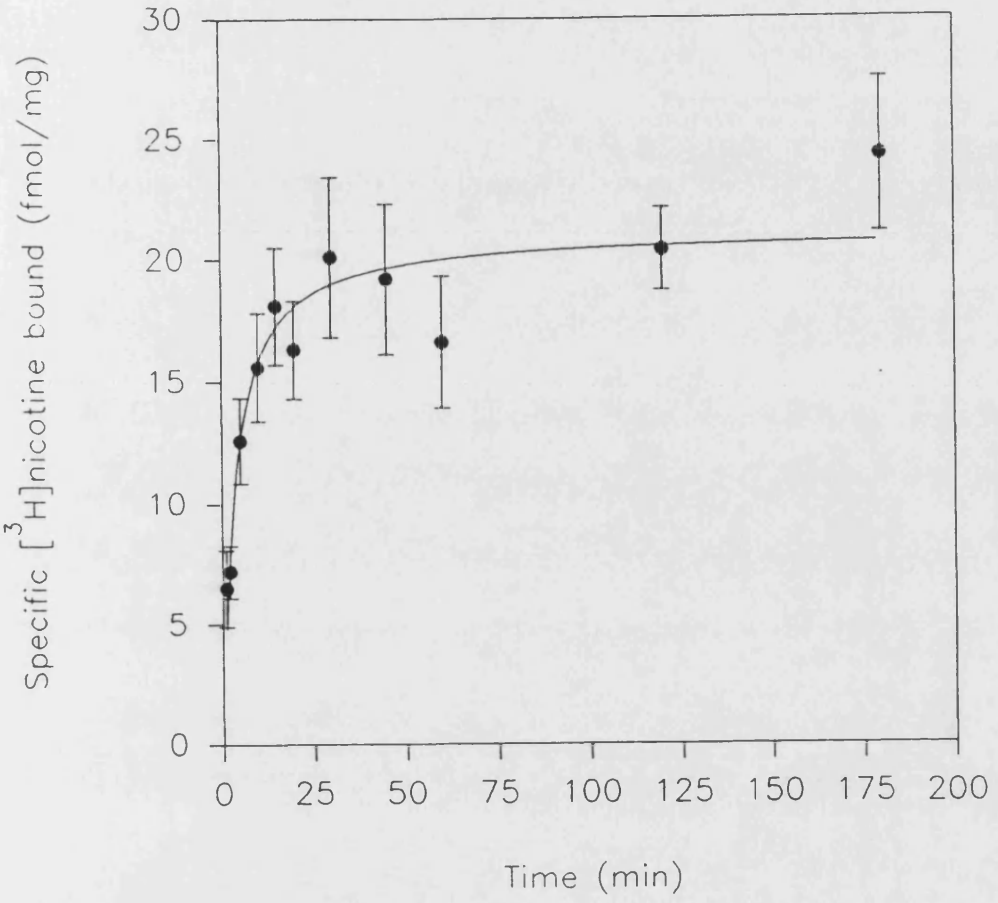

Fig. 4.19 **The time course of 10nM [^{3}H]nicotine binding to Triton extracts.** The protocol and subsequent data analysis are as described previously (see Fig. 4.13). Each data point is the mean ± SEM of between 6 and 12 individual determinations performed in duplicate. The calculated $t_{½}$ was found to be 3.2 minutes.

Fig. 4.20 **The observed association rates (k_{obs}) of 10nM [^{3}H]-nicotine binding to Triton extracts in the absence (A) and presence of mecamylamine (B) and MK-801 (C).** To measure the initial, rapid phase of radioligand association, [^{3}H]nicotine binding (final concentration 10nM) was assayed at intervals up to 30 minutes (see Fig. 4.19) and 180 minutes. Each data point represents the mean ± SEM of 6 (A) or 4 (B,C) separate determinations, each performed in duplicate. **B** and **Be** are the amounts of radioligand bound (in fmol/mg) at time **T** and equilibrium (180 minutes) respectively. The observed association rate (k_{obs}) was measured from the gradient of the plot **ln(Be/Be-B)** against **T** (Lipiello & Fernandes, 1986). Mean k_{obs} values were: control, 0.084$nM^{-1}min^{-1}$; with 180μM mecamylamine, 0.061 $nM^{-1}min^{-1}$; with 500μM MK-801, 0.066$nM^{-1}min^{-1}$.

A

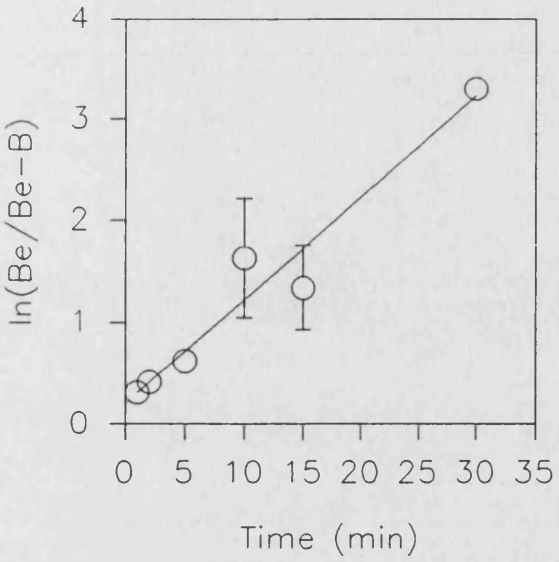
4
3
2
1
0
ln(Be/Be−B)
0 5 10 15 20 25 30 35
Time (min)

B

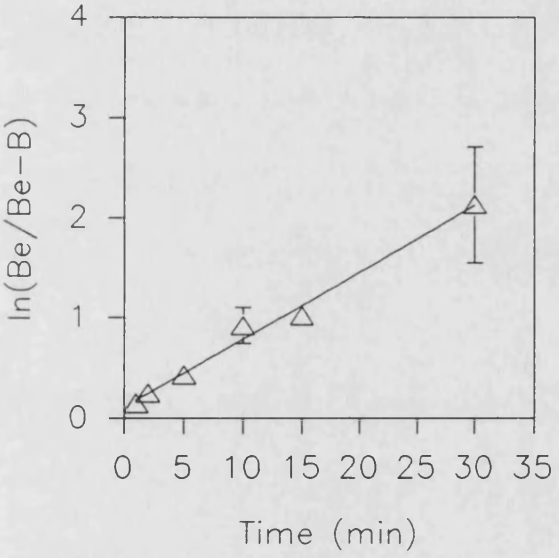
4
3
2
1
0
ln(Be/Be−B)
0 5 10 15 20 25 30 35
Time (min)

C

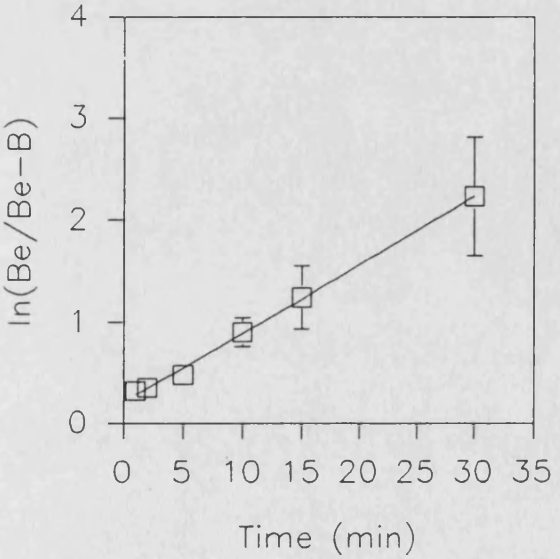
4
3
2
1
0
ln(Be/Be−B)
0 5 10 15 20 25 30 35
Time (min)

Fig. 4.21 **The dissociation rates (k_{-1}) of 10nM [^{3}H]nicotine from Triton extracts in the absence (A) and presence of mecamylamine (B) and MK-801 (C).** Triton extracts were equilibrated with 10nM [^{3}H]nicotine, and the binding assayed. an excess of unlabelled (-)nicotine was then added, and the radioligand remaining bound at intervals up to 30 minutes measured. B_0 and **B** are the amounts of [^{3}H]nicotine bound (in fmol/mg) after equilibration, and at time **T** after addition of unlabelled ligand respectively. The dissociation rate (k_{-1}) was determined from the gradient of the plot $\mathbf{ln(B/B_0 x100)}$ against **T** (Lipiello & Fernandes, 1986). Mean k_{-1} values: control, 0.059min^{-1}; with 180μM mecamylamine, 0.056min^{-1}; with 500μM MK-801, 0.055min^{-1}.

A

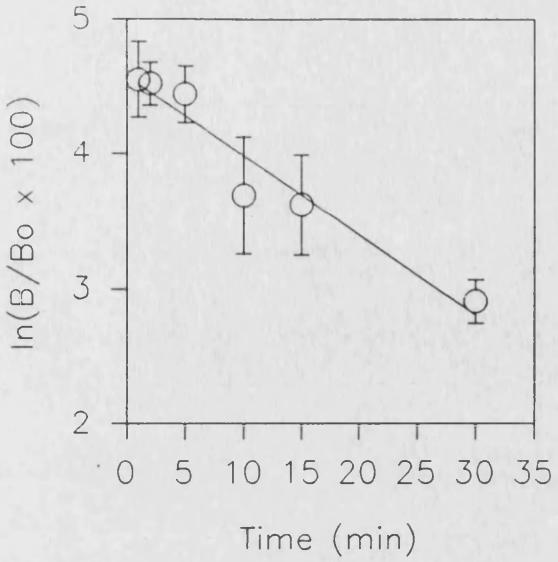
5
4
3
2
ln(B/Bo x 100)
0 5 10 15 20 25 30 35
Time (min)

B

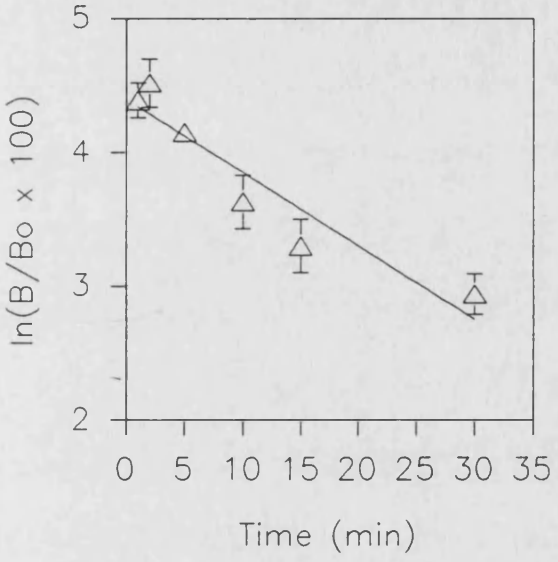
5
4
3
2
ln(B/Bo x 100)
0 5 10 15 20 25 30 35
Time (min)

C

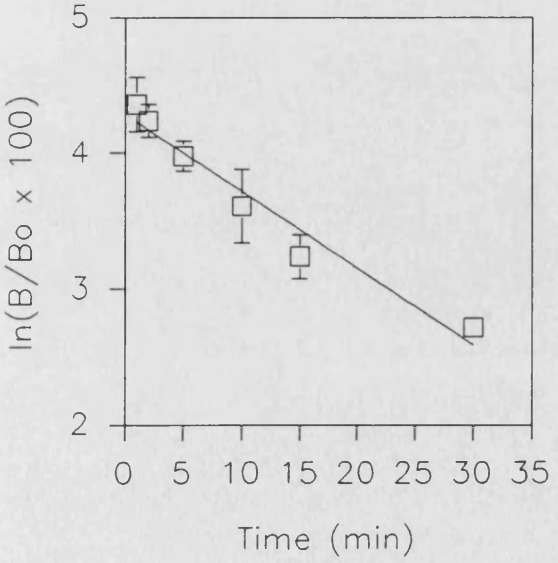
5
4
3
2
ln(B/Bo x 100)
0 5 10 15 20 25 30 35
Time (min)

Fig 4.22 **The time course of 10nM [^{3}H]nicotine binding to Triton extracts in the presence of (A) mecamylamine and (B) MK-801.** The binding data (mean ± SEM, n=4 for each drug) is that shown previously (see Fig. 4.20) curve fitted as for the control data (see Fig. 4.19). The half times of [^{3}H]nicotine association were calculated to be 8.8 and 6.1 minutes in the presence of 180μM mecamylamine and 500μM MK-801 respectively.

A

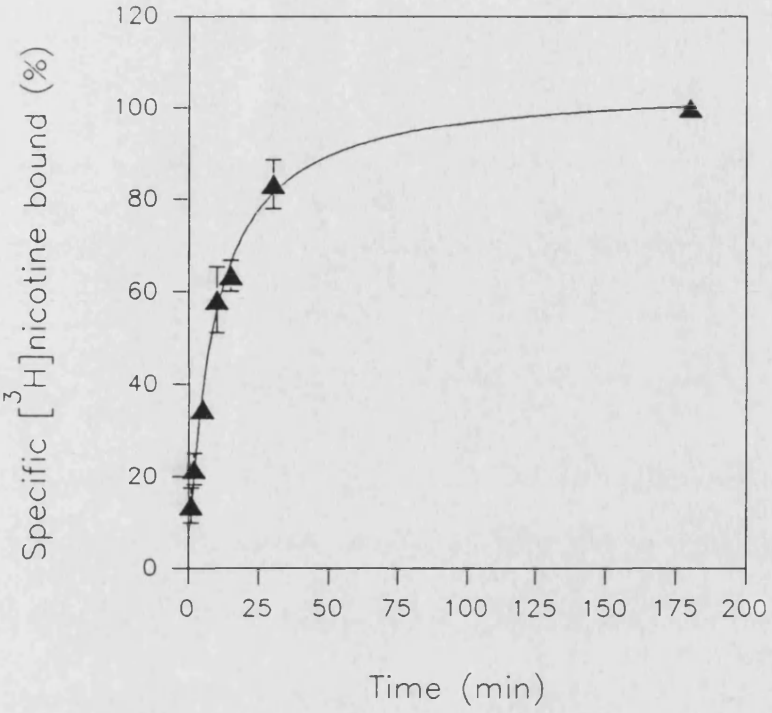
Specific [3H]nicotine bound (%)
120
100
80
60
40
20
0
0
25
50
75
100
125
150
175
200
Time (min)

B

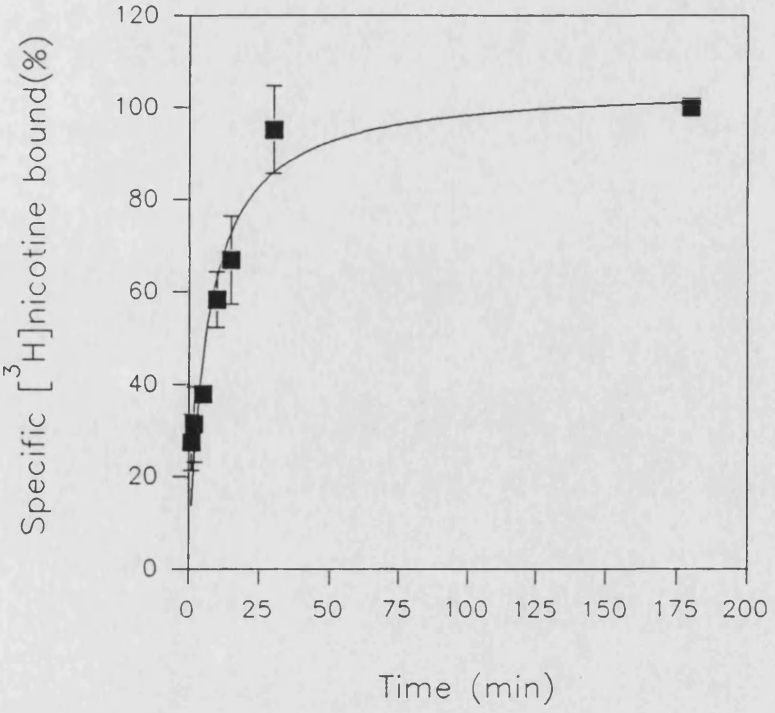
Specific [3H]nicotine bound(%)
120
100
80
60
40
20
0
0
25
50
75
100
125
150
175
200
Time (min)

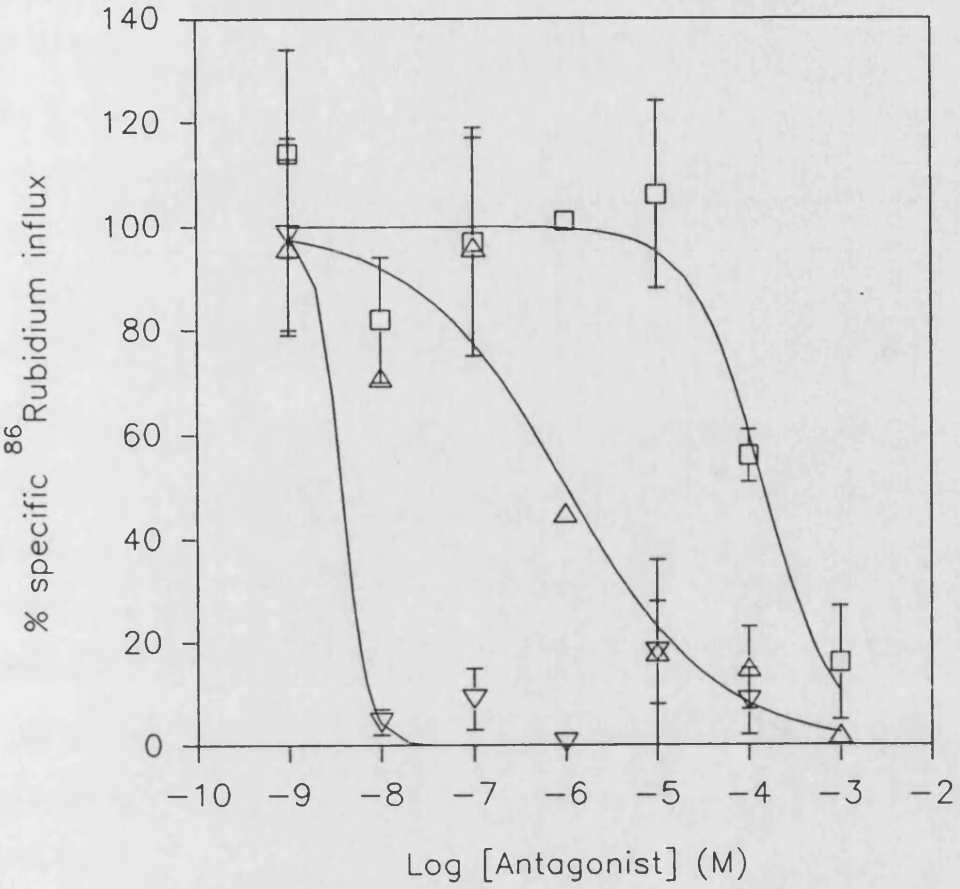

Fig 4.23 **The effects of mecamylamine, MK-801 and chlorisondamine on nicotine-mediated ^{86}Rubidium ion flux into M10 cells.** ^{86}Rubidium influx in response to 1μM (-)-nicotine was measured in the presence of increasing concentrations of mecamylamine (△),MK-801 (□) or chlorisondamine (▽). Data were expressed as a percentage of agonist-induced flux in the absence of either antagonist. Each point represents the mean ± SEM.

5 DISCUSSION

The basic theme underlying nAChR function is one of allosteric modulation of receptor conformation. This is achieved by a wide range of "effectors", a diverse group of relatively small ligands which promote structural rearrangement within the receptor upon binding. The interaction of receptor and effector is thus reliant upon accurate ligand recognition, and the coupling of binding to effect (in what might be termed "signal transduction"). Within this context, the structures of both the effector and the receptor are obviously of great importance. For example, all agonists are of similar size, and conform to a model pharmacophore (see section 5.1). Similarly, whilst homologous, the multiplicity of nAChR receptor subunits has a profound effect on agonist interaction. Thus, subtle structural changes alter binding affinities, leading to distinctive pharmacological profiles for each receptor subtype. For antagonists, a choice of ligand binding sites, and subsequent effector mechanisms, adds further complexity (see section 5.2).

In this section, it is the author's intention to briefly examine the interaction of the two main effector groups - the agonists and antagonists - with nAChR in the terms of this dual mechanism of ligand recognition and signal transduction. Particular reference will be made to those drugs used in this study, and the possible molecular bases of their actions.

5.1 Ligand recognition and receptor activation

All agonists contain a positively charged centre - the POSITIVE POLE - usually a quaternary ammonium salt, and, separated from it by 4.5-5.5Å, a π-electron system which forms a local dipole capable of accepting a hydrogen bond (Cockcroft et al., 1990). Competive antagonists, such as DHßE, are assumed to mimic this arrangement, and thus interfere with agonist binding. In turn, this pharmacophore defines the most important elements of the agonist binding pocket. Thus, a negatively charged subsite was considered an essential complement to the positive pole. Indeed, one of the persuasive features of the cys-loop (see section 1.2.1) as an agonist binding motif was thought to be the presence of an aspartate residue, one of only two invariant acidic amino acids present in the N-terminal domain of the α-subunit (Cockcroft et al., 1990). However, in affinity labelling studies, only aromatic residues in the region of the characteristic cysteines were highlighted (see Sequence 1.1). Whilst such residues could bind the positive pole (Dougherty & Stauffer, 1990), Czajkowski & Karlin (1991) have identified a 60 residue segment immediately prior to the M1 region of the δ-subunit as containing the negative subsite. Subsequent mutation studies showed that at least two of the ten acidic residues in this region (aspartate 180 and glutamate 189) had a significant effect on ACh affinity (Czajkowski et al., 1992). Based on these data, Karlin (1993) has proposed that agonists bridge the binding pocket, extending from the negative subsite to the region

around the disulphide. It is envisaged that ligand binding promotes a decrease in the distance between these two points, in effect moving one subunit relative to the other leading to channel opening. The elegance of this model extends beyond the linkage of ligand recognition and receptor activation however. The closure of the binding cleft around the agonist, a mechanism reminiscent of the "induced fit" of enzymes, may also be the basis of the increase in agonist affinity observed with the shift of the receptor from the R- to D-states (see section 1.3). Such closure would have the twin effects of optimising the interactions between agonist and receptor, and reducing access to the binding pocket; both would tend to increase apparent affinity for agonist. The existence of at least two non-functional conformations (the I- and D-states; see section 1.3.1) suggests that the necessary process of peptide rearrangement is not a smooth one; one might envisage local increases in free energy as neighbouring peptide chains move gradually into closer apposition suddenly relieved by a "flip" into a different conformation.

The kinetics of the ligand-receptor interaction may be influenced by the structure of the agonist; Papke et al. (1988) reported differences in single channel kinetics when subtle changes were made in the steric and ionic character of the acetyl portion of ACh, for example. The distinctive nature of (+)AnTX-induced receptor activation and desensitisation may be a similar phenomenon. The usual

increase in agonist affinity observed in the shift from R- to D-state was limited at transfected M10 cell α4ß2 nAChR; the EC_{50}/IC_{50} ratio for (+)AnTX was approximately 20, compared to 350 for (-)nicotine. In addition, the dose-response curves appeared to be steeper than those of other agonists. Similar observations have been made in other systems. Thus, the curves for (+)AnTX-induced [^{3}H]ACh release from rat hippocampal synaptosomes were steeper than those for (-)nicotine in the same system (Thomas et al., 1992). Using the Ki value for (+)AnTX inhibition of [^{3}H]nicotine binding to rat brain membranes from Wonnacott et al. (1991), the ratio of agonist affinities, approximately 30, was found to be in good agreement with that from the M10 cell line. Interestingly, an equally small shift is evident when the EC_{50} value of α-BgTX-sensitive currents in cultured hippocampal neurons (3.9μM; Thomas et al., 1992) is compared with the ability of (+)AnTX to displace [^{125}I]-αBgTX binding to rat brain membranes (0.38μM; Wonnacott et al., 1991). Data from α7 nAChR expressed in Xenopus oocytes were comparable to those from the cultures. In addition, the (+)AnTX dose response curves were notably steeper than the otherwise comparable (-)nicotine-induced activation curves in this system. The qualitative similarity of the responses of α4ß2 and α7 nAChR to (+)AnTX is particularly striking, despite the large difference in agonist potency between the two receptor subtypes. Relating this back to the model, (+)AnTX may better "fit" the gap between the disulphide and

negative subsites than do other agonists when the receptor is in the R-state. One would predict that the close proximity of ligand and binding subsites would enhance the attraction between the two, and thus lead to a more rapid initial contraction of the agonist binding site. This has the effect of making the agonist more readily able to activate the receptor, giving rise to the steep dose-response curves. Such a theory might also imply that further contraction of the agonist binding site would be rather limited - due to steric interference by the agonist - hence the low EC_{50}/IC_{50} ratios. It is likely that the distance between the two subsites is similar in all nAChR subtypes (they all have the same endogenous agonist), but that the surrounding molecular architecture differs considerably. This would explain the large difference in absolute affinities between the α4ß2 and α7 nAChR subtypes, and is itself simply a reflection of the sequence variation between the extracelluar domains of the different subunits. It would be interesting to see if these features of the (+)AnTX/nAChR interaction were repeated in other subtypes. However, it may require a different approach to that used here. Whilst the initial receptor activation phase is readily accessible to study in all subtypes by use of oocyte expression studies, the shift in affinity during the conversion from R- to D-state may prove more difficult to measure. The desensitised state of the α4ß2 and α7 nAChR subtypes may be directly probed by high affinity ligand binding assays, this is not possible for the other

subtypes. However, a method similar to that employed by Kemp & Morley (1986) might be used; the affinity of the desensitised receptor was calculated from the reduction in conduction observed.

The effect of receptor structure upon the interaction of an agonist and receptor cannot be over emphasised. The difference in subunit composition can, as alluded to above, radically alter the affinity for a given agonist. Thus, if the agonist binding site is formed from both α and (in neuronal nAChR) ß subunits, changes in either one might be expected to have an effect. There is some evidence that changes in subunit composition affect other aspects of the agonist/receptor interaction. Thus, expression studies in Xenopus oocytes have suggested that neuronal nAChRs containing ß2 and ß4 subunits each respond differently to cytisine application; cytisine appeared to be only a partial agonist at ß2-containing subunits (Leutje & Patrick, 1991; see section 3.3.1.2). Chimeric subunits have recently been used to demonstrate the particular importance of the N-terminal domain in this respect (Figl et al., 1992; Papke et al., 1993). The relative efficacy of cytisine in producing functional responses in the ion flux assay used in this study to measure α4ß2 nAChR was thus somewhat surprising (see section 3.3.3).

It is possible that this difference in cytisine's efficacy is a species dependent phenomenon, the expression studies utilising rat- rather than chick-derived receptor subunits. A Xenopus oocyte-expressed avian α4ß2 nAChR has

indeed been recently shown to respond to cytisine as a full agonist, with an affinity very similar to that seen in the M10 cells (Wilkie et al., submitted). However, the same study reported analogous data from rat hippocampal synaptosomes, which suggests a more complicated reason than a simple species difference. Comparison of rat and chick ß2 N-terminal domain sequences suggests little basis for such a theory in any case. There are only six amino acid differences between rat and chick sequences; four of these are conservative. The two residues which Figl et al. (1992) suggested were particularly important for relative insensitivity of rat ß2-containing receptors to cytisine (in the mature protein, phenylalanine 108 and serine 110; see Sequence 5.1), are identical in chick ß2. Papke et al. (1993) were less specific, merely noting that exchange of the first residues between ß2 and ß4 was sufficient to alter cytisine sensitivity. Interestingly the two non-conservative substitutions between rat and chick ß2 occur in this first half of the N-terminal domain (positions 12 and 30; see Sequence 5.1). Examination of the homologous positions in the rat ß4 sequence adds a further dimension. Perhaps purely by circumstance, the residue at position 30 is identical to that in chick ß2 (glutamine instead of glutamate as in rat ß2). In addition, at position 12, the histidine residue of ß2 is replaced with glutamate; both this residue and the tyrosine in this position in chick ß2, could act as hydrogen bond acceptors. Point mutation and oocyte expression could be used to assess the importance of

these residues. They are unlikely to be involved in the negative subsite (acidic residues homologous to those identified by Czajkowski et al. (1992) being present in the region immediately prior to the M1 segment of chick ß2 for example), though may be important in subsequent conformational shifts. Thus, whilst there is some basis for a similarity between chick ß2 and rat ß4, it may not be sufficient to explain the other contradictions in the literature.

Competitive antagonists, such as DHßE, also interact with nAChRs via the agonist binding site. As they are usually larger than the agonists (for example DHßE has a molecular mass of 275, compared with 145 to 190 for the four agonists used in this study), it is possible that whilst spanning the binding pocket, they prevent subsequent structural rearrangements implicit in the model of receptor activation by Karlin (1993). In favour of this hypothesis is the similarity of the antagonist's affinity for the R- and D-states (see section 4.1.1). A greater bulk, and possible difficulties in achieving the correct orientation for recognition by the receptor, are probably the reasons behind the failure to observe a blockade of agonist-induced $^{86}Rb^{+}$ influx by DHßE (see section 4.2.3). The binding of competitive antagonists is capable of eliciting a conformational change however, and is probably a pre-requisite of their action. Mutation and expression of α7 nAChR suggested that DHßE binding lead to channel blockade by the leucine ring of the M2 region (Bertrand et al.,

1992; see section 1.3.2). This may only represent an intermediate step however (an analogue of the agonist-induced I-state perhaps); even with the removal of the leucine ring, currents still desensitised. A two-step inactivation was also suggested by McCarthy & Stroud (1989), though through a somewhat different approach. Using hydrogen exchange as a measure of conformational change, they examined the effects of a number of effectors - agonists, competitive and non-competitive antagonists - on muscle-type nAChR. The largest change was induced by the competitive antagonist, α-BgTX.

5.2 **Modes of antagonism**

Agonist-induced receptor activation depends upon the accurate recognition of the ligand, and the coupling of binding to channel opening; both elements may be disrupted by antagonists. Competitive inhibitors prevent ligand binding by mimicking the agonist, and occupying its site (see section 5.1). Non-competitive inhibitors may allow agonist binding, but prevent subsequent changes in conformation (an "allosteric inhibitor"), or leave both phases of activation undisturbed and sterically block the ion channel. Interestingly, Heidmann et al. (1983) defined three categories of saturable binding sites in their model of NCI interaction with muscle-type nAChR (see section 1.4.1). The implicit site specificity of two of the modes of antagonism - competitive inhibition and channel blockade - suggests a simple correlation between effector binding

site and mechanism. By extending Heidmann's model, a general description of antagonist action at nAChR may be formulated. Basically, the mode of antagonism of any drug depends upon the relative affinity it displays for the three groups of binding sites. Thus, a competitive antagonist will favour the agonist binding site. In theory, as the concentration of the antagonist increases, a sequential occupation of progressively lower affinity site occurs; several mechanisms may thus occur simultaneously at high ligand concentrations. The model provides a useful frame- work within which to describe antagonist action at nAChR, acknowledging the importance of both ligand and receptor structure (which of course define binding affinity) on the mechanism of inhibition. However, it is insufficiently detailed to define the exact molecular basis of action, reflecting the poorly characterised nature of the binding sites. This is especially true of those Heidmann et al. (1983) described as "low affinity sites", a blanket term covering all those not in either the agonist pocket of the ion channel. Thus the mechanisms below must be regarded as speculative.

Chlorisodamine significantly ($p<0.02$) reduced the number of [^{3}H]nicotine binding sites as measured by saturation binding, with the data hinting at an additional effect on radioligand affinity (see section 4.2.2.1.4). When considering the effect of NCIs on high affinity ligand binding, the inevitable agonist-induced change in receptor conformation (see section 5.1) must also be addressed. In

the absence of the agonist, it has been estimated that only some 40% of the receptor population are in the correct conformation to bind [^{3}H]nicotine with nanomolar affinity (Lippiello et al., 1987). The rate of conversion between conformations is dependent upon temperature and agonist concentration. Under the assay conditions utilised (see section 2.2.1.3), the receptor population within the Triton X-100 extracts may be regarded as entirely in the high affinity state. A clear analogy with enzyme/substrate interactions exists. Furthermore, the well characterised mechanisms of enzyme inhibition provide a useful basis for interpretation of the binding data presented here. So, for an enzyme following Michaelis-Menten kinetics, enzyme rate (v) increases as a hyperbolic function of substrate concentration ([S]) to a theoretical maximum (Vmax). The [S] required to attain half maximal rate is given by the Michaelis constant (Km). In the simplest case, Km is assumed to equal the dissociation constant of the enzyme/substrate complex. If one substitutes "binding sites" for "rate", and "ligand" for "substrate", then these parameters are analogous to those in a binding assay: Vmax becomes Bmax, whilst Km is equivalent to Kd. Several patterns of enzyme inhibition have been described. For example, a COMPETITIVE inhibitor increases the Km in proportion to the concentration and affinity (Ki) of that inhibitor; Vmax remains the same. Thus, DHßE likewise reduced the affinity (Kd) of [^{3}H]nicotine binding, but had no effect on Bmax (see section 4.2.2.1.1). This suggests

that the enzyme analogy is a valid one. To continue, an inhibitor which alters only the Vmax is said to be NON-COMPETITIVE. If both Km and Vmax are changed, the mechanism may be one of either MIXED or UNCOMPETITIVE inhibition. The latter is particularly interesting in the context of binding to nAChR, as the inhibitor only binds to the enzyme/substrate complex. Analogy with the classic description of open channel blockade is obvious. Returning to chlorisondamine, a combination of the binding data and its action as reported in the literature (see section 4.1.4) implies an "uncompetitive" action. However, there are certain difficulties associated with this interpretation. For instance, if both chlorisondamine and MK-801 are open channel blockers, why do they have different effects on [^{3}H]nicotine binding? On a more theoretical basis, can binding within the ion channel cause a conformational change in the receptor as well as steric blockade? Whilst the inclusion of an agonist has been widely reported to enhance channel blocker binding in studies using muscle-type receptors (see Heidmann et al., 1983, for example), there is little evidence that NCIs inhibit radioligand binding at anything other than very high concentrations. Thus, whilst the data in this study hinted at an effect by MK-801 on [^{3}H]nicotine binding affinity (see section 4.2.2.1.3A), the model of antagonist action discussed previously would predict direct action at the agonist site. Certainly, lower MK-801 concentrations had no effect on agonist binding, nor did PCP at

concentrations sufficient to abolish [^{3}H]MK-801 binding to immunoimmobilised α4ß2 nAChR (see section 4.2.2.1.3B). These data imply that little, if any, change in conformation accompanies channel blockade. It thus seems likely that the observed effects on high affinity agonist binding are mediated through interaction with a different site.

Lingle & Neely (1986) reported a second component, in addition to channel blockade, in the chlorisondamine inhibition of frog muscle nAChR (see section 4.1.4). Full recovery of agonist-induced currents after incubation with the antagonist was not observed, despite protocol changes. This suggests that chlorisondamine was able to induce or stabilise a conformation in a part of the receptor population which was inactivatable, perhaps permanently. The reduction in the number of binding sites may be interpreted in a similar way; chlorisondamine induces or stabilises a conformation in which the receptor is unable to bind [^{3}H]nicotine with high affinity. It is possible that the two observations are facets of the same phenomenon, and that the chlorisondamine-induced conformation is the same in both assay systems. The form this conformation takes, and the site at which the antagonist must bind to induce it, are unknown. However, the potency of chlorisondamine in attenuating $^{86}Rb^+$ flux ($IC_{50}<1x10^{-8}M$; see section 4.2.3) suggests that whatever the mode of antagonism, the binding affinity of the antagonist is unusually high.

Whilst analogy with enzyme studies provided at least

an indication of the mechanism of chlorisondamine's interaction with nAChR, the same is not true of mecamylamine. The IC_{50} value for the mecamylamine-induced attenuation of $^{86}Rb^{+}$ flux into M10 cells appeared to be in good agreement with those in the literature (see section 4.1.2). However, the effect of mecamylamine on [^{3}H]nicotine to Triton X-100 extracts was found to be quite distinctive, bearing little resemblance to the four patterns outlined previously. To summarise, the curvilinearity observed in the Scatchard transformations of saturation data from assays performed in the presence of mecamylamine, appeared to be due to a more profound inhibition of [^{3}H]nicotine binding at the lower radioligand concentrations. This was reflected by a large decrease in the IC_{50} value for mecamylamine when determined at a representative low (2nM) [^{3}H]nicotine concentration. Paradoxically, [^{3}H]nicotine binding at this concentration, though reduced in comparison to controls, reached equilibrium more quickly. It was concluded that the binding data were indicative of receptor population displaying two comformational states, both inactive, though each with different ligand binding properties. Mecamylamine is an oddity amongst NCIs, examination of the literature suggesting that it displays different modes of antagonism at different receptor subtypes (see section 4.1.2). This is not inconsistent with the model presented earlier however. Differences in subunit composition undoubtedly generate subtle variations in the molecular architecture of a receptor; these could be

sufficient to affect the affinity of one or more of the antagonist binding sites. Thus, it is possible to envisage a reordering of the sequence of site occupation - thus mechanism of inhibition - in different nAChRs. the question here is: what is the site and mechanism of mecamylamine's interaction with the $\alpha 4\beta 2$ subtype?

Of the two conformations, one is undoubtedly the agonist-induced D-state. The other is unclear, but certainly displays a lower affinity for [^{3}H]nicotine than the D-state. Comparable binding conditions (2nM [^{3}H]nicotine, 180μM mecamylamine) lead to a consistent proportion of the receptor population (30-50%) in this conformation at equilibrium, irrespective of assay type. The low affinity conformation is likely to be energetically less stable than the D-state however, as a relatively small increase in the agonist concentration (2nM to 10nM) was able to return binding to approximately control values. As mentioned earlier, Lippiello et al. (1987) reported that only approximately 40% of the receptor population are initially in the correct conformation to bind [^{3}H]nicotine with high affinity. Adding these elements together, it is possible that mecamylamine is able to stabilise the I-state of the receptor. This is probably the equivalent of the "low affinity state" Lippiello and co-workers. This theory has the advantage of providing an explanation of the kinetic data. Thus, at 2nM [^{3}H]nicotine, only that proportion of the receptor population already in the correct conformation to bind the agonist with high affinity

does so; the amount of radioligand bound is reduced in comparison to controls, though the elimination of extensive conformational rearrangements reduces the $t_{½}$ of those receptors which are labelled. At 10nM [^{3}H]nicotine, mecamylamine causes a slight increase in the $t_{½}$ as it attempts to stabilise the less favourable I-state; [^{3}H]nicotine binding approximates to that of controls. As with chlorisondamine, the site of this interaction is unclear, though from oocyte expression studies (Bertrand et al., 1990) there is a clear lack of voltage dependence, ruling out the channel blocker site. (This fits with the previously expressed opinion, that binding at this site does not induce a significant conformational change.) Mecamylamine was found to rely on agonist activation; unsurprising if the antagonist stabilises a conformation intermediate between the R- and D-state. Notably, the action of mecamylamine bears some resemblance to that of progesterone at α4ß2 nAChR expressed in Xenopus oocytes (Valera et al., 1992), which was also found to be voltage-independent, but with some relationship to agonist concentration. Single channel recording techniques may prove a useful tool in the elucidation of mecamylamine's action, as a stabilisation of the I-state might be expected to be reflected in changes in relative contribution of the fast and slow phases of receptor desensitisation.

The M10 cell line provides an excellent tool in the further exploration of the action of these and other antagonists at α4ß2 nAChR. The ability to probe both

antagonists at α4ß2 nAChR. The ability to probe both functional and desensitised states experimentally, and the homogeneity of the system are of great benefit in mechanistic analyses. For example, though not performed in this study, agonist dose-response curves in the presence of fixed concentrations of antagonists might be constructed. These would provide information about the mode of antagonism; competitive inhibitors would increase the concentration of agonist required to achieve full activation, NCIs reduce peak response. The influx assay may prove unsuitable for this style of experiment however, due to the seemingly inherent variability in the response (see section 3.3.3). The use of other radioligands, such as [^{3}H]-MK-801, in binding assays would also provide data about the sites of interaction of various antagonists with nAChR. Competition studies, for example, could be used, though one would have to be aware of the possibility of allosteric modulation.

5.3 Summary

The nAChR is a dynamic protein whose function, that of cation transport across the plasma membrane, is based upon allosteric modulation by a wide variety of "effectors". These effectors bind at one or more of three categories of sites and, depending upon their structure, either activate or inactivate the receptor. In most cases this binding is accompanied by a spatial rearrangement in the peptide chains of the protein which acts as the

action is essentially an "all-or-none" phenomenon, though variation in effector structure around the minimum required for function can modulate elements of the ligand/receptor interaction. In vivo the number of effectors is limited, and this modulation is achieved by varying receptor structure, leading to a multiplicity of nAChR subtypes. This study has been concerned with the action of two groups of effectors - agonists and non-competitive antagonists - on one of these receptor subtypes, the α4ß2 nAChR.

Agonist action appears to be well defined and most rigidly dependent upon effector structure. There are two agonist binding sites, spanning the interface of an α and non-α subunit, which contain two important subsites (the region around the disulphide, and the negative subsite respectively). The interaction of the agonist and receptor leads to a contraction of the site, which, when transmitted to the rest of the protein, gives rise to a transient channel opening. Continued conformational change leads to an enclosure of the agonist, and a concomitant closure of the ion channel; the receptor is "desensitised". The four agonists used in this study show only minor variations in affinity and kinetics.

The mode of action of an antagonist depends upon with which region of the nAChR it interacts. Inactivation mechanisms may be purely steric, allosteric or a combination of the two. However, the presence of multiple sites leads to concentration dependent occupation, and consequently multiple modes of antagonism by a single

inhibitor. MK-801 is primarily a channel blocker, DHßE a competitive antagonist. Chlorisondamine and mecamylamine are both non-channel blocking NCIs, but have dissimilar properties; this may be due to different sites of interaction.

Sequence 5.1 **Comparative alignments of (A) rat ß2/ß4** (from Figl et al., 1992)**, and (B) chick ß2/ß4** (Couturier et al., 1990b).

A

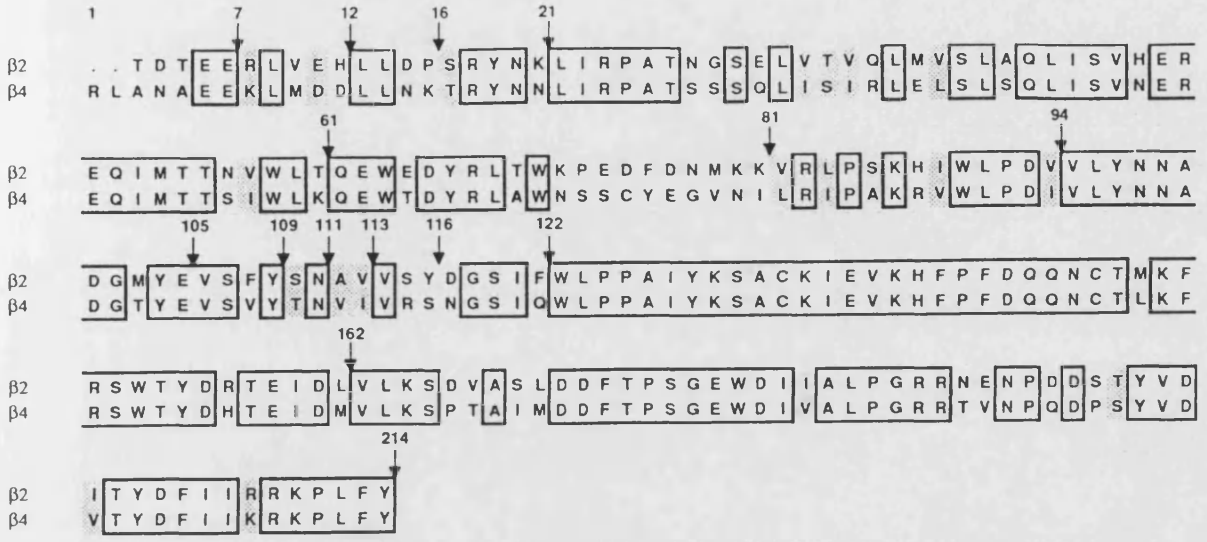
1 7 12 16 21
β2 . . T D T E E R L V E H L L D P S R Y N K L I R P A T N G S E L V T V Q L M V S L A Q L I S V H E R
β4 R L A N A E E K L M D D L L N K T R Y N N L I R P A T S S S Q L I S I R L E L S L S Q L I S V N E R
61 81 94
β2 E Q I M T T N V W L T Q E W E D Y R L T W K P E D F D N M K K V R L P S K H I W L P D V V L Y N N A
β4 E Q I M T T S I W L K Q E W T D Y R L A W N S S C Y E G V N I L R I P A K R V W L P D I V L Y N N A
105 109 111 113 116 122
β2 D G M Y E V S F Y S N A V V S Y D G S I F W L P P A I Y K S A C K I E V K H F P F D Q Q N C T M K F
β4 D G T Y E V S V Y T N V I V R S N G S I Q W L P P A I Y K S A C K I E V K H F P F D Q Q N C T L K F
162
β2 R S W T Y D R T E I D L V L K S D V A S L D D F T P S G E W D I I A L P G R R N E N P D D S T Y V D
β4 R S W T Y D H T E I D M V L K S P T A I M D D F T P S G E W D I V A L P G R R T V N P Q D P S Y V D
214
β2 I T Y D F I I R R K P L F Y
β4 V T Y D F I I K R K P L F Y

B

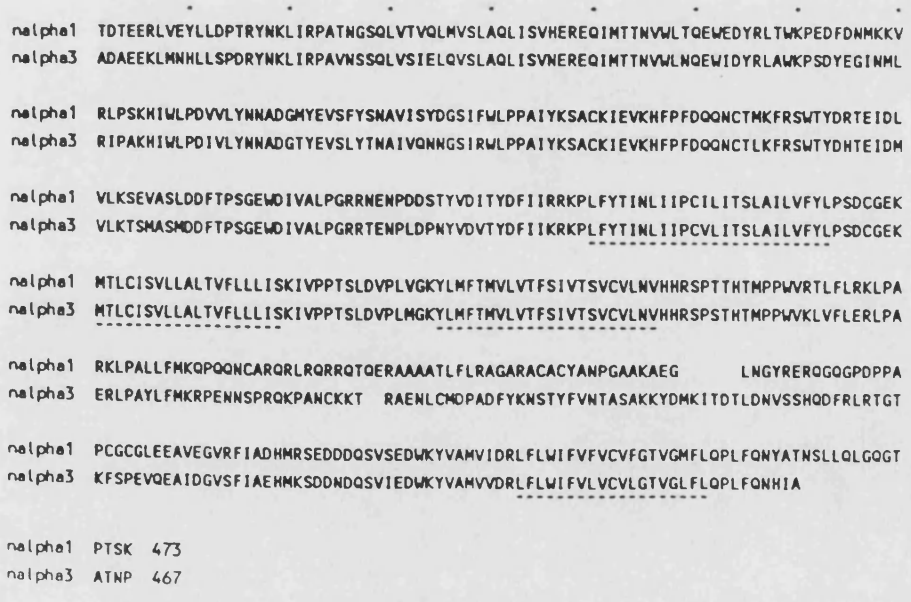
nalpha1 TDTEERLVEYLLDPTRYNKLIRPATNGSQLVTVQLMVSLAQLISVHEREQIMTTNVWLTQEWEDYRLTWKPEDFDNMKKV
nalpha3 ADAEEKLMNHLLSPDRYNKLIRPAVNSSQLVSIELQVSLAQLISVNEREQIMTTNVWLNQEWIDYRLAWKPSDYEGINML
nalpha1 RLPSKHIWLPDVVLYNNADGMYEVSFYSNAVISYDGSIFWLPPAIYKSACKIEVKHFPFDQQNCTMKFRSWTYDRTEIDL
nalpha3 RIPAKHIWLPDIVLYNNADGTYEVSLYTNAIVQNNGSIRWLPPAIYKSACKIEVKHFPFDQQNCTLKFRSWTYDHTEIDM
nalpha1 VLKSEVASLDDFTPSGEWDIVALPGRRNENPDDSTYVDITYDFIIRRKPLFYTINLIIPCILITSLAILVFYLPSDCGEK
nalpha3 VLKTSMASMDDFTPSGEWDIVALPGRRTENPLDPNYVDVTYDFIIKRKPLFYTINLIIPCVLITSLAILVFYLPSDCGEK
nalpha1 MTLCISVLLALTVFLLLISKIVPPTSLDVPLVGKYLMFTMVLVTFSIVTSVCVLNVHHRSPTTHTMPPWVRTLFLRKLPA
nalpha3 MTLCISVLLALTVFLLLISKIVPPTSLDVPLMGKYLMFTMVLVTFSIVTSVCVLNVHHRSPSTHTMPPWVKLVFLERLPA
nalpha1 RKLPALLFMKQPQQNCARQRLRQRRQTQERAAAATLFLRAGARACACYANPGAAKAEG LNGYRERQGQGPDPPA
nalpha3 ERLPAYLFMKRPENNSPRQKPANCKKT RAENLCMDPADFYKNSTYFVNTASAKKYDMKITDTLDNVSSHQDFRLRTGT
nalpha1 PCGCGLEEAVEGVRFIADHMRSEDDDQSVSEDWKYVAMVIDRLFLWIFVFVCVFGTVGMFLQPLFQNYATNSLLQLGQGT
nalpha3 KFSPEVQEAIDGVSFIAEHMKSDDNDQSVIEDWKYVAMVVDRLFLWIFVLVCVLGTVGLFLQPLFQNHIA
nalpha1 PTSK 473
nalpha3 ATNP 467

6 REFERENCES

Akagi, H & Kudo, Y. (1985) Opposite actions of forskolin at pre- and post-synaptic sites in rat sympathetic ganglia. Brain Res. 343 346-349

Albuquerque, E.X., Deshpande, S.S., Aracava, Y., Alkondon, M. & Daly, J.W. (1986) A possible involvement of cAMP in the expression of desensitisation of the nAChR. FEBS Lett. 199 113-120

Alkondon, M. & Albuquerque, E.X. (1993) Diversity of nicotinic acetylcholine receptors in rat hippocampal neurons. 1. Pharmacological and functional evidence for distinct structural subtypes. J. Pharm. Exp. Ther. 265 1455-1475

Alkondon, M., Pereira, E.F.R., Wonnacott, S. & Albuquerque, E.X. (1992) Blockade of nicotinic currents in hippocampal neurons defines methyllycaconitine as a potent specific receptor antagonist. Mol. Pharmacol. 41 802-808

Amar, M., Thomas, P., Johnson, C., Lunt, G.G. & Wonnacott, S. (1993) Agonist pharmacology of the neuronal α7 nicotinic receptor expressed in Xenopus oocytes. FEBS Lett. 327 284-288

Anand, R., Conroy, W.G., Schoepfer, R. Whiting, P. & Lindstrom, J. (1991) Neuronal nAChR expressed in Xenopus oocytes have a pentameric quaternary structure J. Biol. Chem. 17 11192-11198

Ascher, P., Large, W.A. & Rang, H.P. (1979) Studies on the mechanism of action of ACh antagonists in rat parasympathetic ganglion cells. J. Physiol. (Lond.) 295 139-170

Ballivet, M., Nef, P., Couturier, S., Rungger, D., Bader, C.R. (1988) Electrophysiology of a chick neuronal nicotinic acetylcholine receptor expressed in Xenopus oocytes after cDNA injection. Neuron 1 847-852

Bennet, G., Tyler, C. & Zaimis, E. (1957) Mecamylamine and its mode of action. Lancet 273 218-222

Benwell, M.E.M. & Balfour, D.J.K. (1985) Central nicotine binding sites: a study in post-mortem stability. Neuropharamcol. 24 1135-1137

Bertrand, D., Ballivet, M. & Rungger, D. (1990) Activation and blocking of neuronal nAChR reconstituted in Xenopus oocytes. Proc. Nat. Acad. Sci. USA 87 1993-1997

Bertrand, D., Devillers-Thiery, A., Revah, F., Hussy, N., Mulle, C., Bertrand, S., Ballivet, M. & Changeux, J-P. (1992) Unconventional pharmacology of a neuronal nicotinic

receptor mutated in the channel domain. Proc. Nat. Acad. Sci. USA 89 1261-1265

Betz, H. (1990) Ligand gated ion channels in the brain: the amino acid receptor superfamily. Neuron 5 383-392

Blanton, M., McCardy, E., Gallaher, T. & Wong, H.H. (1988) Non-competitive inhibitors reach their binding site in the AChR by two different paths. Mol. Pharmacol. 33 634-642

Blount, P. & Merlie, J.P. (1989) Molecular basis of the two non-equvalent ligand binding sites of the nAChR. Neuron 3 349-357

Boska, P. & Quirion, R. (1987) [^{3}H]N-methyl-carbamylcholine, a new radioligand specific acetylcholine receptors in the brain. Eur. J. Pharmac. 139 323-333

Boulter, J., Connoly, J., Deneris, E., Goldman, D., Heinemann, S. & Patrick, J. (1987) Functional expression of two neuronal nicotinic acetylcholine receptors fron cDNA clones identifies a gene family. Proc. Natl. Acad. Sci. USA 84 7763-7767

Boulter, J., Evans, K., Goldman, D., Martin, G., Treco, D., Heinemann, S. & Patrick, J. (1986) Isolation of a cDNA clone coding for a possible neural nicotinic acetylcholine receptor α-subunit. Nature 319 368-374

Boulter, J., O'Shea-Greenfield, A., Duvoison, R.M., Connolly, J.G., Wada, E., Jensen, A., Gardner, P.D., Ballivet, M., Deneris, E.S., McKinnon, D., Heinemann, S. & Patrick, J. (1990) α3, α5 and ß4: three members of the rat neuronal nicotinic acetylcholine receptor-related gene family form a gene cluster. J. Cell Biol. 265 4472-4482

Boyd, N.D. & Cohen, J.B. (1980) Kinetics of binding of [^{3}H]-acetylcholine and [^{3}H]carbamoylcholine to Torpedo postsynaptic membranes: slow conformational transitions of the cholinergic receptor. Biochemistry 19 5344-5358

Brisson, A. & Unwin, P.N.T. (1985) Quaternary structure of the AChR. Nature 315 474-477

Bruns, R.F., Lawson-Wendling, K. & Pugsley, T.A. (1983) A rapid filtration assay for soluble receptors using polyethylenimine-treated filters. Anal. Biochem. 132 74-81

Cachelin, A.B. & Jaggi, R. (1991) ß subunits determine the time course of desensitisation in rat α3 neuronal nicotinic acetylcholine receptors. Pflugers Arch. 419 579-582

Changeux, J-P. (1990a) Functional architecture and dynamics of the nAChR: an allostreic ligand gated ion channel. Fidia Research Foundation Neuroscience Award Lectures 4 (Raven Press, New York) 21-170

Changeux, J-P. (1990b) The nicotinic acetylcholine receptor: an allosteric protein prototype of ligand-gated ion channels. TIPS 11 485-497

Charnet, P., Labarca, C., Leonard, R.J., Vogelaar, N.J., Czyzk, L., Gouin, A., Davidson, N. & Lester, H.A. (1990) An open channel blocker interacts with adjacent turns of α-helices in the nAChR. Neuron 2 87-95

Cheng, Y.C. & Prusoff, W.H. (1973) Relationship between the inhibiton constant (Ki) and the concentration of inhibitor which causes 50 percent inhibition (I_{50}) of an enzymic reaction. Biochem. Pharmacol. 22 3099-3108

Chiara, D.C. & Cohen, J.B. (1992) Identification of amino acids contributing to high and low affinity d-tubocurarine (dTC) on the Torpedo nicotinic acetylcholine receptor. FASEB J. 6 A106 abstract 611

Chini, B., Clementi, F., Hukovic, N. & Sher, E. (1992) Neuronal-type α-bungarotoxin receptors and the α5 nicotinic receptor subunit gene are expressed in neuronal and non-neuronal cell lines. Proc. Natl. Acad. Sci. USA 89 1572-1576

Clarke, P.B.S. (1984) Chronic central nicotinic blockade after a single administration of the bisquaternary ganglion-blocking drug, chlorisondamine. Br. J. Pharmac. 83 527-535

Clarke, P.B.S. & Kumar, R. (1983) Characterisation of the locomotor stimulation of nicotine in tolerant rats. Br.J. Pharmac. 80 587-594

Claudio, A., Ballivet, M., Patrick, J. & Heinemann, S. (1983) Nucleotide and deduced amino acid sequences of Torpedo californica AChR τ subunit. Proc. Nat. Acad. Sci. USA 80 1111-1115

Cockcroft, V.B., Osguthorpe, D.J., Barnard, E.A., Friday, A.E. & Lunt, G.G. (1990) Ligand-gated ion channels: homology and diversity. Mol. Neurobiol. 4 129-169

Conroy, W.G., Vernallis, A.B. & Berg, D.K. (1992) The α5 gene product assambles with multiple acetylcholine receptor subunits to form distinctive receptor subtypes in the brain. Neuron 9 679-691

Cooper, E., Coutuner, S. & Ballivet, M. (1991) Pentameric structure and subunit stoichiometry of a neuronal AChR. Nature 350 235-238

Couturier, S., Bertrand, D., Matter, J-M., Hernandez M-C., Bertrand, S., Millar, M., Valera, S., Barkas, T. & Ballivet, M. (1990a) A neuronal nicotinic acetylcholine receptor subunit (α7) is developmentally regulated and

forms a homo-oligomeric channel blocked by α-bungarotoxin. Neuron 5 847-856

Couturier, S., Erkman, L., Valera, S., Rungger, D., Bertrand, S., Boulter, J., Ballivet, D. & Bertrand, D. (1990b) α3, α5 and non-α3: three clustered avian genes encoding neuronal nicotinic acetylcholine receptor-related subunits. J. Biol. Chem. 265 17560-17567

Czajkowski, C. & Karlin, A. (1991) Agonist binding site of Torpedo electric tissue nicotinic acetylcholine receptor. A negatively charged region of the δ subunit within 0.9nm of the α subunit binding site disulphide. J. Biol. Chem. 266 22603-22612

Czajkowski, C., Kaufmann, & Karlin, A. (1992) Nicotinic receptor δ subunit aspartate 180 and glutamate 189 contribute to the binding of acetylcholine. Soc. Neurosci. Abs. 259.2

Daly, J.W., Nishizawa, Y., Edwards, M.W. Waters, J.A. & Aronstam, R.S. (1991) Nicotinic receptor elicited sodium flux in rat pheochromocytoma PC12 cells: effects of agonists, antagonists and non-competitive blockers. Neurochem. Res. 16 489-500

Dani, J.A. (1989) Open channel structure and ion binding sites of the nAChR channel. J.Neurosci. 9 884-892

DeLean, A. & Rodbard, D. (1979) Kinetics of cooperative binding, in The Receptors: a comprehensive treatise (Ed. O'Brien, R.D.) 143-192 (Plenum Press, New York)

Deneris, E.S., Boulter, J., Swanson, L.W., Patrick, J. & Heinemann, S. (1989) ß3: a new member of the nicotinic acetylcholine receptor gene family is expressed in brain. J. Biol. Chem. 264 6268-6272

Deneris, E.S., Connolly, J., Boulter, J., Wada, E., Wada, K., Swanson, L.W., Patrick, J & Heinemann, S. (1988) Primary structure and expression of ß2: a novel subunit of neuronal nicotinic acetylcholine receptor. Neuron 1 45-54

Deneris, E.S., Connolly, J., Rogers, S.W. & Duvoisin, R. (1991) Pharmacological and functional diversity of neuronal nicotinic acetylcholine receptors. TIPS 12 34-40

Devillers-Thierry, A., Giraudat, J., Bentaboulet, M. & Changeux, J-P. (1983) Complete mRNA coding sequence of the ACh-binding α subunit of Torpedo marmorata AChR: a model for the transmembrane organisation of the polypetide. Proc. Nat. Acad. Sci. USA 80 2067-2070

Dionne, V.E., Steinbach, J.H. & Stevens, C.F. (1978) An analysis of the doce-response relationshipat voltage clamped frog neuromuscular junctions. J. Physiol. (Lond.)

281 421-444

Dougherty, D.A. & Stauffer, D.A. (1990) Acetylcholine binding by a synthetic receptor: implications for biological recognition. Science 250 1558-1560

Duvoisin, R.M., Deneris, E.M., Patrick, J. & Heinemann, S. (1989) The functional diversity of neuronal nicotinic acetylcholine receptors is increased by a novel subunit: ß4. Neuron 3 487-496

Dwyer, T.M., Adams, D.J. & Hille, B. (1980) The permeability of the end-plate channel to organic cations in frog muscle. J. Gen. Physiol. 75 469-492

Eusebi, F., Molinaro, M. & Zani, B.M. (1985) Agents that activate protein kinase C Reduce ACh sensitivity in cultured myotubes. J. Cell. Biol. 100 1339-1342

Figl, A., Cohen, B.N., Quick, M.W., Davidson, N. & Lester, H.A. (1992) Regions of ß4.ß2 subunit chimeras that contribute to the agonist selectivity of neuronal nicotinic receptors. FEBS Lett. 308 245-248

Finer-Moore, J. & Stroud, R.M. (1984) Amphipathic analysis and possible formation of the ion channel in an AChR. Proc. Nat. Acad. Sci. USA 81 155-159

Flores, C.M., Rogers, S.W., Pabreza, L.A. Wolfe, B.B. & Kellar, K.J. (1991) A subtype of nicotinic acetylcholine receptor in rat brain is composed of α4 and ß2 subunits and is upregulated by chronic nicotine treatment. Mol. Pharmacol. 29 250-257

Furois-Corbin, S. & Pullman, A. (1989) A possible model for the inner wall of the AChR channel. Biochim. Biophys. Acta 984 339-350

Giraudat, J., Dennis, M., Heidmann, T., Chang, J-Y. & Changeux, J-P. (1986a) Structure of the high affinity binding site for non-competitive blockers of the nAChR: serine 262 of the δ subunit is labelled by [^{3}H]CPZ. Proc. Nat. Acad. Sci. USA 2719-2723

Giraudat, J., Dennis, M., Heidmann, T., Haumant, P-Y., Lederer, F. & Changeux, J-P. (1986b) Structuer of the high affinity binding site for non-competitive blockers of the AChR: [^{3}H]CPZ labels homologous residuesin the ß and δ chains. Biochem. 26 2410-2418

Giraudat, J., Galzi, J-L., Revah, F., Changeux, J-P., Haumant, R-Y. & Lederer, F. (1989) The non-competitiveblocker [^{3}H]CPZ labels segment M2 but not segment M1 of the nAChR α subunit. FEBS Lett. 253 198-198

Goldman, D., Deneris, E., Luyten, W., Kochlar, A., Patrick,

J. & Heinemann, S. (1987) Members of a nicotinic acetylcholine receptor family are expressed in different regions of the mammalian central nervous system. Cell 48 965-975

Gordon, A.S., Davis, C.G. & Diamond, I. (1977a) Phosphorylation of membranes at the cholinergic synapse. Proc. Nat. Acad. Sci. USA 74 263-267

Gordon, A.S., Davis, C.G., Milfray, D. & Diamond, I. (1977b) Phosphorylation of AChR by endogenous membrane protein kinase in receptor rich membranes of Torpedo californica. Nature 267 539-540

Grady, S.R., Marks, M.J., Wonnacott, S. & Collins, A.C. (1992) Characterisation of nicotinic receptor-mediated [^{3}H]dopamine release from synaptosomes prepared from the mouse striatum. J. Neurochem. 59 848-856

Greene, L.A. & Tischler, A.S. Establishment of a noradrenergic clonal linee of rat adrenal pheochromocytoma cells which respond to nerve growth factor. Proc. Nat. Acad. Sci. USA 73 2424-2428

Gross, A., Ballivet, M., Rungger, D. & Bertrand, D. (1991) Neuronal nicotinic acetylcholine receptors expressed in Xenopus oocytes: role of the α subunit in agonist sensitivity and desensitisation. Pflugers Arch. 419 545-551

Gurney, A.M. & Rang, H.P. (1984) The channel blocking action of methonium compounds on rat submandibular ganglion cells. Br. J. Pharm. 82 623-642

Guy, H.R. (1984) Structural model of the AChR channel based on the partition energy and helix packing calculations. Biophys. J. 45 249-261

Halliwell, R.F., Peters, J.A. & Lambert, J.J. (1989) The mechanism of action and pharmacological specificity of the anticolvulsant NMDA antagonist MK-801: a voltage clamp study on neuronal cells. Br. J. Pharm. 96 480-494

Heidmann, T. & Changeux, J-P. (1979) Fast kinetic studies on the interaction of a fluorescent agonist with the membrane-bound acetylcholine receptor from Torpedo marmorata. Eur. J. Biochem. 4 281-296

Heidmann, T., Oswald, R.E. & Changeux, J-P. (1983) Multiple sites of action for non-competitive blockers on AChR rich membrane fragments from Torpedo marmorata. Biochem. 22 3112-3117

Herz, J.M., Johnson, D.A. & P. Taylor (1987) Interaction of non-competitive inhibitors with the AChR. J. Biol. Chem. 262 7238-7247

Heuttner, J.E. & Bean, B.P. (1988) Block of N-methyl-D-aspartate activated current by the anticonvulsant MK-801: selective binding to open channels. Proc. Nat. Acad. Sci. USA 85 1367-1371

Hucho, F., Oberthur, W. & Lottspeich, F. (1986) The ion channel of the nAChR is formed by homologous helices MII of the receptor subunits. FEBS Lett. 205 137-142

Huganir, R.L., Albert, K.A. Greengard, P. (1983) Phosphorylation of the nAChR by Ca^{2+}/phospholipid dependent protein kinase, and comparison with its phosphorylation by cAMP-dependent protein kinase. Soc. Neurosci. Abs. 9 578

Huganir, R.L. & Greengard, P. (1983) cAMP-dependent protein kinase phoshorylates the nAChR. Proc. Nat. Acad. Sci. USA 80 1130-1134

Huganir, R.L., Miles, K. & Greengard, P. (1984) Phosphorylation of the nAChR by an endogenous tyrosine specific protein kinase. Proc. Nat. Acad. Sci. USA 81 6968-6972

Huganir, R.L., Delcour, A.H., Greengard, P. & Hess, G.P. (1986) Phosphorylation of the nAChR regulates its desensitisation. Nature 321 774-776

Imoto, K., Methfessel, C., Sakmann, B., Mishina, M., Mori, Y., Konno, T., Fukada, K., Kurasaki, M., Bujo, H.,Fujita, Y. & Numa, S. (1986) Location of a δ subunit region dtermining ion transport through the AChR channel. Nature 324 670-674

Imoto, K., Busch, C., Sakmann, B., Mishina, M.,Konno, T., Nakai, J., Bujo, H., Mori, Y., Fukada, K. & Numa, S. (1988) Rings of negatively charged amino acids determineAChR channel conductance. Nature 335 645-648

Imoto, K., Konno, T., Nakai, J., Wang, F., Mishina, M. & Numa, S. (1991) A ring of uncharged polar amino acids as a component of channel constriction in the nAChR. FEBS Lett. 289 193-200

Javitt, D.C. & Zukin, S.R. (1989) Interaction of [^{3}H]MK-801 with multiplestates of the N-methyl-D-aspartate receptor complex of rat brain. Proc. Nat. Acad. Sci. USA 86 740-744

Jones, S.V.P., Harvey, A.L. & Marshall, I.G. (1986) The effects of two Erythrina alkaloids on endplate currents. Br. J. Pharm. 86 587P

Karlin, A. (1993) Structure of nicotinic acetylcholine receptors. Current Opinion Neurobiol. 3 299-309

Katz, B. & Thesleff, J. (1957) A study of the

"desensitisation" produced by acetylcholine at the motor end-plate. J. Physiol. (Lond.) 138 63-80

Kavanaugh, M.P., Tester, B.A. & Weber, R. (1989) Interaction of MK-801 with the nAChR associated ion channel from electroplax. Eur. J. Pharmacol. 164 397-398

Kemp, G. & Morley, B.J. (1986) Ganglionic nAChRs and high affinity nicotinic binding sites are not equivalent. FEBS Lett. 205 265-268

Kermode, J.C. (1989) The curvilinear scatchard plot. Experimental artifact or receptor heterogeneity? Biochem. Pharmacol. 38 2053-2060

Klymkowski, M.W. & Stroud, R.M. (1979) Immunospecific identification and three-dimensional structure of a membrane bound AChR from Torpedo californica. J. Mol. Biol. 128 319-354

Kofuji, P., Aracava, Y., Swanson, K.L., Aronstam, R.S., Rapoport, H. & Albuquerque, E.X. (1990) Activation and blockade of the acetylcholine receptor ion channel by the agonists (+)-anatoxin-a, the n-methyl derivative and the enantiomer. J. Pharm. Exp. Ther. 252 517-525

Konno. T., Busch, C., von Kitzing, E., Imoto, K., Wang, F., Nakai, J., Mishina, M., Numa, S. & Sakmann, B. Rings of anionic amino acids as structural determinants of ion selectivity in the acetylcholine receptor channel. Proc. R. Soc. Lond. Ser. B 244 69-79

Kozikowski, A.P. & Pang, Y-P. (1989) Structural determinants of affinity for the phencyclidine binding site of the NMDA receptor complex: discovery of a rigid phencyclidine analogue of high binding affinity. Mol. Pharmacol. 37 352-357

Kubalek, E., Ralston, S., Lindstrom, J. & Unwin, N. (1987) Location of subunits with the AChR by electron image analysis of tubular crystals from Torpedo marmorata. J. Cell. Biol. 105 9-18

Large, W.A. & Sim, J.A. (1986) A comparison between mechanisms of action of different nicotinic blocking agents on rat submandibular ganglia. Br. J. Pharm. 89 583-592

Leeson, P.D., Carling, R.W., James, K., Smith, J.D., Modre, K.W., Wong, E.H.F. & Baker, R. (1990) The role of hydrogen bonding ion ligand interection with the N-methyl-D-aspartate receptor ion channel. J. Med. Chem. 33 1296-1305

Lena, C. & Changeux, J-P. (1993) Allosteric modulation of the nicotinic acetylcholine receptor. TINS 16 181-186

Leonard, R.S., Labarca, C.G., Charnet, P., Davidson, N.,

Lester, H.A. (1988) Evidence that the M2 membrane spanning region lines the ion channelof the nicotinic receptor. Science 242 1578-1581

Leutje, C.W. & Patrick, J. (1991) Both α- and ß-subunits contribute to the agonist senstivity of neuronal nAChR. J. Neurosci. 11 837-845

Lingle, C. (1983) Blockade of cholinergic channels by chlorisondamine on a crustacean muscle. J.Physiol (Lond.) 339 395-417

Lippiello, P.M. & Fernandes, K.G. (1986) The binding of L-[^{3}H]nicotine to a single class of high affinity sites in rat brain membranes. Mol. Pharmacol. 29 448-454

Lippiello, P.M., Sears, S.B. & Fernandes, K.G. (1987) Kinetics and mechanism of L-[^{3}H]nicotine binding to putative high affinity receptor sites in rat brain. Mol. Pharmacol. 31 392-400

Listeraud, M., Brussard, A.B., Devay, P., Colman, D.R. & Role, L.W. (1991) Functional contribution of neuronal AChR subunits revealed by antisense oligonucleotides. Science 254 1518-1521

Lowry, O.H., Rosebrough, N.J., Farr, A.L. & Randall, R.J. (1951) Protein measurement with the Folin phenol reagent. J. Biol. Chem. 193 265-275

Lukas, R.J. (1989) Pharmacological distinctions between functional nicotinic acetylcholine receptors in the PC12 rat pheochromacytoma and the TE671 human medulloblastoma cell lines. J. Pharm. Exp. Ther. 251 175-182

Macallan, D.R.E., Lunt, G.G., Wonnacott, S., Swanson, K.L. Rapoport, H. & Albuquerque, E.X. (1988) Methyllycaconitine and (+)anatoxin-a differentiate between nicotinic receptors in vertebrate and invertebrtae systems. FEBS Lett. 226 357-363

McCarthy, M.P. & Moore, M.A. (1992) Effects of lipids and detergents on the conformation of the nicotinic acetylcholine receptor from Torpedo californica. J. Biol. Chem. 267 7655-7663

McCarthy, M.P. & Stroud, R.M. (1989) Conformational states of the nicotinic acetylcholine receptor from Torpedo californica induced by the binding of agonists, antagonists and local anesthetics. Equilibrium measurements using tritium-hydrogen exchange. Biochem 28 40-48

McCrea, P.D., Popot, P.L. & Engelman, D.M. (1987) Transmembrane topography of the nAChR δ subunit. EMBO J. 6 3619-3626

McGee, R. & Liepe, B. (1984) Acute elevation of cAMP does

not alter the ion conducting properties of the neuronal nAChR of PC12 cells. Mol. Pharmacol. 26 51-56

McHugh, E.M. & McGee, R. (1986) Direct anesthetic-like effects of forskolin on the nicotinic nAChR of PC12 cells. J. Biol. Chem. 261 3103-3106

Maelicke, A. (1988) Structural similarities between ion channel proteins. TIBS 13 199-202

Margiotta, J.F., Berg, D.K. & Dionne, V.E. (1987) Cyclic AMP regulates the propotion of functional AChR on chicken ciliary ganglia. Proc. Nat. Acad. Sci. USA 84 8155-8159

Marks, M.J., Farnham, D.A., Grady, S.R. & Collins, A.C. (1993) Nicotinic receptor function determined by stimulation of Rubidium efflux from mouse brain synaptosomes. J. Pharm. Exp. Ther. 264 542-552

Marks, M.J., Stitzel, J.A., Romm, E., Wehner, J.M. & Collins, A.C. (1986) Nicotinic binding sites in rat and mouse brain: comparison of acetylcholine, nicotine and α-bungarotoxin. Mol. Pharmacol. 30 427-436

Martino-Barrows, A.M. & Kellar, K.J. (1987) [^{3}H]Acetyl-choline and [^{3}H](-)nicotine label the same recognition site in rat brain. Mol. Pharmacol. 31 169-174

Middleton, P., Jaramillo, F. & Scheutze, S.M. (1986) Forskoloin increases the rate of acetylcholine receptor desensitisation at rat soleus endplates. Proc. Nat. Acad. Sci. USA 83 4967-4971

Miles, K., Anthony, D.T., Rubin, L.L., Greengard, P. & Huganir, R.L. (1987) Regulation of nAChR phosphorylation in rat myotubes by forskolin and cAMP. Proc. Nat. Acad. Sci. USA 84 6591-6595

Mishina, M., Tobimatsu, T., Imoto, K., Tanaka, K., Fujita, Y., Kurasaki, M., Takahashi, H., Morimoto, T., Hirose, T., Inayama, S., Tajahashi, T., Kuno, M. & Numa, S. (1985) Location of functional regions of AChR α-subunits by site-directed mutagenesis. Nature 313 364-369

Monod, J. Wyman, J. & Changeux, J-P (1965) On the nature of allosteric transitions: a plausible model. J. Mol. Biol. 12 88-118

Monod, J., Changeux, J-P & Jacob, F. (1963) Allosteric proteins and cellular control mechanisms. J. Mol. Biol. 6 306-329

Moriyoshi, K., Masu, M., Ishii, T., Shigemoto, R, Mizono, N. & Nakanshi, S. (1991) Molecular cloning and characterisation of the rat NMDA receptor. Nature 354 31-37

Musil, L.S., Frail, D.E. & Merlie, J.P. (1989) The mammalian 43kD AChR-associated protein (RAPsyn) is expressed in some non-muscle cells. J. Cell. Biol. 1833-1840

Nakayama, H., Nakashima, T. & Kuragahi, Y. (1991) α4 is a major acetylcholine binding subunit of cholinergic ligand affinty-purified nicotinic acetylcholine receptor from rat brains. Neurosci. Lett. 121 122-124

Neely, A. & Lingle, C.J. (1986) Trapping of an open-channel blocker at frog neuromuscular acetylcholine channel. Biophys. J. 50 981-986

Nef, P., Oneyser, C., Alliod, C., Couturier, S. & Ballivet, M. (1988) Genes expressed in the brain define three distinct neuronal nicotinic acetylcholine receptors. EMBO J. 7 595-601

Neher, E. & Steinbach, J.H. (1978) Local anesthetics transiently block cuurents through single AChR channels. J. Physiol. (Lond.) 277 153-176

Neubig, R.R., Boyd, N.D. & Cohen, J.B. (1982) Conformations of Torpedo acetylcholine receptor associated with ion transport and desensitisation. Biochemistry 21 3460-3467

Noda, M., Takahashi, H., Tanabe, T., Toyosato, M., Furutani, Y., Hirose, T., Asai, M., Inayama, S., Miyata, T. & Numa, S. (1982) Primary structure of α-subunit precursor of Torpedo californica AChR deduced from cDNA sequence. Nature 299 793-797

Noda, M., Takahashi, H., Tanabe, T., Toyosato, M., Kikyotani, S., Furutani, Y., Hirose, T., Takashima, H., Inayama, S., Miyata, T. & Numa, S. (1983) Structural homolgy of Torpedo californica AChR subunits. Nature 302 528-532

Ochoa, E.L.M., Chattopadhyay, A. & McNamee, M.G. (1989) Desensitisation of the nicotinic acetylcholine receptor: molecular mechanisms and the effect of modulators. Cell. Mol. Neurobiol. 9 141-177

Oswald, R.E. & Changeux, J-P (1982) Cross-linking of α-bungarotxin to the acetylcholine receptor from Torpedo marmorata by ultraviolet light irradiation. FEBS Lett. 139 225-229

Pabreza, L.A., Dhawan, S. & Kellar, K.J. (1991) [^{3}H]Cytisine binding to nicotinic cholinergic receptors in the brain. Mol. Pharmacol. 89 9-12

Papke, R.L., Duvoisin, R.M. & Heinemann, S.F. (1993) The amino terminal half of the nicotinic ß-subunit extracellular domain regulates the kinetics of inhibition

by neuronal bungarotoxin. Proc. R. Soc. Lond. B 252 141-148

Papke, R.L., Millhauser, G., Lieberman, Z. & Oswald, R.E. (1988) Relationships of agonist properties to the single channel kinetics of nicotinic acetylcholine receptors. Biophys. J. 53 1-10

Partick, J. & Stallcup, B. (1977) α-Bungarotoxin binding and cholinergic receptor function on a rat sympathetic nerve line. J. Biol. Chem. 252 8629-8633

Pedersen, S.E. & Cohen, J.B. (1990) d-Tubocurarine binding sites are located at α-τ and α-δ subunit interfaces in the nAChR. Proc. Nat. Acad. Sci. USA 87 2785-2789

Perutz, M.F. (1989) Mechanisms of cooperativity and allosteric regulation in proteins. Q. Rev. Biophys. 22 139-236

Raftery, M.A., Hunkapiller, M.W., Strader, C.D. & Hood, L.E. (1980) Acetylcholine receptor: complex of homologous subunits. Science 208 1454-1457

Ramoa, A.S., Alkondon, M., Aracava, Y., Irons, J., Lunt, G.G., Deshpande, S.S., Wonnacott, S., Aronstam, R. & Albuquerque, E.X. (1990) The anticonvulsant MK-801 interacts with with peripheral and central nAChR ion channels. J. Pharm. Exp. Ther. 254 71-82

Rapier, C., Lunt, G.G. & Wonnacott, S.(1988) Stereoselective nicotine induced release of dopamine from striatal synaptosomes: concentration dependence and repetitive stimulation. J. Neurochem. 50 1123-1130

Rapier, C., Lunt, G.G. & Wonnacott, S (1990) Nicotinic modulation of [^{3}H]dopamine release from striatal synaptosomes: pharmacological characterisation. J. Neurochem. 54 937-945

Reavill, C., Stollerman, I.P., Kumar, R. & Garcha, H.S. (1986) Chlorisondamine blocks acquisition of the conditioned taste aversion produced by (-)nicotine. Neuropharm. 25 1067-1069

Reavill, C., Walther, B., Stolerman, I.P. & Testa, B. (1990) Behavioural and pharmacokinetic studies on nicotine, cytisine and lobeline. Neuropharm. 29 619-624

Revah, F., Bertrand, D., Galzi, J-L., Devillers-Thiery, A., Mulle, C., Hussy, N., Bertrand, S., Ballivet, M. & Changeux, J-P. Mutations in the channel domain alter desensitisation of a neuronal nicotinic receptor. Nature 353 846-848

Revah, F., Galzi, J-L., Giraudat, J., Haumant, P-Y., Lederer, F. & Changeux, J-P. (1990) The non-competitive

blocker [^{3}H]CPZ labels three amino acids of the AChR τ subunit; implications for the α-helical organisation of region MII and for the structure of the ion channel. Proc. Nat. Acad. Sci. USA 87 4675-4679

Reynolds, J.A. & Karlin, A. (1978) Molecular weight in detergent solution of AChR from Torpedo californica. Biochem. 17 2035-2038

Rogers, S.W., Mandelzys, A., Deneris, E.S., Cooper, E. & Heinemann, S. (1992) The expression of nicotinic acetylcholine receptors by PC12 cells treated with NGF. J.Neurosci. 12 4611-4623

Romano, C. & Goldstein, A. (1980) Stereospecific nicotine receptors on rat brain membranes. Science 210 647-650

Romm, E., Lippiello, P.M., Marks, M.J. & Collins, A.C. (1990) Purification of L-[^{3}H]nicotine eliminates low affinity binding. Life Sci. 46 935-945

Ross, A.F., Rapauno, M., Schmidt, J.H. & Prives, J.M. (1987) Phosphorylation and assembly of nAChR subunits in cultured chick muscle cells. J. Biol. Chem. 262 14640-14647

Ross, M.J., Klymkowsky, M.W., Agard, D.A. Stroud, R.M. (1977) Structural studies of a membrane bound acetylcholine receptor from Torpedo californica. J. Mol. Biol. 116 635-659

Rowell, P.P. & Wonnacott, S. (1992) Evidence for functional activity of up-regulated nicotine binding sites in rat brain synsptosomes J. Neurochem. 55 2105-2110

Rubin, M.M. & Changeux, J-P. (1966) On the nature of allosteric transitions: implications of non-exclusive ligand binding. J. Mol. Biol. 21 265-274

Saitoh, T. & Changeux, J-P. (1981) Change in the state of phosphorylation of the AChR during maturation of the electromotor synapse in Torpedo marmorata electric organ. Proc. Nat. Acad. Sci. USA 78 4430-4434

Scatchard, G. (1949) Ann. N.Y. Acad. Sci 51 660-672

Schoepfer, R., Conroy, W.G., Whiting, P., Gore, M. & Lindstrom, J. (1990) Brain α-bungarotoxin binding protein cDNAs and mABs reveal subtypes of this branch of the ligand-gated ion channel superfamily. Neuron 5 35-48

Schoepfer, R., Whiting, P., Esch, F., Blacher, R., Shimasaki, S. & Lindstrom, J. (1988) cDNA clones coding for the structural subunit of a chicken brain nicotinic acetylcholine receptor. Neuron 1 241-248

Smith, M.M, Merlie, J.P. & Lawrence, J.C. (1987) Regulation

of phosphorylation of nAChR in mouse BC3HI myocytes. Proc. Nat. Acad. Sci. USA 84 6601-6605

Snell, L.D. & Johnson, K.M. (1989) effects of nicotinic agonists and antagonists on NMDA induced ^{3}H-norepinephrine release and ^{3}H-(1-[1-(2-Thienyl)cyclohexyl]-Piperidine) binding in rat hippocampus. Synapse 3 129-135

Stolerman, I.P., Albuquerque, E.X. & Garcha, H.S. (1992) Behavioural effects of anatoxin, a potent nicotinic agonist, in rats. Neuropharm. 31 311-314

Sumikawa, K. & Gehle, V.M. (1992) Assembly of mutant subunits of the nicotinic acetylcholine receptor laking the conserved disulphide loop structure. J. Biol. Chem. 267 6286-6290

Swanson, K.L., Allen. C.N., Aronstam, R.S., Raport, H. & Albuquerque, E.X. Molecular mechanisms of the potent and stereospecifc nicotinic agonist (+)-anatoxin-a. Mol. Pharmacol. 29 250-257

Takayama, H., Majewska, M.D. & London, E.D. (1989) Interaction of non-competitive inhibitors with nicotinic receptors in the brain. J. Pharm. Exp. Ther. 253 1083-1089

Tank, D.W., Huganir, R.L., Greengard, P. & Webb, W.W. (1983) Patch recorded single channel currents of the purified and reconstituted Torpedo acetylcholine receptor. Proc. Nat. Acad. Sci. USA 80 5129-5133

Thomas, P., Stephens, M., Wilkie, G., Amar, M., Lunt, G.G., Whiting. P., Gallagher, T., Pereira, E., Alkondon, M., Albuquerque, E.X. & Wonnacott, S. (1992) (+)Anatoxin is a potent agonist at neuronal nicotinic acetylcholine receptors. J. Neurochem. 60 2308-2311

Unwin, N. (1989) The structure of ion channels in excitable membranes. Neuron 3 665-676

Unwin, N. (1993) Nicotinic acetylcholine receptor at 9A resolution. J. Mol. Biol. 229 1101-1124

Valera, S. Ballivet, M., Bertrand, D. (1992) Progesterone modulates a neuronal nicotinic acetylcholine receptor. Proc. Natl. Acad. Sci. USA 89 9949-9953

Van Rossum, J.M. (1962) Classification and molecular pharmacology of ganglionic blocking agents II. Mode of action of competitive and non-competitive ganglionic blocking agents. Int. J. Neuropharmacol. 1 403-421

Varanda, W.A., Aracava, Y., Sherby, S.M., Van Meter, W.G., Eldefrawi, M.E. & Albuquerque, E.X. (1985) The AChR of the neuro-muscular junction recognises mecamylamine as a non-competitve antagonist. Mol. Pharmacol. 28 128-137

Vernallis, A.B., Conroy, W.G. & Berg, D.K. (1993) Neurons asseble acetylcholine receptors with as many as three kinds of subunits while maintaining subunit segregation among receptor subtypes. Neuron 10 451-464

Vijayaraghavan, S., Schmidt, H.A., Halvorsen, S.W. & Berg, D.K. (1990) Cyclic AMP-dependent phosphorylation of a neuronal AChR α-Type subunit. J. Neurosci. 10 3255-3262

Wada, K., Ballivet, M., Boulter, J., Connolly, J., Wada, E., Deneris, E.S., Swanson, L.W., Heinemann, S. & Patrick, J. (1988) Functional expression of a new pharmacological subtype of brain nicotinic acetylcholine receptor. Science 240 330-334

Wada, E., Wada, K., Boulter, J., Deneris, E., Heinemann, S., Patrick, J. & Swanson, L.W. (1989) Distribution of α2, α3, α4 and ß2 neuronal nicotinic receptor subunit mRNAs in the central nervous system: a hybridisation histochemical study in the rat. J. Comp. Neurol. 284 314-335

Wada, E., McKinnon, D., Heinemann, S., Patrick, J. & Swanson L.W. (1990) The distribution of messenger-RNA encoded by a new member of the neuronal nicotinic acetylcholine receptor gene family (α5) in the rat cental nervous system. Brain Res. 526 45-53

Walker, J.W., Takeyasu, K. & McNamee, M.G. (1982) Activation and inactivation kinetics of Torpedo californica acetylcholine receptor in reconstituted membranes. Biochemistry 21 5384-5382

Weber, M. & Changeux, J-P. (1974) Binding of Naja nigricollis ^{3}H-α-toxin to membrane fragments from Electrophorus and Torpedo electric organs. II. Effect of cholinergic agonists and antagonists on the binding of the tritiated α-neurotoxin. Mol. Pharmacol. 10 13-34

White, B.H. & Cohen, J.B. (1992) Agonist-induced changes in the structure of the acetylcholine receptor M2 regions revealed by photoincorporation of an uncharged nicotinic noncompetitive antagonist. J. Biol. Chem. 267 15770-15783

Whiting, P., Esch, F., Shimasaki, S. & Lindstrom, J. (1988) Neuronal nicotinic acetylcholine receptor ß subunit is coded for by the cDNA clone α4. FEBS Lett. 219 459-463

Whiting, P. & Lindstrom, J. (1986) Purification and characterisation of a nAChR from chick brain. Biochem. 25 2082-2093

Whiting, P., Schoepfer, R., Lindstrom, J. & Preistly, T. (1991) Structural and pharmacological characterisation of the major brain nAChR subtype stably expressed in mouse fibroblasts. Mol. Pharmacol. 40 463-472

Wilkie, G.I., Stephens, M.W., Whiting, P., Hutson, P.H., Bertrand, S., Bertrand, D. & Wonnacott, S. (1993) Pharmacological comparison of a nicotinic autoreceptor with the reconstituted α4ß2 nicotinic receptor. Br. J. Pharm. (submitted)

Williams, M. & Robinson, J.L. (1984) Binding of the nicotinic cholinergic antagonist, dihydro-ß-erythroidine, to rat brain tissue. J. Neurosci. 4 2906-2911

Wise, D.S., Schoenborn, B.P. & Karlin, A. (1981) Structure of an AChR dimer determined by neutron scattering and electron microscopy. J. Biol. Chem. 256 4124-4126

Wong, E.H.F., Kemp. J.A., Priestly, T., Knight, A.R., Woodruff, G.N. & Iverson, L.L. (1986) The anticonvulsant MK-801 is a potent N-methyl-D-aspartate antagonist. Proc. Nat. Acad. Sci. USA 83 7104-7108

Wonnacott, S. (1987a) Brain nicotine binding sites. Human Toxicol. 6 343-353

Wonnacott, S. (1987b) Neurotoxin probes for neuronal nicotinic receptors, in Neurotoxins and their pharmacological implications (Ed. Jenner, P.) 209-231 (Raven Press, New York)

Wonnacott, S. (1990) The paradox of nicotinic acetylcholine receptor upregulation by nicotine. TIPS 11 216-219

Wonnacott, S., Jackman, S., Swanson, K.L., Rapoport, H. & Albuquerque, E.X. (1991) Nicotinic pharmacology of anatoxin analogues: II. Side chain structure-activity relationships at neuronal nicotinic ligand binding sites. J. Pharm. Exp. Ther. 259 387-391

Zhang, X., Stjernlof, P., Aden, A. & Nordberg, A. (1987) Anatoxin-a: a potent ligand for nicotinic cholinergic receptors in rat brain. Eur. J.Pharmacol. 135 457-458

TABLE 1. *Comparison of EC_{50} values for AnTx, (−)-nicotine, and ACh in different neuronal nAChR preparations*

nAChR preparation	EC_{50} (*M*)		
	(+)-AnTx	(−)-Nicotine	ACh
Presynaptic nAChR	$1.4 \pm 0.4 \times 10^{-7}$ (3)	$4.9 \pm 0.9 \times 10^{-7}$ (4)	ND
$\alpha4\beta2$ nAChR	$4.8 \pm 1.8 \times 10^{-8}$ (4)	$2.7 \pm 0.7 \times 10^{-6}$ (5)	$9.0 \pm 4.0 \times 10^{-7}$ (4)
$\alpha7$ nAChR	$5.8 \pm 0.9 \times 10^{-7}$ (5)	$2.4 \pm 0.7 \times 10^{-5}$ (4)	$1.3 \pm 0.1 \times 10^{-4}$ (5)
Hippocampal neurones	$3.9 \pm 0.6 \times 10^{-6}$ (6)	$2.7 \pm 0.5 \times 10^{-5}$ (5)	$1.3 \pm 0.2 \times 10^{-4}$ (7)

Data are mean ± SE values (no. of preparations). ND, not determined.

tine gives an EC_{50} of 2.7 μM, whereas AnTx is ~50 times more potent. Again AnTx produced a steeper dose–response curve than nicotine, and the dose–response curves for both drugs are sharper than those obtained from synaptosomes; this may reflect the longer agonist exposure time in the ion flux assay.

Dual-electrode voltage-clamp recordings from *Xenopus* oocytes expressing the $\alpha7$ receptor resulted in characteristically fast currents that exhibited rapid desensitisation (Couturier et al., 1990). Three-second applications of several concentrations of agonist generated the dose–response curves depicted in Fig. 1c. At this nAChR subtype, nicotine is a weaker agonist. Its EC_{50} value of 24 μM is in good agreement with the previously published value of 10 μM (Bertrand et al., 1992). AnTx is 40 times more potent than nicotine (Table 1). Again the curve for AnTx is steeper (n_H = 2.6) than that for nicotine (n_H = 1.4).

A physiological correlate of the $\alpha7$ nAChR may occur in hippocampal neurones (Alkondon et al., 1992). These neurones express at least three different nAChRs, based on the kinetic properties of agonist-evoked whole-cell currents and their relative sensitivities to agonists and antagonists (Alkondon and Albuquerque, 1993). Two types of currents, referred to as IA and IB, could be blocked by α-Bgt. The type of current most frequently recorded (occurring in >80% of the hippocampal neurones tested) was IA, which exhibited a fast decay, reminiscent of $\alpha7$ expressed in oocytes. In the present study, AnTx, nicotine, and ACh were compared on type IA nAChRs (Fig. 2). AnTx was the most potent and efficacious agonist, being seven times more potent than nicotine and 30 times more potent than ACh (Table 1). EC_{50} values for nicotine and ACh at the hippocampal type IA nAChR were in good agreement with values obtained for the reconstituted $\alpha7$ nAChR, but AnTx appeared to be more potent at the latter (Table 1).

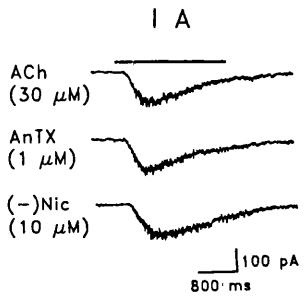

FIG. 2. Sample recordings of whole-cell currents (type IA) elicited in a cultured hippocampal neuron by AnTx (1 μM), nicotine (Nic; 10 μM), and ACh (30 μM). The holding potential was −50 mV, and the cell was cultured for 30 days.

In all four nAChR preparations studied here, representing at least two distinct nAChR subtypes, namely, $\alpha4\beta2$ and $\alpha7$, AnTx is a potent agonist, with submicromolar EC_{50} values in most cases (Table 1). EC_{50} values for nicotine range from 0.5 μM in hippocampal synaptosomes to ~25 μM at the α-Bgt-sensitive nAChR; in each preparation, nicotine has at least a threefold lower potency than AnTx. The endogenous agonist ACh had a potency similar to or less than that of (−)-nicotine and was clearly less potent than AnTx in each case (Table 1).

In ligand binding assays for [^{3}H]nicotine or ^{125}I-α-Bgt binding sites the rank order of potency of AnTx, (−)-nicotine, and ACh is similar to that in Table 1 (MacAllan et al., 1988; Wonnacott et al., 1991; Grady et al., 1992). Comparison of K_i and EC_{50} values shows the former to be generally one or two orders of magnitude higher. This is considered to reflect the propensity of agonists to convert the receptor into a high-affinity desensitised configuration and precludes the quantitative comparison of equilibrium binding data with functional estimates of agonist potency (Grady et al., 1992). Binding studies suggest that cytisine is a more potent ligand than (−)-nicotine (Whiting et al., 1991; Grady et al., 1992). However, the *agonist* potency of cytisine is very dependent on the subunit composition of the nAChR (Luetje and Patrick, 1991), and EC_{50} values for cytisine at different nAChR subtypes are similar to those for (−)-nicotine (Bertrand et al., 1992; Grady et al., 1992). In the four preparations described here, cytisine had potencies similar to or less than that of (−)-nicotine (data not shown) and was clearly less potent than AnTx. When its potency at the muscle nAChR (Swanson et al., 1986) is also considered, AnTx is the most potent nicotinic agonist thus far identified.

Because of the rigid structure of the azabicyclononene ring of AnTx, its high (probably exclusive) stereoselectivity for the (+)-enantiomer, and the available synthetic chemistry, AnTx is an attractive lead compound for structure–activity studies (Swanson et al., 1991; Wonnacott et al., 1991, 1992). Furthermore, the ability of AnTx, a secondary amine, to enter the brain from the systemic circulation (Stolerman et al., 1992) and its potential for chemical modification to create radiolabelled and affinity ligands (Huby et al., 1991; Wonnacott et al., 1992) make AnTx an excellent probe for the neuronal nAChR.

Acknowledgment: We are grateful to Dr. H. Rapoport for providing the AnTx, to Dr. Marc Ballivet for the $\alpha7$ cDNA, and to Dr. Daniel Bertrand for advice regarding the oocyte recording. These studies were supported by grants from R. J. Reynolds Tobacco Co. (G.G.L. and S.W.), the National Institutes of Health, the NIMH Center for Neuroscience and Schizophrenia, and the U.S. Army Medical Research Development Command (E.X.A.). Further support

was provided by SERC Postgraduate Training Awards to M.S. and G.W., an EMBO Fellowship to M.A., and a NATO Collaborative Award to S.W. and E.X.A.

REFERENCES

Alkondon M. and Albuquerque E. X. (1990) Alpha-cobratoxin blocks the nicotinic acetylcholine receptor in rat hippocampal neurons. *Eur. J. Pharmacol.* **191,** 505–506.

Alkondon M. and Albuquerque E. X. (1993) Diversity of nicotinic acetylcholine receptors in rat hippocampal neurons: I. Pharmacological and functional evidence for distinct structural subtypes. *J. Pharmacol. Exp. Ther.* (in press).

Alkondon M., Pereira E. F. R., Wonnacott S., and Albuquerque E. X. (1992) Blockade of nicotine currents in hippocampal neurons defines methyllycaconitine as a potent and specific receptor antagonist. *Mol. Pharmacol.* **41,** 802–808.

Amar M., Pichon Y., and Inove I. (1991) Micromolar concentrations of veratridine activate sodium channels in embryonic cockroach neurons in culture. *Pflugers Arch.* **417,** 500–508.

Aracava Y., Deshpande S. S., Swanson K. L., Rapoport H., Wonnacott S., Lunt G. G., and Albuquerque E. X. (1987) Nicotinic acetylcholine receptors in cultured neurons from the hippocampus and brain stem of the rat characterised by single channel recording. *FEBS Lett.* **226,** 63–70.

Bertrand D., Bertrand S., and Ballivet M. (1992) Pharmacological properties of the homomeric $\alpha 7$ receptor. *Neurosci. Lett.* **146,** 87–90.

Couturier S., Bertrand D., Matter J.-H., Hernandez M.-C., Bertrand S., Millar N., Valera S., Barkas T., and Ballivet M. (1990) A neuronal nicotinic acetylcholine receptor subunit ($\alpha 7$) is developmentally regulated and forms a homo-oligomeric channel blocked by α-BTX. *Neuron* **5,** 847–856.

Flores C.C. M., Rogers S. W., Pabreza L. A., Wolfe B. B., and Kellar K. J. J. (1992) A subtype of nicotinic cholinergic receptor in rat brain is composed of $\alpha 4$ and $\beta 2$ subunits and is upregulated by chronic nicotine treatment. *Mol. Pharmacol.* **41,** 31–37.

Grady S.S., Marks M. J., Wonnacott S., and Collins A. C. (1992) Characterization of nicotinic receptor-mediated [^{3}H]dopamine release from synaptosomes prepared from mouse striatum. *J. Neurochem.* **59,** 848–856.

Hamill O.O., Marty A., Beher E., Sakmann B., and Sigworth F. (1981) Improved patch-clamp techniques for high resolution current recording from cells and cell-free membrane patches. *Pflugers Archch.* **391,** 85–100.

Huby N.N. J. S., Thompson P., Wonnacott S., and Gallagher T. (1991) Structural modification of anatoxin-a. Synthesis of model affinity ligands for the nicotinic acetylcholine receptor. *J. Chem. Soc. Chem. Commun.* **4,** 243–245.

Luetje C. W. and Patrick J. (1991) Both α- and β-subunits contribute to the agonist sensitivity of neuronal nicotinic acetylcholine receptors. *J. Neurosci.* **11,** 837–845.

MacAllan D. R. E., Lunt G. G., Wonnacott S., Swanson K. L., Rapoport H., and Albuquerque E. X. (1988) Methyllycaconitine and anatoxin-a differentiate between nicotinic receptors in vertebrate and invertebrate nervous systems. *FEBS Lett.* **226,** 357–363.

Robinson D. and McGee R. (1985) Agonist-induced regulation of the neuronal nicotinic acetylcholine receptor of PC12 cells. *Mol. Pharmacol.* **27,** 409–417.

Rowell P. P. and Wonnacott S. (1990) Evidence for functional activity of up-regulated nicotine binding sites in rat striatal synaptosomes. *J. Neurochem.* **55,** 2105–2110.

Schoepfer R., Conroy W. G., Whiting P., Gore M., and Lindstrom J. (1990) Brain α-bungarotoxin binding protein cDNAs and mABs reveal subtypes of this branch of the ligand-gated ion channel gene superfamily. *Neuron* **5,** 35–48.

Stolerman I. P., Albuquerque E. X., and Garcha H. S. (1992) Behavioural effects of anatoxin, a potent nicotinic agonist, in rats. *Neuropharmacology* **31,** 311–314.

Swanson K. L., Allen C. N., Aronstam R. S., Rapoport H., and Albuquerque E. X. (1986) Molecular mechanisms of the potent and stereospecific nicotinic receptor agonist (+)-anatoxin-a. *Mol. Pharmacol.* **29,** 250–257.

Swanson K. L., Aronstam R. S., Wonnacott S., Rapoport H., and Albuquerque E. X. (1991) Nicotinic pharmacology of anatoxin analogs: I. Side-chain relationships at peripheral agonist and noncompetitive antagonist sites. *J. Pharmacol. Exp. Ther.* **259,** 377–386.

Thorne B., Irons J., Lunt G. G., Wonnacott S., and Dunkley P. R. (1988) Comparison of methods for rapid isolation of synaptosomes from brain regions, for uptake and release studies. *Biochem. Soc. Trans.* **16,** 309–310.

Thorne B., Wonnacott S., and Dunkley P. R. (1991) Isolation of hippocampal synaptosomes on Percoll gradients: cholinergic markers and ligand binding sites. *J. Neurochem.* **56,** 479–484.

Whiting P., Schoepfer R., Lindstrom J., and Priestley T. (1991) Structural and pharmacological characterisation of the major brain nicotinic acetylcholine receptor subtype stably expressed in mouse fibroblasts. *Mol. Pharmacol.* **40,** 463–472.

Wonnacott S., Jackman S., Swanson K. L., Rapoport H., and Albuquerque E. X. (1991) Nicotinic pharmacology of anatoxin analogs: II. Side chain structure–activity relationships at neuronal nicotinic ligand binding sites. *J. Pharmacol. Exp. Ther.* **259,** 387–391.

Wonnacott S., Swanson K. L., Albuquerque E. X., Huby N. J. S., Thompson P., and Gallagher T. (1992) Homoanatoxin: a potent analogue of anatoxin-a. *Biochem. Pharmacol.* **43,** 419–423.

Neurochem. Int. Vol. 19, No. 4, pp. 619–620, 1991
Printed in Great Britain

0197-0186/91 $3.00 + 0.00
Pergamon Press plc

BOOK REVIEWS

Fidia Research Foundation Neuroscience Award Lectures, Vol. 4, 1988–1989. ISBN 0-88167-671-3. Price: U.S. $109.50. Raven Press Ltd, New York, 1990.

This is the fourth volume in the rather good series of invited lectures organized by the Fidia Research Foundation, and presented at Georgetown University, Washington, during 1988 and 1989. This volume comprises contributions from Jean-Pierre Changeux, Rudolfo Llinás, Dale Purves and Floyd Bloom, each preceded by a short biographical sketch of the eminent neuroscientist in whose honour the lecture was given. This feature, together with the historical context of their topic offered by some of the contributors, provides an interesting perspective for the modern student of neuroscience.

This volume commences with an additional contribution by Edmund Pellegrino on Medical Ethics, a topic oddly out of place here. It is not an essay on the ethics of brain grafts, or genetic counselling in relation to inherited neurological diseases, but rather debates the relevance of Hippocratic ethics to modern medicine. There is little or no mention of Neuroscience and, contrary to the title of the volume, this is not offered as a Neuroscience Award Lecture. One wonders, therefore, what this essay is doing here.

The second contribution, which rather dominates the book, is an extensive yet highly readable review of the nicotinic acetylcholine receptor: "An alosteric ligand-gated ion channel", by Jean-Pierre Changeux. The author's attempt to integrate a historical narrative with a discussion of current models of structure and function works well. Thus we are introduced to Claude Bernard's studies with curare, and Langley's concept of a "receptive substance". This idea is developed to give a lucid account of the prototypical allosteric transmembrane protein.

The 'intrinsic electroresponsive properties' of nerve cells form the basis of Rudolfo Llanás' lecture. The author provides evidence for different electrical properties between cell types, adding weight to the view that even if all other things were identical (synaptic connectivity and transmitter output) a neuron of a given type could not be replaced by another. Ending with a model integrating these properties, the author envisages the brain operating "not as a slumbering machine awoken by ... sensory information", but as a "continuously humming" entity.

Is neuronal circuitry more or less structurally fixed or can it be altered during learning for example? Dale Purves, though accepting such changes are unlikely in the short term, believes that slowly developing, long term behavioural changes may, quite plausibly, be due to ongoing alterations in the connections between pre- and post-synaptic processes. Presenting evidence from both the peripheral and central nervous systems, the author suggests such changes may be commonplace, particularly in systems where multiple innervation of target cells is seen.

Floyd Bloom attempts to review the role of peptides as regulators of cell function in the brain. Acknowledging that a comprehensive survey is impossible when the number of peptides seems to be increasing almost exponentially, the author chooses to look at the detection, localization and characterization of a few specific examples. These include his own work on an immunoglobulin-like brain specific adhesion molecule (1B236). Also addressed is the interplay between peptides and classical neurotransmitters (such as somatostatin and ACh).

In conclusion, although the character of the contributions is rather varied (ranging from Changeux's comprehensive review to the briefer, more personal accounts of the other authors), this is an attractive collection of essays that many neuroscientists will find enjoyable and instructive to read.

M. W. Stephens and S. Wonnacott
Drs Stephens and Wonnacott are at the Department of Biochemistry, University of Bath, Bath, Avon, U.K.

Neurology and Neurobiology, Vol. 57, Catecholamine Genes. Edited by T. H. Joh. ISBN 0-471-56769-8. Price: U.S. $79.95. Wiley–Liss, 1990.

The rapid expansion of molecular neurobiology in the world of neuroscience fully justify the edition of the present volume of the series *Neurology and Neurobiology*. Many genes related to neuronal activities have been characterized and structure–function relationships of these genes are now extensively studied. The genes of the catecholamines-related enzymes are probably among the more fully characterized. The present volume, *Catecholamines Genes*, was then devoted to the summary of recent progress in this field.

We can however regret that the J. Mallet's group, one of the major contributors to this field and well recognized since their works are cited in 7 on 10 chapters of this book, lacks as a contributor of this up-to-date volume.

This volume focuses mostly, in 5 on 10 chapters, on the rate limiting enzyme in catecholamine biosynthesis, tyrosine hydroxylase (TH). Two chapters review recent findings on multiple messenger RNA (mRNA) of human TH. They characterized the human TH gene and the alternative RNA splicing producing four types of TH mRNA from the same primary transcripts. Tissue-specific expression of these four types of human TH, transcriptional regulation in the promoter region, and finally generation of stable mammalian cell lines independently expressing individual TH isoenzymes are developed in these chapters. The problem of transcriptional and post-transcriptional regulation of TH mRNA is more deeply examined in two additional chapters. The last chapter reviews the data on the evolution of TH. The authors state that TH gene belongs to a gene family constituted by the three aromatic acid hydroxylase genes and propose a model based on current genomic structures for the evolution of the ancestral hydroxylase gene.

Three chapters focus on the phenyletanolamine *N*-methyltransferase (PNMT), an enzyme serving as a specific cell marker for the adrenergic phenotype. The isolation, identification and nucleotide sequence of a cDNA and genomic DNA clone encoding bovine PNMT; the study of the PNMT promoter including the characterization of a glucocorticoid response element; and the different aspects of transcriptional regulation of this PNMT mRNA are developed in these chapters.

Unfortunately, making the history incomplete, no chapters were devoted to the two other enzymes in catecholamine biosynthesis: aromatic L-amino acid decarboxylase (AADC) and dopamine beta-hydroxylase (DBH) despite both being recently cloned. However, in its introductory chapter Tong Joh, the editor, briefly summarizes recent data on AADC and DBH.

Finally and interestingly, the last chapter of this issue concerns the cloning and expression of human monoamine oxidase A and B, two catecholamines metabolizing enzymes. These recently reported results open the way for a better understanding of these enzymes and a better use of their inhibitors in therapeutics.

All chapters of this book mix up-to-date reviews and precise and concise description of results and used methods and they demonstrate how large is the part taken by molecular neurobiology in the advance in understanding of catecholamine enzyme. It will be very useful for all pharmacologists and neuroscientists, particularly those involved in neurotransmitter research and also for neurologists involved in neurodegenerative diseases.

We are waiting now for an equally useful issue of the *Neurology and Neurobiology* series on catecholamine receptor genes.

PROFESSOR JEAN-JACQUES VANDERHAEGHEN
Professor Vanderhaeghen is at the Neuropathology–Neuropeptides Laboratory, Université Libre de Bruxelles, Campus Erasme Anderlecht, Bâtiment C, CP 601, 808 route de Lennik, 1070 Brussels, Belgium.

Trophic Factors and the Nervous System. Fidia Research Foundation Symposium Series. Vol. 3. Edited by L. A. HORROCKS, N. H. NEFF, A. J. YATES and M. HADJICONSTANTINOU. ISBN 0-88167-671-3. Price: US$109.50. Raven Press, New York, 1990.

Factors which promote growth, development and differentiation of neurons are currently the topic of numerous experimental studies and therefore it seems justified to collect reviews concerning these factors. As is often the case the nerve growth factor attracts most of the attention and in this collection of papers from a Symposium held at the Ohio State University in 1989 9 out of 24 contributions specifically deal with this important protein. However, many other substances influencing neuronal differentiation are described ranging from classical neurotransmitters over gangliosides to different peptides. A couple of papers are devoted to a detailed discussion of the role of calcium in the control of neuronal growth. Particularly the chapter by Stanley Kater and coworkers gives an excellent overview of the importance of the level of the intracellular free calcium concentration for the behavior of the neuronal growth cone. With regard to the understanding of the molecular events at the gene level which regulate neuronal differentiation, the introductory chapter by Erminio Costa is very useful. Also the chapter by Silvio Varon and coworkers on *in vivo* effects of nerve growth factor on degenerating cholinergic neurons is interesting.

Altogether this collection of review papers gives a very useful up-to-date picture of this extremely active field. The subject index gives easy access to the book and as is customary for these types of books there is a list of contributors. The book will be useful for those interested in neurodegenerative diseases with special emphasis on regeneration processes.

ARNE SCHOUSBOE
Professor Schousboe is at the PharmaBiotec Research Center, Department of Biological Sciences, Royal Danish School of Pharmacy, 2100 Copenhagen Ø, Denmark.